
Masters Theses

Student Theses and Dissertations

Fall 2020

On the investigation of hot tearing behavior of continuous cast steel

Yanru Lu

Follow this and additional works at: https://scholarsmine.mst.edu/masters_theses



Part of the [Materials Science and Engineering Commons](#), [Mechanical Engineering Commons](#), and the [Mining Engineering Commons](#)

Department:

Recommended Citation

Lu, Yanru, "On the investigation of hot tearing behavior of continuous cast steel" (2020). *Masters Theses*. 7966.

https://scholarsmine.mst.edu/masters_theses/7966

This thesis is brought to you by Scholars' Mine, a service of the Missouri S&T Library and Learning Resources. This work is protected by U. S. Copyright Law. Unauthorized use including reproduction for redistribution requires the permission of the copyright holder. For more information, please contact scholarsmine@mst.edu.

ON THE INVESTIGATION OF HOT TEARING BEHAVIOR OF CONTINUOUS
CAST STEEL

by

YANRU LU

A THESIS

Presented to the Graduate Faculty of the
MISSOURI UNIVERSITY OF SCIENCE AND TECHNOLOGY

In Partial Fulfillment of the Requirements for the Degree

MASTER OF SCIENCE

in

MATERIALS SCIENCE AND ENGINEERING

2020

Approved by:

Dr. Laura N. Bartlett, Advisor
Dr. Ronald J. O'Malley
Dr. Simon N. Lekakh

© 2020

Yanru Lu

All Rights Reserved

PUBLICATION THESIS OPTION

This thesis consists of the following three articles, formatted in the style used by the Missouri University of Science and Technology:

Paper I, found on pages 6–52, is intended for submission to *International Journal of Metalcasting*.

Paper II, found on pages 53–74, was published on the proceedings of AISTech 2020.

Paper III, found on pages 75–100, is intended for submission to *Steel Research International*.

ABSTRACT

Hot tearing has long been recognized as a major problem that plagues the development of the continuous casting process and results in low-quality products. Understanding of the mechanisms and the required conditions for the hot tearing formation is important for industries but has not been well-established yet. Thus, this research focuses on the hot tearing issue observed in continuous cast steel, by providing a summary of the current research progress and then introducing a new laboratory method to determine the thermo-mechanical properties relevant to hot tearing of different steel grades under different solidification conditions. In this method, an apparatus was developed to apply a certain amount of the strain to the solidifying steel shell at a controlled strain rate. A special mold, equipped with two water-cooled copper chills and an insulation sleeve, was designed to control the dendrite growth in the direction perpendicular to the applied strain and to ensure that the strain was applied in the region of controlled shell growth. The temperature, displacement and force were monitored and recorded as a function of time by a computer system during the test.

The in-situ hot tensile test was performed for a medium carbon steel using this apparatus to determine the thermo-mechanical properties of the solidifying casting. Filling and solidification simulation software was used to predict the temperature profile during the experiment. It was found that the calculated temperature was in good agreement with the measured temperature in experiments. The fracture strength obtained with this method was comparable with that measured by the submerged-split chill tensile test, but was lower than that determined by the conventional hot tensile test.

ACKNOWLEDGMENTS

First and foremost, I would like to thank my husband, Jie Wan, and my family for their unwavering support and understanding throughout the courses of my master's degree while attending Missouri University of Science and Technology. It has been my greatest honor to work with my advisors, Dr. Laura Bartlett, Dr. Ronald O'Malley and Dr. Simon Lekakh, on this project and I'm grateful for their exceptional guidance, knowledge, and dedication they provided. Many thanks to Dr. Mario Buchely who has helped me enormously with my experimentation and test program. I would like to also recognize Mr. Brian Bullock for his good advice and help with my experimental setup manufacture.

This project has been supported by the Peaslee Steel Manufacturing Research Center (PSMRC). A great appreciation to the PSMRC participating member companies for their financial and resource support as well as their insightful technical guidance.

I also appreciate my fellow graduate and undergraduate students for their help with my tests and sample preparation on this project.

Last but not least, I would like to extend my thanks to the staff of the MSE department who make our work and life easier and smoother. I am extremely grateful for their never-ending support and many cherished memories during my time at Missouri S&T.

TABLE OF CONTENTS

	Page
PUBLICATION THESIS OPTION.....	iii
ABSTRACT.....	iv
ACKNOWLEDGMENTS	v
LIST OF ILLUSTRATIONS.....	x
LIST OF TABLES	xiv
 SECTION	
1. INTRODUCTION.....	1
 PAPER	
I. A REVIEW ON HOT TEARING OF STEELS	6
ABSTRACT	6
1. INTRODUCTION.....	7
2. HOT TEARING CRITERION.....	12
2.1. NON-MECHANICAL CRITERIA	13
2.2. MECHANICAL CRITERIA	15
2.2.1. Critical Stress Based Criteria	15
2.2.2. Critical Strain Based Criteria	16
2.2.3. Critical Strain Rate Based Criteria	17
2.2.4. Other Criteria Specifically Related to the Continuous Casting Process	18
3. EXPERIMENTAL METHODS.....	20
3.1. CONSTRAINED SHAPE CASTING TEST.....	20

3.2. HOT TENSILE TESTS	22
3.3. BENDING TESTS.....	24
3.4. SUBMERGED SPLIT-CHILL TENSILE (SSCT) TEST	27
3.5. CONTROLLED DEFORMATION TEST FOR SOLIDIFYING STEEL SHELL.....	28
4. FACTORS INFLUENCING HOT TEARING	31
4.1. COMPOSITION.....	31
4.1.1. Carbon	31
4.1.2. Sulfur and Mn/S Ratio.....	35
4.1.3. Phosphorus	37
4.2. SOLIDIFICATION STRUCTURE	38
4.3. STRESS, STRAIN AND STRAIN RATE	41
5. CONCLUSION	42
ACKNOWLEDGEMENT.....	43
REFERENCES.....	43
II. NEW EXPERIMENTAL APPARATUS TO INVESTIGATE HOT TEARING BEHAVIOR IN STEEL.....	53
ABSTRACT.....	53
1. INTRODUCTION.....	54
2. EXPERIMENTAL PROCEDURE.....	58
2.1. CASTING AND MOLD DESIGN.....	59
2.2. TEST APPARATUS.....	60
2.3. TEST PROCEDURE	62
3. RESULTS AND DISCUSSION	64

3.1. THERMODYNAMIC MODELING	64
3.2. CASTING SOLIDIFICATION SIMULATION	65
3.3. CDT RESULTS	66
4. CONCLUSIONS	71
ACKNOWLEDGEMENTS	72
REFERENCES	72
III. DEVELOPING A METHOD TO INVESTIGATE MECHANICAL BEHAVIOR OF STEEL NEAR ITS SOLIDUS TEMPERATURE	75
ABSTRACT	75
1. INTRODUCTION	76
2. EXPERIMENTAL PROCEDURE	79
2.1. CONTROLLED DEFORMATION TEST (CDT)	79
2.1.1. Experimental Apparatus	79
2.1.2. Experimental Tests	82
2.2. THERMAL ANALYSIS	83
2.2.1. Cooling Curve Analysis	83
2.2.2. Temperature Profile Simulation	85
3. RESULTS	86
3.1. SOLIDIFICATION PATTERN OF THE CASTING IN INSULATING AREA	86
3.2. THERMAL ANALYSIS	87
3.3. CDT RESULTS	89
4. DISCUSSION	91
4.1. TEMPERATURE PROFILE AND SOLID SHELL	91

4.2. FRACTURE STRENGTH.....	92
4.3. COMPARISON OF FRACTURE STRENGTH DETERMINED BY DIFFERENT EXPERIMENTAL METHODS.....	93
5. CONCLUSIONS.....	95
ACKNOWLEDGEMENT.....	95
REFERENCES.....	96
SECTION	
2. CONCLUSIONS AND RECOMMENDATIONS.....	101
2.1. CONCLUSIONS.....	101
2.2. RECOMMENDATIONS.....	103
BIBLIOGRAPHY.....	106
VITA.....	109

LIST OF ILLUSTRATIONS

PAPER I	Page
Figure 1. Schematic of mechanical properties in mushy zone and the corresponding structures	9
Figure 2. Schematic of continuous casting process	11
Figure 3. Schematic of the test setup using a constrained T-shaped casting	21
Figure 4. Schematic of the experimental setup using a permanent steel mold	22
Figure 5. Schematic of the hot tensile test apparatus and specimen	23
Figure 6. Schematic of thermal and deformation history for tensile test using Gleeble system	24
Figure 7. Schematic of the three points bending test apparatus	25
Figure 8. Schematic of ingot bending test apparatus	26
Figure 9. Schematic of the SSCT test apparatus	27
Figure 10. Schematic of the controlled deformation test apparatus	29
Figure 11. (a) Typical non-equilibrium binary Fe-C phase diagram of carbon steel and (b) total thermal strain (ϵ_c^{TH}), strain caused by cooling (ϵ_c^*) and strain caused by phase transformation ($\epsilon_c^{\delta-\gamma}$) as a function of carbon content	33
Figure 12. The calculated crack susceptibility (Sc), strain in brittle temperature range and measured crack index as a function of carbon content	34
Figure 13. Crack index as a function of carbon content	35
Figure 14. The influence of sulfur content on the BTR for different carbon steels	36
Figure 15. Influence of the phosphorus content on the critical strain	38
Figure 16. The liquid permeability in the mushy zone with different grain morphologies	39

Figure 17. Solidification structure and internal cracks for (a) Al-Si killed steel and (b) low C-Al killed steel, revealed by sulfur print	40
Figure 18. Critical strain with different grain sizes at different temperatures	40
PAPER II	
Figure 1. Schematic diagram of mechanical properties in the mushy zone during continuous casting of steels	54
Figure 2. Schematic of different designs of constrained rod castings used to determine hot tearing sensitivity in aluminum and magnesium castings	56
Figure 3. Schematic diagram of the SSCT test method	58
Figure 4. Similarity of the solidification patterns in the continuous casting process and the proposed testing method	59
Figure 5. Side view of the test casting design showing the cylindrical test casting, insulation sleeve used to delay solidification in the test area, and water cooled copper chills on each side of the casting used to induce solidification and allow mechanical locking of the test casting	60
Figure 6. (a) Schematic of the Controlled Deformation Test (CDT) setup showing the main components of this apparatus, and (b) a detailed view of the attachment between the clamping bolts and the copper chill	61
Figure 7. The controlled deformation test setup shows how the mold box and electric cylinder were attached to the steel frame, and the blue arrow in the picture indicates the direction of the movement of the electric cylinder.	61
Figure 8. (a) Assembly of the experimental setup, and (b) detail view of the position of the LVDT and load cell	62
Figure 9. Calculated solid fraction and temperature curve for the studied steel by Scheil equation, which was used to estimate the LIT (dotted lines)	64
Figure 10. MAGMASOFT solidification modeling shows (a) the solidification sequence of the casting and (b) the cross sectional view of liquid fraction in the insulated area	65
Figure 11. (a) Cross sectional view of the insulated area with the position of the simulated thermocouples and, (b) simulated temperature history in different positions of the casting	66

Figure 12. Load and displacement change during (a) Test 1 and (b) Test 2.....	68
Figure 13. Results of the casting.....	69
Figure 14. (a) An overview of the fracture surface after Test 1; (b) zoom of part of the fracture surface to show the growth direction of the dendrites; and (c) higher magnification SEM image to show a signal dendrite structure on the fracture surface.	70
Figure 15. (a) and (c) Internal cracks that were observed in the insulated part after the test 2; (b) and (d) EDS mapping in the area of (a) and (c) to show the sulfur distribution in those area	71
 PAPER III	
Figure 1. Schematic of the CDT apparatus (front view).....	80
Figure 2. (a) Schematic of the mold and casting design (front view) and (b) the last solidified cross section in insulation area with the positions of the simulated thermocouples	81
Figure 3. (a) Geometry of the casting with thermocouple tube and (b) the macro structure of the insulated area.....	86
Figure 4. Cooling curve recorded during the test (T_c), its first derivative (T'_c) and the calculated Fourier Z curve.....	87
Figure 5. Comparison of the solid fraction calculated with Fourier method and that in MAGMASOFT.	88
Figure 6. Comparison of the measured temperature in experiment and calculated temperature with MAGMASOFT at two locations: center and 10mm position away from the surface on the last solidified cross section	89
Figure 7. Force and displacement change during experimental tests	90
Figure 8. Insulation part of the casting after (a) Test 1, (b) Test 2 and (c) Test 3	91
Figure 9. Comparison of fracture strength tested by CDT, SSCT test and CHT test at different representative temperature.....	94

SECTION

Figure 2.1. Solidification structure of the insulated area with (a) 10mm thick insulation sleeve, (b) 4mm thick insulation sleeve..... 104

LIST OF TABLES

PAPER I	Page
Table 1. List of abbreviations in this paper.....	11
Table 2. A summary of different experimental methods used for investigation of the hot tearing of steels.	30
PAPER II	
Table 1. Measured steel chemistry in two tests (wt.%).	67
PAPER III	
Table 1. Compositions of steels used in this study (weight percent).....	83
Table 2. Test conditions and calculated fracture strength for different tests	93

1. INTRODUCTION

Continuous casting (CC) process is nowadays the dominating technology that is used to produce over 90% of the steels in the world owing to its inherent advantages of low cost, high yield, flexibility of operation, and ability to a high quality product. Although much research and development work has been performed to optimize the casting process and improve product quality, hot tearing has long been recognized as a severe problem in the CC process due to the poor mechanical properties of the mushy zone and the complex thermal-mechanical conditions encountered during the casting process.

Hot tearing is known as a common defect in steel casting that usually appears as a crack or fracture, either on the surface or inside of the casting [1]. It is generally considered to form in the mushy zone at the later stages of solidification in response to a localized applied load and resulting strain, which may arise from both thermal contraction and mechanical constraint [2] [3] [4]. As explained by Campbell [5], the hot tear is a failure of a weak material, proceeded by a separation of dendrites, frequently recognizable in micrographs in the form of segregated paths due to suction of solute-enriched liquid. The hot tears in continuously casting steel are mostly observed as dendritic cracks. That is because the dendritic structure is intrinsically more brittle along interdendritic region than within single dendrite due to the existence of low melting point liquid film between dendrites [6].

Hot tearing formation is significantly influenced by the mechanical properties of the steel shell during its solidification. According to the solidification theory, the mushy

zone can be divided into several different stages based on the mechanical properties of the material. These stages are identified by temperature and solid fraction values [7] [8] [9]. They are:

- Dendrite coherency point (DCP): dendrite branches start to touch with each other until a coherent dendritic network is formed. While the dendrites are still separated by surrounding liquid and the material is permeable to liquid phase. Only after the temperature drops below the coherency point, the “real” mushy zone is formed [10]. Above which the material is in a slurry state [11] [12] .
- Zero strength temperature (ZST): it is defined as the temperature during cooling at which forces can first be transmitted perpendicular to the solidification direction [8]. A segregated thin liquid film still exists between the dendrites. The ZST corresponds to a solid fraction in the range of 0.6 to 0.8 [13].
- Liquid impenetrable temperature (LIT): the dendrite arms are close enough to cut off the liquid feeding path. With increasing solid fraction, solute enriched liquid film is isolated in the inter-dendritic region. The LIT is commonly associated with a solid fraction of about 0.9.
- Zero ductility temperature (ZDT): as the solid fraction increases, the strength of the material increases and at some point, the material acquires plasticity (ductility) [14]. The transition temperature is defined as ZDT and the corresponding solid fraction is between 0.98~1 [6] [9].

Hot tear can easily occur in the mushy zone even a small amount of the strain is applied to the material. For the hot tears formed above the LIT, the deformation of the material can create a new path for the liquid feeding, so the cracks can be “healed” by the surrounding liquid. While when the temperature drops below the LIT, the liquid film is isolated to resist feeding to the cracking area through the dendrite arms. In this case, the cracks will be maintained. Based on this theory, the mushy zone is divided into the liquid feeding zone and the cracking zone by the LIT [14] [15]. And the temperature interval between the LIT and the ZDT is defined as the brittle temperature range (BTR), in which the material is vulnerable to the crack.

Over the years, much effort has been devoted to understand the mechanisms of the crack formation and to correlate the conditions required for hot tearing occurrence, as summarized by D. G. Eskin et al. [10]. Two steps should be taken into consideration in terms of crack formation: the nucleation and propagation. Porosities or voids are commonly considered as the initiation sites for the hot tear, although the pores should not necessarily develop into a crack [16] [17]. The liquid film surrounding the grain at late stages of solidification is believed as a stress concentration of semi-solid body, so the liquid-filled cavity acts as a crack initiator [18]. In addition, the dissolved gas, oxide bi-film and other inclusions that entrained in the mushy zone can also work as the nuclei of the hot tear [5] [19]. The propagation of the crack, however, can be triggered by the rupture of the liquid film [20], through liquid film by sliding [21], and diffusion of vacancies from the solid to the crack [22], and so on. It is worth to note that the propagation of the crack is significantly determined by the applied stress or strain, and when it comes to the nucleation and propagation of the hot tears, experimental proof is

frequently replaced by an educated assumption. Therefore, in practical application, most of the existing hot tearing criteria deal with the conditions rather than with the mechanisms of hot tearing [10].

To estimate the hot tearing tendency in continuous casting steels, different casting conditions were investigated by many researchers and numerous hot tearing criteria were proposed. Most of these indicators are based upon the considerations of the solidification interval, brittle temperature range, thermal and mechanical conditions in the mushy zone, then associate with the mechanical properties of the material. Accordingly, many experimental approaches and validated numerical models have been developed, as summarized later in the first paper in this work. However, in most of the existing testing methods, hot tears were induced by the constraint of the solidification contraction. While for different steel grades, the amount of the solidification contraction is different due to the combined influences of the alloying elements and casting parameters, which makes it difficult to evaluate the hot tearing tendency for different steel grades. Moreover, since each of the existing criteria still has its own limitations to predict the occurrence of the hot tearing and most of the experimental approaches are still relatively simple that can only consider several factors, there's no doubt that a standard hot tear testing system and evaluation method of hot tearing severity still need to be developed and established.

Hot tear in steels is a difficult research topic due to the complexity of the hot tearing mechanisms and the various casting processes. A well-established knowledge of this phenomenon is important for the industry to produce defect-free high quality products and develop new steel grades.

This study was performed to bring a better understanding of the hot tearing phenomenon and provide a new method to investigate the hot tearing behavior that can be applied for a wide range of steel grades.

PAPER

I. A REVIEW ON HOT TEARING OF STEELS

Yanru Lu, Laura N. Bartlett, Ronald J. O'Malley

Peaslee Steel Manufacturing Research Center, Department of Materials Science and
Engineering

Missouri University of Science and Technology

1400 N Bishop Avenue, Rolla, MO, USA, 65409-034

Phone: 573-341-4711

Email: lnmkvf@mst.edu

ABSTRACT

Hot tearing is a common solidification defect in both continuous cast steels and mold castings, which has a significant impact on the quality of the final products. It is a complex phenomenon that involves in both the thermal and mechanical conditions and chemical element segregation that evolves during casting process. Over several decades, much effort has been invested into improving our understanding of the conditions required for the occurrence of hot tearing and to relate these conditions with casting parameters, like casting speed in continuous cast process, alloy composition, cooling conditions, etc. This review summarizes the results from previous investigations that have focused on the hot tearing phenomenon of steels, including criteria for hot tearing, experimental methods, and several validated models for different testing methods. The

factors that influence hot tearing sensitivity are also reviewed and discussed in the present work.

Keywords: Hot tearing; Hot tearing criterion; Experimental method; Influence factor.

1. INTRODUCTION

Hot tearing is a common solidification defect that usually appears as a crack or fracture in different alloys and steel castings [1]. It occurs when a casting is strained to failure in the semi-solid region during solidification and can lead to alloy and impurity element segregation, porosity formation, and precipitation of inclusions [2] [3]. The ability to understand and predict the conditions that cause hot tearing is important to steel mills and foundries for process design, quality control, and development of new steel grades.

Studies of the hot tearing have been started since the 1950s [4] [5]. A summary of hot tearing mechanisms given by D.G. Eskin [6], included both the nucleation and propagation of the hot tearing. Differing from cold cracking, hot tearing initiates above the solidus in mushy zone with a high solid fraction above about 90%. The hot tearing usually appears as solute enriched interdendritic cracks [7] [8], which is observed in the subsurface [9], halfway [10] [11] and centerline [12] [13] regions in the casting. These cracks may work as a weakened site that can result in void formation in the final product or fracture during the rolling process [14]. Owing to its deleterious effect on the casting quality, much effort has been expended to improve our understanding of the conditions that lead to the formation of the hot tearing in different casting processes.

To better understand hot tear formation, the solidification process can be divided into three stages:

Stage 1: Formation of the primary dendrite during solidification from liquid steel. As cooling goes on, secondary dendrite arms start to form behind the primary dendrite tips. At this stage, since the dendrite arms do not touch with each other, there is no mechanical bonding between the dendrites. If there is thermal or mechanical strain that is applied on the material in this stage, the deformation will be filled by surrounding liquid immediately.

Stage 2: As the temperature going down, the primary dendrites start to coarsen and the secondary dendrite arms start to reach out. Once the secondary dendrite arms start to interlock with each other, it will give the solid shell some strength. This point is defined as the zero strength temperature (ZST), above which the strength of material remains zero and below which the strength of the material starts to increase as the temperature drops. In the later of this stage, the secondary dendrite arms become compact and the free liquid feeding path is blocked [15] [16]. The liquid is isolated into liquid droplets in the interdendritic region. Under the applied strain, the hot tearing can easily occur during this stage. The deformation of the material creates a new liquid feeding path. Therefore, the cracks formed in this stage can be “healed” by the surrounding liquid and leave no internal crack. While even no internal cracks left, the hot tearing can still be detected by chemistry analysis because the that feeding liquid is solute enriched liquid resulting from microsegregation [8].

Stage 3: As the coarsening and compacting of dendrite arms, the interlocked secondary dendrite branches become indistinguishable and the material structure starts to

form columns without visible dendrite branches. The elements segregation lowers the melting point of the last liquid film. Thus, a thin liquid film can still exist between the columns structures during this stage, which makes the ductility of the material remains zero [17]. If there is strain that is perpendicular to the direction of the column structure, the hot tearing can still occur. The cracks formed in this stage cannot be refilled anymore, which will lead to the internal cracks in the final products. The critical temperature point below which the crack cannot be refilled by liquid metal is called liquid impenetrable temperature (LIT), which is commonly associated with a solid fraction of 0.9. And the temperature point below which there is no continuous liquid film existing is called zero ductility temperature (ZDT), which corresponds to a solid fraction of 0.98 to 1 [8]. The temperature difference between LIT and ZDT is defined as brittle temperature range (BTR). During continuous casting of steels, most of the internal cracks tend to occur in the BTR due to the thermal and mechanical constraint [18]. Thus, the BTR provides a qualitative guide to the hot tearing susceptibility [8] [19] [20] [21].

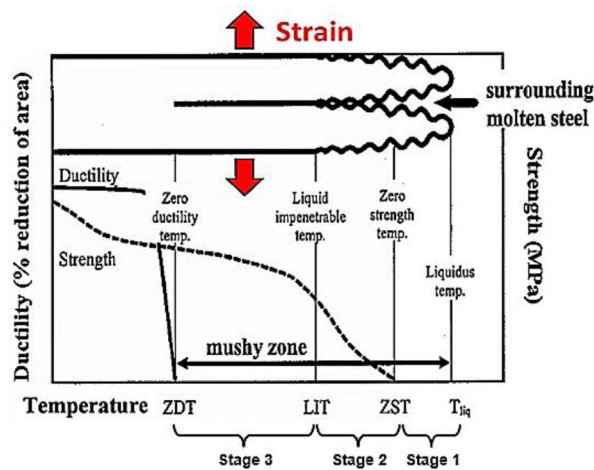


Figure 1. Schematic of mechanical properties in mushy zone and the corresponding structures [8].

Figure 1 shows a schematic diagram of the mechanical properties in the semi-solid region and corresponding solidification structures, including several key temperature points [8] [22]: ZST, LIT and ZDT.

To evaluate the hot tearing tendency for different alloys, many researchers have proposed different criteria and developed experimental methods to quantitatively study the cracking conditions, such as the alloy composition, thermal and mechanical conditions. A review on hot tearing criteria and experimental setups for aluminum alloys and magnesium alloys was given by D.G. Eskin et al. [16] and J. Song, et al [23], respectively. For foundry shaped casting, the hot tearing is mainly induced by the solidification shrinkage caused strain, which is significantly influenced by the casting geometry and steel compositions [24] [25]. For continuous casting steels, as shown in Figure 2, the thermo-mechanical conditions are much more complex. During the casting process, the strand shell experiences both mechanical and thermal loads resulting from contraction and phase transformation, non-uniform cooling rates from surface to center, friction between the mold and strand, bending and straightening, soft reduction and so on. Besides, the thickness of solid shell changes as a function of time, which leads to the changes of the position of mushy zone and changes of the stress and strain profile in the mushy zone as a function of temperature. Therefore, much effort has been devoted to the understanding of the relationship between the hot tearing phenomenon and the casting parameters in continuous casting process, like casting speed, alloy composition, cooling and machine conditions. The objective of the present paper is to provide an overview of the current progress of the hot tearing studies for different steels. Thus, the hot tearing criteria and the experimental methods developed to study the hot tearing behavior are

summarized and compared. The factors that have influence on the hot tearing susceptibility are also discussed in this work.

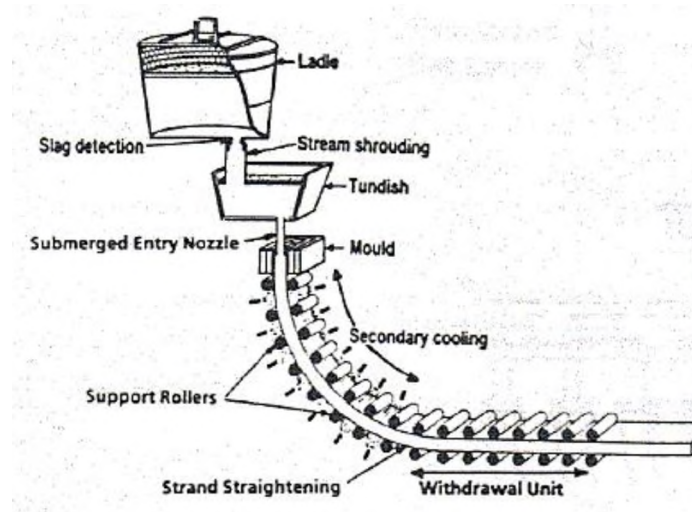


Figure 2. Schematic of continuous casting process [21]

A summary of the common abbreviations used in this paper was provided in Table 1.

Table 1. List of abbreviations in this paper.

ZST	Zero strength temperature
LIT	Liquid impenetrable temperature
ZDT	Zero ductility temperature
BTR (ΔT_B)	Brittle temperature range
HCS	Hot cracking susceptibility
CRC	Constrained rod casting
SSCT Test	Submerged split-chill tensile test

2. HOT TEARING CRITERION

To predict the occurrence or tendency of the hot tearing, many theories and criteria have been proposed over the last few decades. The existing hot tearing criteria focus more on the conditions or causes of the hot tearing instead of the mechanisms, like nucleation or propagation. These criteria, which have been reviewed elsewhere [6] [23], can be generally divided into two categories: non-mechanical criteria and mechanical criteria. The non-mechanical criteria that consider the brittle temperature range, phase diagram, steel composition and so on, have been proposed by Clyne and Davies, Feurer, Katgerman, Suyitno and Kou [6] [16] [23]. Mechanical criteria have mainly been derived from the mechanical behavior of semi-solid metals and involves critical stress [26] [27] [28], critical strain [29] [30] or critical strain rate [31] criteria.

Different casting processes require specific considerations for hot tearing criteria. For foundry casting, most of the criteria that consider composition sensitivity are successful in predicting hot tearing, since the steel compositions have essential effect on the amount of solidification shrinkage and brittle temperature range. In most of these predictions and the experimental results, the hot tearing susceptibility increases with increasing in the alloy element content and then it decreases with further increasing in the content of that alloy element, which indicating that there is a maximum susceptibility of material at a certain composition [23]. However, these criteria cannot applied for dynamic processes, such as continuous casting. For the continuous casting process, a viable hot tearing criterion should correctly predict damage based on both composition

and caster operating conditions. Thus, different hot tearing criteria that consider different aspects are introduced in this section.

2.1. NON-MECHANICAL CRITERIA

Clyne et al. [19] proposed the Hot Crack Susceptibility (HCS) criterion to estimate the cracking tendency. The criterion considers the local solidification time when the structure is most vulnerable to cracking, as shown below:

$$\text{HCS} = \frac{t_v}{t_R} = \frac{t_{99} - t_{90}}{t_{90} - t_{40}} \quad (1)$$

here, t_v is the vulnerable time period where the hot tearing can occur and t_R is the time available for the stress relief. t_{99} , t_{90} , t_{40} correspond to the time when the local solid fraction is 0.99, 0.9 and 0.4, respectively.

In general, they suggest that the hot tearing occurs when the solid fraction is between 0.9 and 0.99 and that the stress relaxation and after-feeding can take place at a solid fraction between 0.4 and 0.9 [16]. With specific reference to the continuous casting steels, they estimate the period for which the material will be vulnerable to cracking as a function of depth below the strand surface. To do this, they apply a micro-segregation model to describe the segregation of carbon and phosphorus and consider this to examine the influence of the δ - γ phase transformation on hot tearing sensitivity. This approach was used to predict hot tearing for continuous casting steel with varying levels of carbon [32].

Feurer's criterion [33] considers that hot tearing occurs when the liquid feeding no longer accommodates shrinkage during solidification. Two terms proposed by Feuerer are SPV and SRG. SPV is the maximum volumetric flow rate per unit volume and SRG

is the velocity of volume solidification shrinkage caused by density different between solid and liquid phase. SPV is formulated as follows:

$$SPV = \frac{f_l^2 d^2 P_s}{24\pi c^3 \eta L^2} \quad (2)$$

where f_l is the liquid volume fraction; d is the secondary dendrite arm spacing; P_s is the effective feeding pressure; L is the length of porous network; c is the tortuosity constant of dendrite network; and η is the viscosity of the liquid phase.

SRG is given by the following equation:

$$SRG = \left(\frac{\partial \ln V}{\partial t} \right) = -\frac{1}{\rho} \frac{\partial \bar{p}}{\partial t} \quad (3)$$

where V is a volume element of the solidifying mush with constant mass and t is time.

The Feurer's criterion says that hot tearing is not possible if:

$$SPV > SRG. \quad (4)$$

Based on the HCS proposed by Clyne et al. and the Feurer's criterion, Katgerman [34] proposed a new HCS, as follows:

$$HCS = \frac{t_{99} - t_{cr}}{t_{cr} - t_{40}} \quad (5)$$

where the t_{99} and t_{40} correspond to the time when the local solid fraction is 0.99 and 0.4, respectively. And the t_{cr} is the time when liquid feeding can no longer occur. The time t_{cr} is determined using Feurer's criterion when the SPV equals to the SRG.

The Katgerman's criterion along with the Feurer's criterion have been widely used to study the influence of the casting speed on the hot tearing formation in the continuous casting process [6] [16] [33] [35]. It has also been used to predict and evaluate the hot tearing susceptibility for shape casting [36].

2.2. MECHANICAL CRITERIA

2.2.1. Critical Stress Based Criteria. Typical strain rates encountered in continuous casting process have been reported to be on the order of $10^{-4}/s$ to $10^{-3}/s$ [37]. However, higher strain rates of $10^{-1}/s$ to $1/s$ were chosen by several researchers to minimize the shell growth during testing and measure the shell's fracture stress directly [38] [39]. In order to estimate the critical fracture stress, a critical stress based criterion was proposed by Y. M. Won et al. [8] also considering the influence of strain rate. To achieve this, the critical fracture stress of δ phase and γ phase for internal crack formation in the mushy zone was calculated using constitutive equations for each phase as follows:

$$\begin{aligned}\sigma_c^\delta &= \frac{\varepsilon_c^{n\delta}}{\beta_\delta} * \sin h^{-1} \left[\frac{\dot{\varepsilon}}{A_\delta} \exp \left(\frac{Q_\delta}{RT} \right) \right]^{m\delta} \\ &= \frac{\varphi^{n\delta}}{\dot{\varepsilon}^{m^* \cdot n\delta} \Delta T_B^{n^* \cdot n\delta} \beta_\delta} \cdot \sin h^{-1} \left[\frac{\dot{\varepsilon}}{A_\delta} \exp \left(\frac{Q_\delta}{RT} \right) \right]^{m\delta}\end{aligned}\quad (6)$$

$$\begin{aligned}\sigma_c^\gamma &= \frac{\varepsilon_c^{n\delta}}{\beta_\gamma} \cdot \sin h^{-1} \left[\frac{\dot{\varepsilon}}{A_\gamma} \exp \left(\frac{Q_\gamma}{RT} \right) \right]^{m\gamma} \\ &= \frac{\varphi^{n\delta}}{\dot{\varepsilon}^{m^* \cdot n\gamma} \Delta T_B^{n^* \cdot n\gamma} \beta_\gamma} \cdot \sin h^{-1} \left[\frac{\dot{\varepsilon}}{A_\gamma} \exp \left(\frac{Q_\gamma}{RT} \right) \right]^{m\gamma}\end{aligned}\quad (7)$$

here, A and β are constants; m is constant related to strain-rate sensitivity; n is the strain-hardening exponent; Q is the activation energy for deformation; and R is the gas constant. The value of A, β , m and n can be found based on the experimental measured data reported in [8].

The critical stress of steels for crack formation is predicted using equation [3], as follows:

$$\sigma_c = \left(\frac{f_s - c f_s}{1 - c f_s} \right) * [\delta f_s \sigma_c^\delta + \gamma f_s \sigma_c^\gamma] \quad \text{for } ZDT \leq T \leq ZST \quad (8)$$

The relationship between δf_s and γf_s can be determined using a microsegregation model, which takes composition and cooling conditions into consideration. σ_c is the critical stress when the solid fraction is c_s . The predicted hot tearing trends were in good agreement with the experimental results reported by [38] [40].

2.2.2. Critical Strain Based Criteria. In recent studies, it has been suggested that critical strain and/or strain rate is a better criterion for hot tearing than stress [24]. Studies on residual strain/stress have shown that tensile stress is not required to generate hot tearing but that tensile strain is required to form a hot tear. Thereby, if the true strain is higher than the critical fracture strain, hot tearing will occur [23].

A. Yamanaka et al. [41] proposed a critical fracture strain by performing experiments using a tensile test on a cylindrical ingot with liquid core. The critical strain was determined to be 1.6% by comparing the occurrence of the cracks with the applied effective strain. The effective strain was defined as the accumulated strain in the BTR. To calculate the effective strain, the movement of the BTR needs to be considered. By correlating the time-strain history and the movement of the BTR, the effective strain can be estimated.

Many researchers [42] [43] [44] have suggested that critical strain decreases with increasing strain rate and solute element content because the BTR widens. A relationship for the critical strain as a function of the BTR and strain rate has been developed by Y. M. Won et al. [8]:

$$\varepsilon_c = \frac{\phi}{\dot{\varepsilon}^{m^*} \Delta T_B^{n^*}} \quad (9)$$

where ϕ is a constant; and m^* and n^* are the strain rate sensitivity and the BTR exponent on the critical rate, respectively. The BTR (ΔT_B) has been expressed as follows:

$$\Delta T_B = \text{LIT} - \text{ZDT} = T(f_s = 0.9) - T(f_s = 0.99) \quad (10)$$

in which the LIT and ZDT correspond to the temperature at which the solid fractions are 0.9 and 0.99, respectively, which is reported by many researchers [22] [19] [20]. The BTR is calculated using a microsegregation analysis, in which incomplete solute back-diffusion, diffusion length scale, cooling rate, alloy composition, and phase transformations are considered [45].

2.2.3. Critical Strain Rate Based Criteria. In addition to critical stress and critical strain based criteria, a strain rate based criterion, the RDG criterion, has also been proposed by M. Rappaz et al. [3] and applied by different researchers [46] [47] [48]. The RDG criterion was proposed based on the maximum strain rate ($\dot{\epsilon}$) that the mushy zone can sustain before the hot tear occurs. It considers a mass balance for the liquid and solid phases and allows for calculating the pressure drop contributions in the mushy zone. This model was derived from columnar dendritic structure assuming that the tensile deformation is perpendicular to the growth direction of the dendrites. When the interdendritic liquid feeding cannot compensate for the thermal contraction and solidification shrinkage at a given strain rate, hot tearing will initiate. The maximum strain rate can be expressed as follows [46]:

$$\dot{\epsilon}_{\text{crit}} = \frac{G}{(1+\beta)B} \left[\frac{\lambda_2^2 G \Delta p_{\text{max}}}{180\mu} - v_T \beta A \right]$$

$$\text{With } A = \int_{T_c}^{T_l} \frac{(1-f_s) f_s^2}{(1-f_s)^3} dT \quad \text{and} \quad B = \int_{T_c}^{T_l} \frac{f_s^2 \left(\int_{T_c}^T f_s dT \right)}{(1-f_s)^3} dT \quad (11)$$

where μ is the dynamic viscosity of the liquid phase, G is the thermal gradient, v_T is the velocity of the isotherms, β is the solidification shrinkage factor, A and B are integrals over the temperature interval between the coalescence T_c and the liquidus temperature T_l ,

the value of the T_c varies based on alloy chemistry, morphology and precipitates. And f_s is the fraction of solid. The Δp_{\max} is the maximum pressure drop that the mushy zone can bear, which was estimated to be around 90 kPa for stainless steel in welding process [49]. The RDG criterion has been widely used and further developed in simulations of hot tear formation [46] [47].

2.2.4. Other Criteria Specifically Related to the Continuous Casting Process.

Y. M. Won et al. [50] developed a specific crack susceptibility to describe the possibility of hot tearing of the strand during continuous casting within the mold. The development of the specific crack susceptibility involves in the analysis of critical strain and a crack susceptibility coefficient. The critical strain was calculated by equation [4], as discussed previously. The crack susceptibility was expressed as follows:

$$s_c = \frac{\sigma_{\max}(T)}{\sigma_c(T)} \quad \text{for } ZDT \leq T \leq LIT$$

$$s_c = 0 \quad \text{for } LIT < T \leq T_L \text{ or } \sigma_{\max}(T) < 0 \quad (12)$$

The crack susceptibility coefficient, S_c , is defined as the instantaneous possibility of solidification cracking at a position, and the specific crack susceptibility, sS_C , was proposed as follows:

$$^sS_C = \frac{\int_{A_m} \int_0^{t_c} S_c dt dA_m}{\int_{A_s} \int_0^{t_c} dt dA_s} \quad (13)$$

here A_m is the area of mushy zone in the brittle temperature range, A_s is the area of solidified shell, t_c is the casting time. The specific crack susceptibility is reported to successfully predict the effect of carbon content, slab width, narrow face taper and casting speed on the hot tearing of continuous cast steels.

Z. Han et al. [51] proposed a critical strain based model to predict hot tearing near the solidifying front in slab casting. The tensile strains at the solidifying front caused by bulging, straightening, and misalignment of the support rollers in a four-point-unbending bow-type caster was calculated, respectively:

$$\varepsilon_B = \frac{1600S\delta_B}{l^2} \quad (14)$$

$$\varepsilon_s = 100 * \left(\frac{d}{2} - S\right) * \left|\frac{1}{R_{n-1}} - \frac{1}{R_n}\right| \quad (15)$$

$$\varepsilon_M = \frac{300S\delta_M}{l^2} \quad (16)$$

here, S is solidified shell thickness, l is roll pitch, δ_B is slab bulging deflection, d is slab thickness, R_{n-1} and R_n are the unbending radii, and δ_M is the roll misalignment. The bulging deflection is calculated by the equation [12]:

$$\delta_B = \frac{Pl^4}{32E_e S^3} \sqrt{t} \quad (17)$$

where P is the ferrostatic pressure of liquid steel, t is the time for slab to travel a roll-pitch, and E_e is the equivalent elastic modulus that can be calculated using the following equation:

$$E_e = \frac{T_s - T_m}{T_s - 100} * 10^6 \text{ N/cm}^2 \quad (18)$$

here, T_s is solidus and T_m is the average of the surface temperature and the solidus temperature. Thus, the total strain at the solidifying front was calculated by the sum of ε_B , ε_s and ε_M . When the total strain exceeds the critical strain, the hot tears will occur. Their prediction matches with the experimental results and was further developed by coupling this model with a microsegregation model [51].

3. EXPERIMENTAL METHODS

Over the years, researchers have developed many different experimental tools to investigate hot tearing. For example, the ring mold test [52] [53] [54] and several different constrained rod casting (CRC) [55] [56] tests were widely used in the investigation of the hot tearing susceptibility for aluminum alloys and magnesium alloys. Several different constrained shape castings were also used to study the hot tearing in steel casting. These testing methods employ different constraint conditions to induce stress or strain during solidification to promote the formation of hot tearing. For the continuous casting steel, as discussed in the previous section, the solidifying strand shell is always in a dynamic state and it experiences much more complicated thermomechanical conditions. Therefore, more sophisticated setups were designed to study the mechanical properties of solidifying steels and reproduce the condition of the hot tear formation in the continuous casting process. Thus, these typical testing methods used for different casting processes are discussed in this section and summarized in Table 2.

3.1. CONSTRAINED SHAPE CASTING TEST

Different constrained sand casting tests have been developed to study the hot tearing behavior in shape steel castings. One of the most widely used tests is the constrained T-shaped casting using sand mold, as shown in Figure 3. Monroe and Beckermann [57] [58] used a T section sand mold with force and displacement measurement devices to quantitatively study the hot tearing behavior of low carbon low

alloy steels. The measured force and displacement in this approach were in good agreement with their simulated force and displacement predictions, respectively.

Bhiogade et al. [24] used the constrained T-shaped casting to study the influence of the stress, strain and strain rate on the hot tearing susceptibility of a stainless steel. Their results showed that the strain or strain rate are better predictors for hot tearing than stress.

A bracket-shaped sand casting with different size of sand cores was designed by D. Galles et al. [59] to study the casting distortion. The distortion was caused by the combination of core expansion and steel contraction during solidification. The stress during the test was simulated with the commercial software ABAOUS² using a user-defined elasto-visco-plastic model and the distortion was predicted accurately in their work.

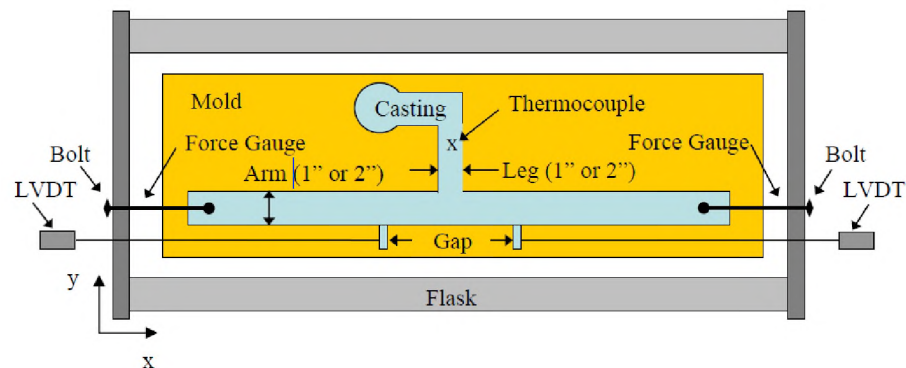


Figure 3. Schematic of the test setup using a constrained T-shaped casting [58].

In addition to sand molding processes, a permanent mold was developed by Cerri et al. [60] and was used by Hadzic et al. [61] to develop a viscoplastic damage model to predict hot tear formation in the steel casting, as shown in Figure 4. The water-cooled chills were used to ensure the directional solidification in the casting and to constrain the

ends of the casting to induce tensile stresses during solidification process. The damage model for hot tearing prediction was developed based on Cocks constitutive model using commercial software MAGMASOFT and ABAQUS. A good correlation between experimental findings and predicted damage is observed in their works [61].

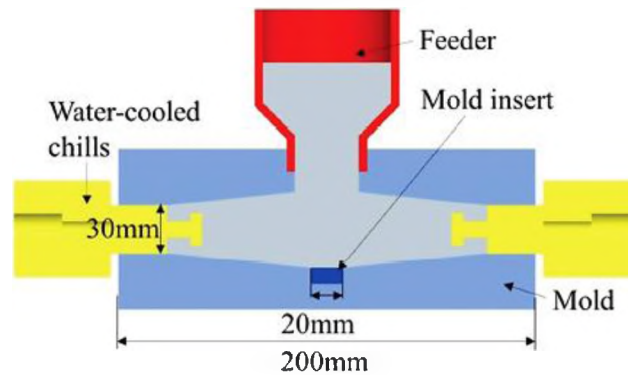


Figure 4. Schematic of the experimental setup using a permanent steel mold [61].

3.2. HOT TENSILE TESTS

As discussed in the previous section, the brittle temperature range (ΔT_B), which was defined by the temperature different between the ZST (or LIT) and ZDT, gives a qualitative indication of the hot tearing susceptibility [6] [16]. Therefore, it is of great interest to experimentally determine these critical temperature points. M. B. Santillana [22] proposed an apparatus that can be used to perform the hot tensile test at a temperature range from 1100°C to 1520°C. The schematic of this apparatus is shown in Figure 5. A high frequency induction coil was used to heat the central region of a cylindrical sample, which has a diameter of 10mm and a length of 100mm. The temperature of the molten zone was controlled by an R-type thermocouple welded to the

sample surface. A load cell and a two-color optical pyrometer were used to measure the force and temperature during the test, respectively. The sample was heated, melted and solidified sequentially under controlled conditions. The hot tensile test was conducted between the temperature range of liquidus and solidus in 10°C increments. After testing, the ZST and ZDT were determined based on post-mortem analysis of the tensile specimens.

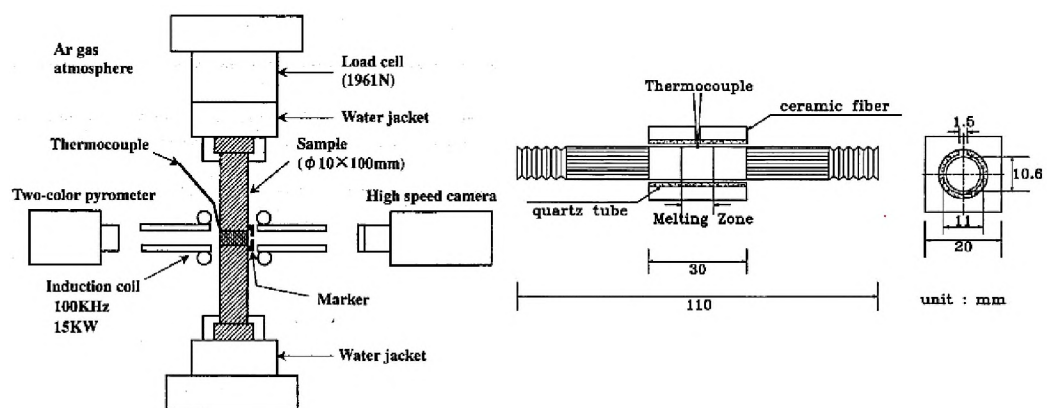


Figure 5. Schematic of the hot tensile test apparatus and specimen [22]

Similar hot tensile tests have also been performed using Gleeble™ systems to study the high temperature mechanical properties for different steel grades. D. J. Seol and his coworkers [62] have used Gleeble™ 1500 system to study the mechanical behaviors of carbon steel in the temperature range of mushy zone; Wenli et al. [63] have used Gleeble™ 3800 system to determine the ZST and ZDT for a 6.5 wt.% electrical steel. W.T. Lankford [64] has used Gleeble™ 510 to study the effects of isothermal treatments, temperature, and cooling rate on the hot ductility for low carbon steels with different amount of alloy elements. A typical thermal and deformation historical cycle of the

tensile test is shown in Figure 6. The test was performed at different temperature in the mushy zone. Thus the critical temperature points were determined by analyzing the strength and displacement under different temperatures.

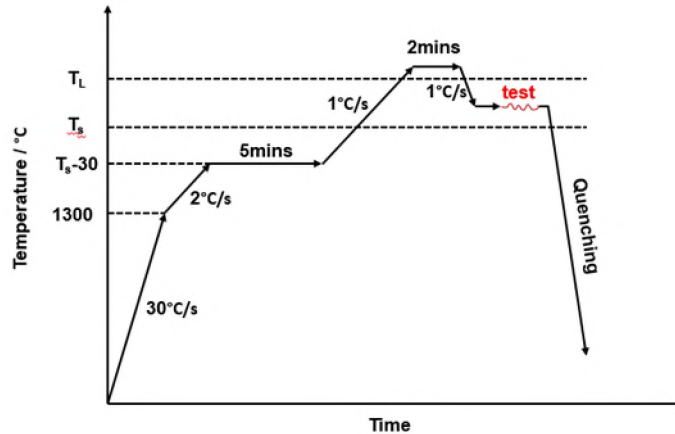


Figure 6. Schematic of thermal and deformation history for tensile test using Gleeble system.

3.3. BENDING TESTS

Bending tests were designed by several researchers to study the hot tearing phenomenon in continuous casting process [65] [66] [67] [68] to estimate the critical strain for the hot tearing formation under different conditions. Matsumiya et al. [69] used a horizontal three point bending test to investigate the critical strain for six different carbon steels. The schematic of the testing apparatus is shown in Figure 7. The specimen was 45cm long, 8cm wide and 3.5cm high that was cut off from the columnar crystal zone to ensure that the longitudinal direction of the specimen was consistent with the casting direction. The center of the top surface of the specimen was heated by a specially designed high-frequency induction heater to ensure uniform temperature distribution in

the width direction. The test was conducted at various degrees of bending. By analyzing the amount of the strain that was applied to the liquid-solid interface and comparing with the existence or nonexistence of the crack, the critical strain for the hot tearing formation was determined.

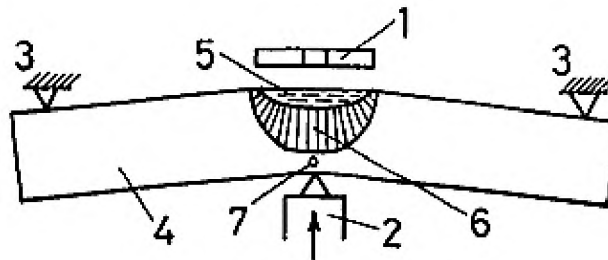


Figure 7. Schematic of the three points bending test apparatus (1-induction heating coil, 2- ram, 3-fulcra, 4-specimen being bent, 5-liquid pool, 6-mushy zone, 7-thermocouple) [69]

The horizontal three points bending test provides a quantitative way to estimate the critical strain for different grades of steel. To better compare with the continuous casting process, larger scale experiments were also proposed [70] [71]. Moreover, since the hot tearing formation in continuous casting steel also involves element segregation, more sophisticated experimental methods have been developed to study the hot tearing as well as to reveal the macrosegregation.

Koshikawa et al. [72] [73] [74] [75] proposed an ingot bending test (also called the “ingot punching test”), which consists of a tool that applies deformation at the surface of a solidifying 450 kg steel ingot. Figure 8 (a) shows the schematic of the initial state of the test apparatus that was developed at Nippon Steel & Sumitomo Metal Corporation. The molten metal was poured at 1640°C and after a certain amount of time, the top right

mold was removed. Then, a cylinder tool was used to push the solidifying ingot perpendicular to the surface of the ingot. The velocity and displacement of the punching tool were controlled by a hydraulic system and temperature was measured by thermocouple during the test. More details about the experiment procedure can be found in [74].

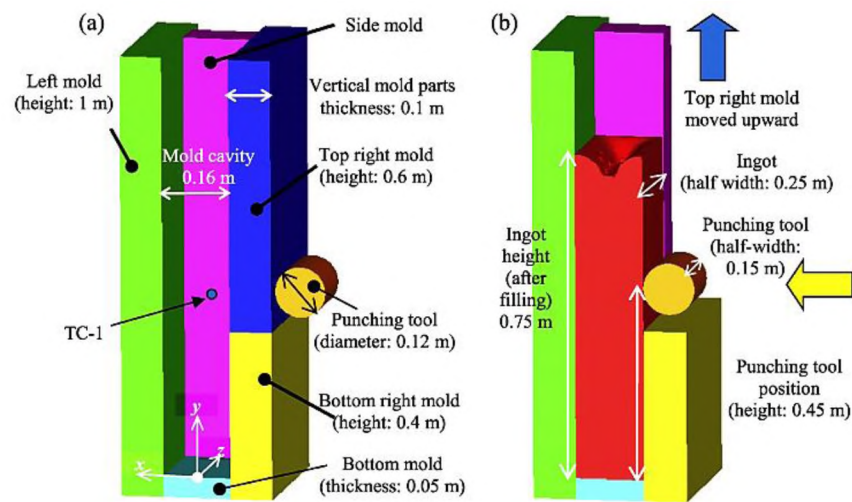


Figure 8. Schematic of ingot bending test apparatus [74].

Valuable information about the hot tearing formation and segregation is provided by the ingot bending test. Koshikawa et al. [72] [73] developed a so-called “two-phase” model, which considers the macrosegregation resulting from both the solid phase deformation and liquid flow in the mushy zone, to simulate the macrosegregation and compare with their experimental results. A finite element model was developed to analyze the thermomechanical stress/strain in the bending test [74]. Excellent agreement was found between the simulation results and the position and intensity of the hot tears obtained from the measurements.

3.4. SUBMERGED SPLIT-CHILL TENSILE (SSCT) TEST

The submerged split-chill tensile (SSCT) test, which was initially proposed by Ackermann et al. [76] to study the high temperature mechanical properties of aluminum alloys, was developed and applied by Hiebler and other researchers [38] [40] [77] [78] to study the mechanical behavior of the solidifying steel shell and investigate the relationship between the hot tearing susceptibility and process parameters encountered in the continuous casting process. Figure 9 shows a schematic of the SSCT test apparatus and the relationship of the SSCT test with continuous casting conditions. A water-cooled copper or steel test body, which can be split into two halves, was submerged into the liquid steel contained in an induction furnace. After a shell of sufficient thickness has formed around the test body, the lower part was moved downwards at a controlled velocity. The force and displacement were recorded during the test.

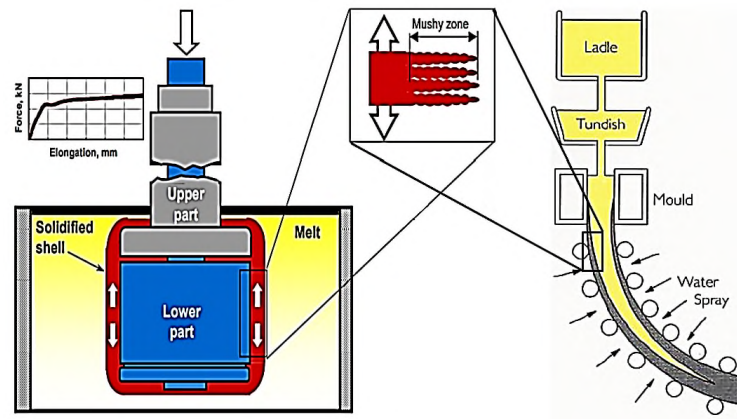


Figure 9. Schematic of the SSCT test apparatus [79]

Different experiments were carried out based on the SSCT test. Suzuki et al. [40] used the SSCT test to study the fracture strength of solidifying steel shells containing

0.004 to 0.7 wt.% C. Their test results show that the fracture strength at a very early stage of solidification of the shell thickness with a thickness of 1 to 5mm was around 1 to 3.5 MPa. After analyzing the friction force between the shell and the mold and comparing with the measured data, a reasonable upper limit of the casting speed of a caster with sinusoidally oscillating mold was suggested to be about 8.5 m/min. Bernhard et al. [38] used the SSCT test to study the effect of phosphorous content on the hot tearing susceptibility for different carbon steels. By analyzing the relationship between the P content and the shell strength and comparing with the characterizations of the solid shell, the authors observed that hot ductility decreased with an increasing P content for both high carbon and low carbon steels over a wide range of strain rates. Reiter et al. [79], Bernhard et al. [39] and Hiebler et al. [80] developed different computational models to simulate the thermomechanical behavior in SSCT test, such as temperature history, shell thickness, solidification force, and failure location to analyze the stress and strain profile in the test and determine the critical strain for hot tear formation. Due to the high cooling rate and thin solid shell during SSCT test, this method is more suitable for analysis of the cracking susceptibility of the steel shell in the mold region or early stage out of the mold.

3.5. CONTROLLED DEFORMATION TEST FOR SOLIDIFYING STEEL SHELL

In recent study, the concept of the controlled deformation test for solidifying steel shell was proposed by the Lu et al. [81], which can be used to study the mechanical properties of the steel shell in different solidification stages. The steel shell was deformed by the applied strain, which was controlled by the electric cylinder coupled with a servomotor. A special mold configuration, with two water-cooled cooper chills and an

insulation sleeve, was developed to control the dendrite growth in the direction perpendicular to the applied strain and to ensure that the strain is applied in the region of controlled shell growth. Figure 10 shows the schematic of the setup with illustration of the solidification pattern in testing area and applied strain during the test. The force, displacement and temperature were monitored as a function of time. The temperature field in the whole casting was simulated by MAGMASOFT 5.3.1.

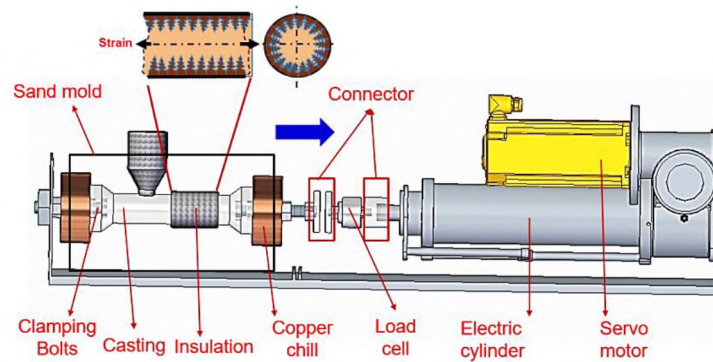


Figure 10. Schematic of the controlled deformation test apparatus.

Various experiments can be carried out using this method. The cooling rate and solidification structure in the testing area can be controlled and adjusted by the material type and thickness of the insulation sleeve. The shell thickness during the test can be controlled by the solidification time, which corresponds to the different stages during solidification process. Thus, several types of studies can be performed: solidification behavior under constrained mold design; mechanical properties of the material in a wide temperature range; critical stress/strain for the cracking formation in different stages of solidification, and so on. The numerical deformation model of the current method is also under development now and will be released soon.

Table 2. A summary of different experimental methods used for investigation of the hot tearing of steels

Experimental Methods	Application scenarios	limitations	References
Constrained shape casting test	Mostly used in mold casting, based on the severity of cracks determine hot tearing susceptibility, critical stress and/or critical strain.	Cannot control the amount of strain. Limited application in continuous casting process.	[24], [57-61]
Hot tensile test	Used to determine the critical temperature points and study the high temperature mechanical properties.	Re-melting the specimen, cannot represent the real solidification condition. Limited consideration of segregation.	[6], [16], [22], [62-64]
Bending test	Mostly used in continuous cast steel, determine the critical strain/stress. Ingot bending test has good correlation with continuous cast process.	Re-melting the specimen, cannot represent the real solidification condition. Limited application in mold casting.	[65-75]
SSCT test	Mostly used in continuous cast steel, determine the fracture strength, critical strain/stress. Good correlation with continuous casting process in the mold region or early stage out of the mold.	Limited application in mold casting and later stage out of the mold in continuous casting process. Hard to determine real strain during the test.	[38-40], [76-80]
Controlled deformation test	Can be used in mold casting and continuous cast steel, determine the amount of solidification shrinkage, fracture strength, critical strain/stress.	Limited application in mold region or early stage out of the mold region in continuous casting process. Hard to determine real strain during the test.	[81]

4. FACTORS INFLUENCING HOT TEARING

The factors that have an influence on hot tearing susceptibility have been discussed for many years. Both alloy constitution and processing parameters are influential. Wide freezing range alloys tend to promote increased hot tearing susceptibility because these alloys spend more time in a vulnerable state during solidification, where hot tearing easily occurs [6]. The existence of segregating elements widens the BTR by forming low melting point liquid films in the interdendritic region and on grain boundaries. Processing parameters, such as casting speed, primary and secondary cooling intensity, mold taper, strand bending, soft-reduction, and so on, affect hot tearing by their influence on the solid shell thickness, solidification structure, thermal and mechanical strain profile in mushy zone. Common factors that have a direct influence on the hot tearing sensitivity are summarized in this section.

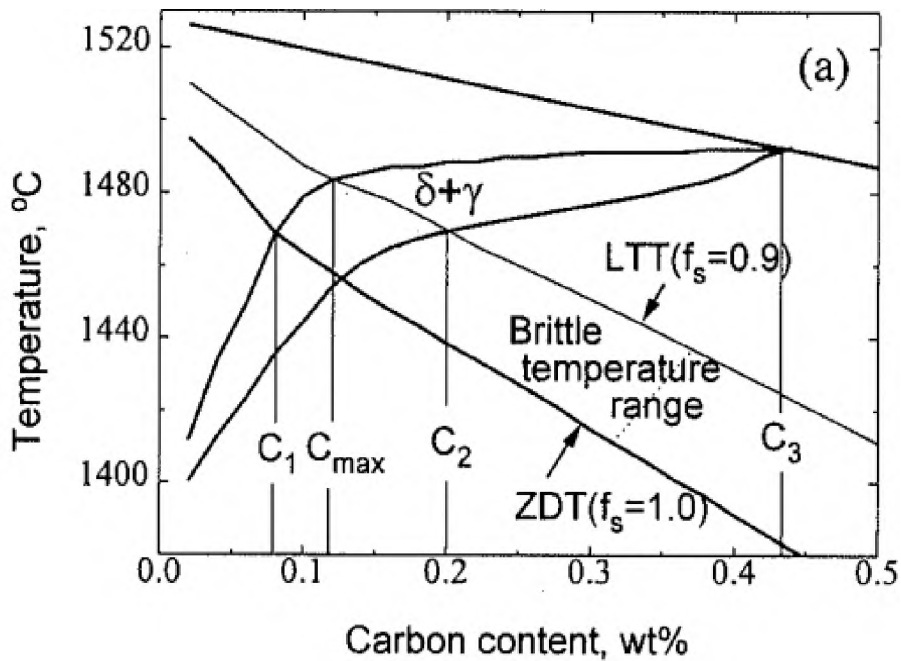
4.1. COMPOSITION

It is well established that high purity metals are not prone to hot tearing because the pure metal does not exhibit a semi-solid stage during solidification [82]. For commercial alloyed steels, different alloying elements have different influences on the hot tearing susceptibility based on their effects on the solidification process and their segregation tendency.

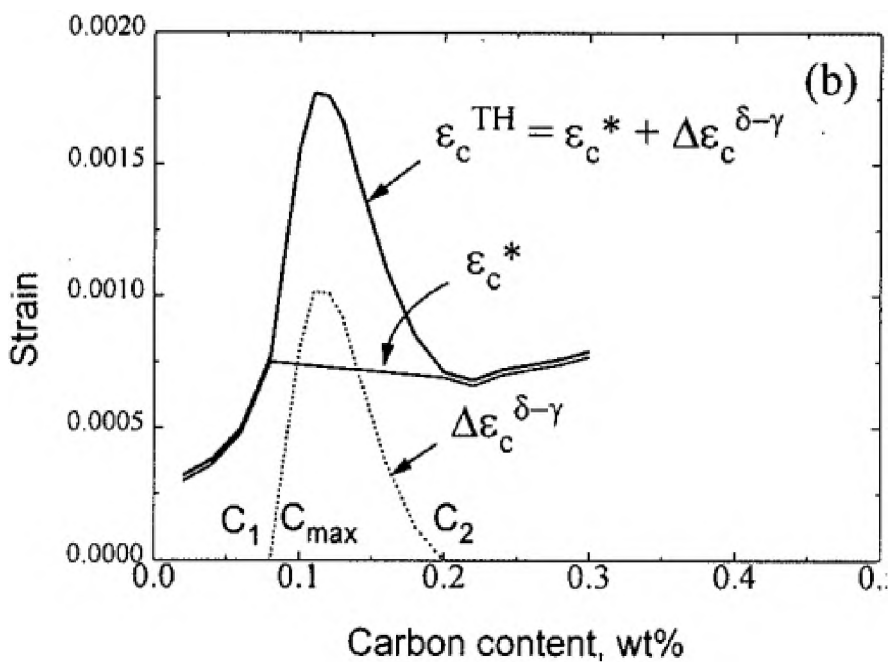
4.1.1. Carbon. Carbon is one of the most important alloying elements in steels. It affects the hot tearing susceptibility not only by changing the BTR but also through the δ - γ phase transformation. The total thermal strain of steel is generally expressed as the sum

of the strain caused by cooling and the strain caused by phase transformation [83]. Figure 11 (a) and (b) show a typical non-equilibrium binary Fe-C phase diagram of carbon steel and thermal strains as a function of carbon content, respectively. The BTR changes as a function of carbon content as shown in Figure 11 (a). For the steel with a carbon content below C_1 , the total thermal strain is only a function of temperature because solidification is already completed before the δ - γ phase transformation begins. For steels with a carbon content above C_2 , the total thermal strain is only a function of temperature because the δ - γ phase transformation finished above the LIT. For steels with a carbon content between C_1 and C_2 , the total internal strain varies by changing of the phase transformation induced strain $\epsilon_c \delta$ - γ , as shown in Figure 11 (b). Thus, there is a C_{\max} at which all the δ - γ phase transformation occurs in the BTR, which causes a maximum total internal thermal strain, or in another words, a maximum tendency to the hot tearing.

Since the BTR and δ - γ phase transformation are influenced by solute elements such as sulfur and phosphorus, the values of C_1 , C_2 and C_{\max} also vary with different steel composition. In previous studies, both experimental measurements and computational models were used to analyze the effect of carbon content on the hot tearing susceptibility for different grades of steel. Won et al. [50] have investigated the steels with the compositions of (0.05–0.6)C–0.03Si–0.4Mn–0.02P–0.02S. The relationship between the crack susceptibility and the carbon content is shown in Figure 12. Based on their work, the maximum hot tearing tendency appears at a carbon content of 0.12%, which is consistent with Kim's [83] results.



(a)



(b)

Figure 11. (a) Typical non-equilibrium binary Fe-C phase diagram of carbon steel and (b) total thermal strain (ϵ_c^{TH}), strain caused by cooling (ϵ_c^*) and strain caused by phase transformation ($\epsilon_c^{\delta-\gamma}$) as a function of carbon content [83].

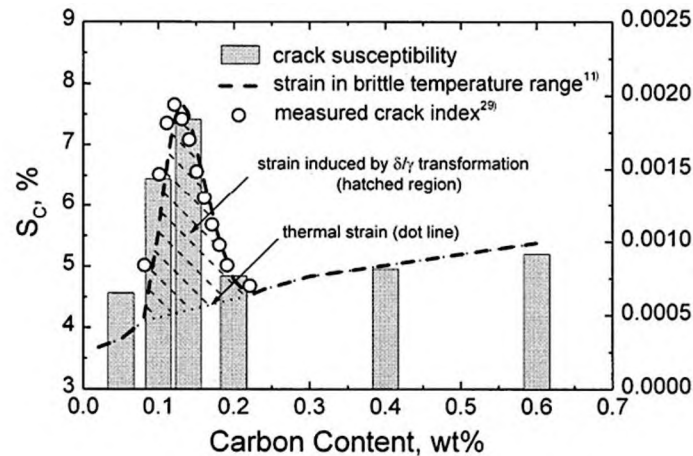


Figure 12. The calculated crack susceptibility (S_c), strain in brittle temperature range and measured crack index as a function of carbon content [50].

For steels with a medium or high carbon content, the relationship of hot tearing susceptibility and the carbon content was given by K. Wunnenberg and R. Flender [84]. They used a crack index to reflect steel's susceptibility to hot tearing. The crack index was developed to combine individual parameters measured on microsections, including crack length, crack opening, spacing between adjoining cracks, and number of cracks. A high index means that the steel is more vulnerable to the hot tearing. This study was performed using steels containing (0.09-1.16)C-(1.5-1.6)Mn-0.025S. Between 0.2 and 0.35% carbon, the crack index is reduced. For steels over 0.4% carbon, the susceptibility increases rapidly to a maximum at 0.86% and at 1.16%C, the susceptibility to cracking drops again, and is equivalent to a 0.6%C steel.

Additional studies on the effects of carbon on the hot tearing susceptibility were also performed by many researchers [13] [19] [64] [85]. However, it is difficult to quantitatively analyze the effects of carbon on cracking in isolation because of the interactions among other alloying elements in these studies.

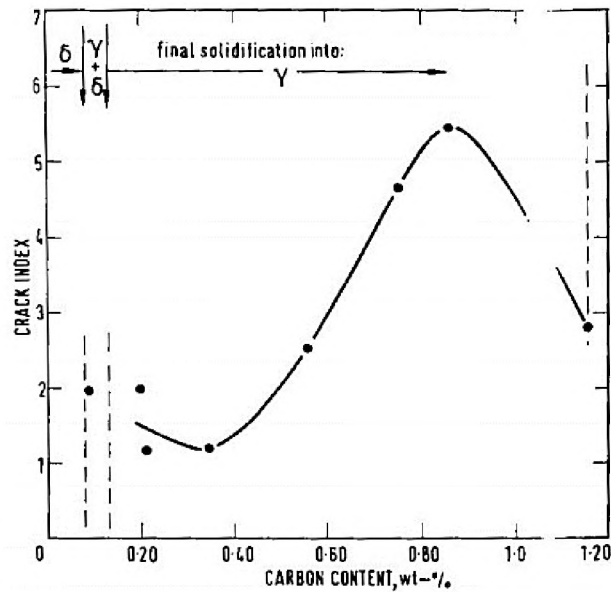


Figure 13. Crack index as a function of carbon content [84].

4.1.2. Sulfur and Mn/S Ratio. Sulfur has been shown to have a significant influence on hot tearing in many studies. It is well established that sulfur will increase the hot tearing vulnerability of steels by forming a low melting point liquid films in the interdendritic region or on grain boundaries. With its low partition ratio, sulfur has a very strong tendency to segregate during solidification, which will lower the non-equilibrium solidus temperature where the last solidified liquid phase [86] is present. As a result, even when the temperature of the bulk alloy drops below the equilibrium solidus temperature, there can still be a liquid film that exists interdendritically and along the grain boundaries. As a result, the segregation of sulfur widens the BTR and creates a path for hot tear formation [22] [21] [83] [87]. A. Chojecki et al. [88] studied the influence of sulfur content on the BTR for different carbon steels, as shown in Figure 14. Even small amounts of sulfur significantly increases the BTR [89].

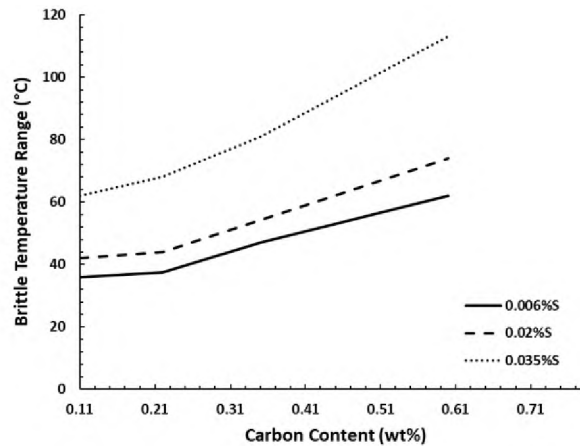


Figure 14. The influence of sulfur content on the BTR for different carbon steels [88].

As solidification takes place, the existence of sulfur will result in the formation of either MnS or FeS. When the local interdendritic concentration of Mn and S in the residual liquid is higher than the solubility product constant of MnS, it will begin to precipitate [90]. The formation of MnS or FeS is determined by the relative concentration of Mn and S. Under equilibrium conditions, MnS is generally more stable than FeS. During solidification, however, sulfur is expected to segregate strongly to inter-dendritic region due to its low partition ratio. If the content of sulfur is much higher than Mn, or there is residual segregated sulfur in liquid unreacted with Mn, FeS will form. The formation of pure FeS will dramatically decrease the solidification temperature of the interdendritic liquid because the FeS has a low melting point of approximately 1200 °C [22].

Many investigators [13] [84] [64] [90] [41] [91] have demonstrated that there is a critical value of the Mn/S ratio below which a high susceptibility to cracking is expected. Alvarez de Toledo et al. [90] developed a critical value of Mn/S based on literature data and their results from rolling continuous cast billets, which they expressed as:

$$(\text{Mn/S})_c = 1.345 * \text{S}^{-0.7934} \quad (18)$$

A reasonable agreement between the experimental data and their theoretically equation was observed. Steel grades with high Mn/S ratio, or more specifically higher Mn, are not as prone to the hot tearing as steels with a low Mn/S ratio.

4.1.3. Phosphorus. Compared with carbon and sulfur, less research has been reported that studies the influences of phosphorus on the hot tearing. Phosphorus is generally deleterious to steel ductility, but it is employed in some alloys to strengthen steels where carbon content is restricted. However, phosphorus not only affects hot tearing tendency, but also can lead to cold work embrittlement [92]. To ensure the product quality, the amount of phosphorus in steels is normally minimized. The segregation tendency of phosphorus to the grain boundaries is weak compared with that of sulfur [93]. According to F. Weinberg [94], under equilibrium conditions, P is enriched in γ and δ iron by a factor between 10^2 and 10^3 on a monolayer at the grain boundary, and S by a factor of 10^4 . However, it is still possible that the incipient melting may occur at grain boundaries due to the segregation of phosphorus.

Several studies [8] [19] [64] [87] [89] have been conducted to theoretically or experimentally study the influence of the phosphorus on the hot tearing. W. Wang et al. [89] used a coupled macro-heat transfer and micro-segregation model to investigate the effect of phosphorus on crack susceptibility. Their results show that, for hypo-peritectic steels, increasing phosphorus widens the BTR. The study showed that both the thermal strain and the difference in deformation energy will increase. The effects of the observed difference in deformation energy is demonstrated and discussed in [8]. Qualitatively, the deformation energy change influences the possibility of cracking in the BTR. Thus, hypo-

peritectic steel is more sensitive to cracking than other steels. A similar conclusion was obtained in Young Mok Won's work [8], in which the steel with a higher phosphorus content tended to crack at a lower strain. This tendency was observed in steels over a wide carbon range, as shown in Figure 15.

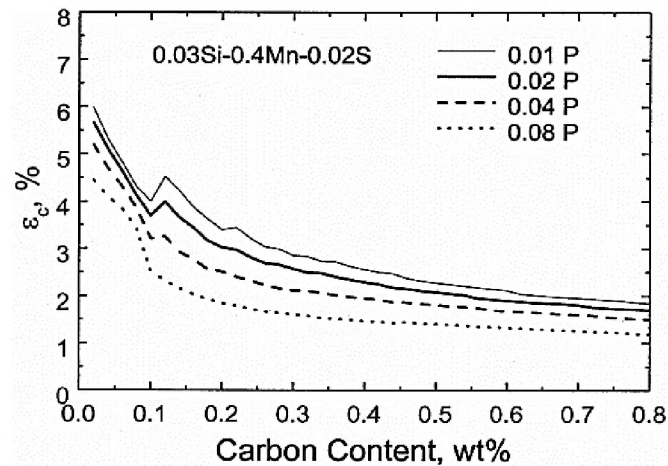


Figure 15. Influence of the phosphorus content on the critical strain [8]. When the accumulated strain exceeds the critical strain, the hot tearing will occur.

4.2. SOLIDIFICATION STRUCTURE

The hot tearing susceptibility of steel is influenced by both the grain morphology and the grain size. Due to the change of the grain morphology and size, the liquid feeding ability, amount of strain and strain rate, the propagation paths of hot tears will also change. Y. Li [95] highlighted the impact of grain morphology on the liquid permeability in the mushy zone in Figure 16, which further influences the liquid feeding ability. Lower liquid permeability at the late stage of solidification will cause the incomplete feeding, thus increase the hot tearing tendency.

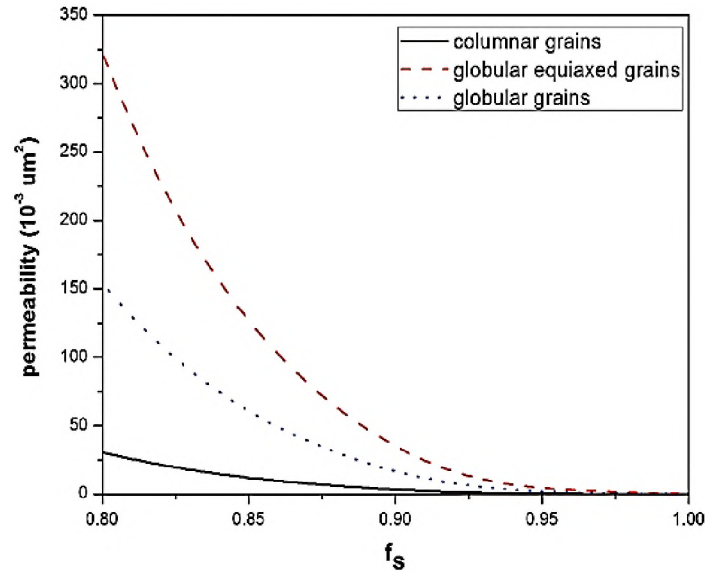


Figure 16. The liquid permeability in the mushy zone with different grain morphologies [95].

H. Fujii et al. [96] studied the influence of the solidification structure on the hot tearing formation by comparing the hot cracks formed in two different steels with different structures. One steel was Al-Si killed and another one was low C-Al killed. These two steels were cast on a bow-type casting machine. The Al-Si killed steel contained different grain structures on the inner-radius side and outer-radius side of the slab: the outer-radius side being an equiaxed structure (due to equiaxed grain settling) and the inner-radius side being a columnar structure. The low C-Al killed steel exhibited a fully columnar structure on both sides. The internal cracks were revealed by the sulfur print technique, as shown in Figure 17. By comparing the hot tear formation during the casting for the two steels, the author suggested that the columnar cast structure was more susceptible to hot tearing compared with equiaxed cast structure.

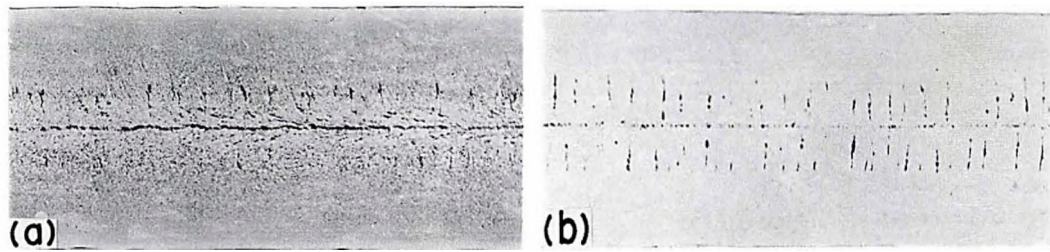


Figure 17. Solidification structure and internal cracks for (a) Al-Si killed steel and (b) low C-Al killed steel, revealed by sulfur print [96].

An investigation on the influence of the grain size on the hot tearing susceptibility was performed by Shinozaki et al. [97]. They carried out experiments to study the critical strain for a 347 stainless steel in the liquidus-solidus temperature range. The columnar grain size of the specimen varies from 69 to 210 μm . Figure 18 shows their measured critical strain values for different grain sizes and temperatures. In general, the larger grain sizes exhibited a lower critical strain at all temperatures. A similar conclusion was reached in a study of different Al alloys by Y. Yoshida [98] and F. Matsuda [99].

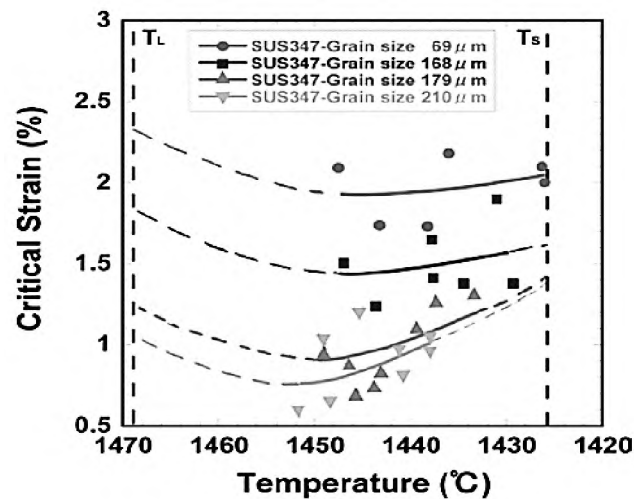


Figure 18. Critical strain with different grain sizes at different temperatures [97].

4.3. STRESS, STRAIN AND STRAIN RATE

It is well known that stress and/or strain is required for the formation of the hot tears. In the continuous casting process, the stress or strain can originate from mold friction, thermal stress, ferrostatic pressure, gravity forces from the weight of the casting, bending and straightening, and other mechanically induced forces resulting from operating irregularities, such as misalignment between successive support rolls or mold distortion [64]. Some researchers [17] [100] [101] have suggested that hot tearing occurs in the mushy zone when the maximum principle stress exceeds the local yield stress at temperature, while other researchers [102] [29] suggest that the material will crack if the local strain exceeds a critical value. However, Won et al. [50] stated that neither the absolute stress nor strain value is enough to predict the possibility of cracking during continuous casting process because the stress and strain in the solidifying shell both change as a function of temperature and movement of the semi-solid region. Moreover, in the continuous casting process, a large portion of the mushy zone solidifies in a stress-free state due to the existence of liquid. Thus, efforts in their investigation were focused on the influence of both strain and strain rate on hot tearing susceptibility.

To explore the combined effects of strain and strain rate on the hot tearing susceptibility, both theoretical studies and experimental measurement have been carried out. Some researchers [50] [102] [103] found that the critical strain for internal cracking is independent of strain rate, while others have reported contradicting results [64] [87] [42] [43]. An informative interpretation on how to determine the critical value of strain that can lead to the hot tearing was given by A. Yamanaka et al. [41]. They defined an effective strain, which is defined as the accumulated strain that occurs in the BTR. For

different strain rates, especially under the conditions with low strain rate and high cooling rate, the movement of mushy zone is large during the deformation. When the effective strain at the solid shell exceeded the critical strain, hot tearing occurs. The effective strain that accumulated in the solid shell depends on not only the strain rate, but also the BTR. Currently, the combined effects of these many different influencing factors make it difficult to select a single model to describe the hot tearing susceptibility that is valid for a broad range of alloys and process conditions.

5. CONCLUSION

In this review, the basic mechanisms and factors influencing the hot tearing phenomenon have been reviewed and discussed, and hot tearing criteria and the experimental methods used for investigating the hot tearing of steels have been summarized. From these analyses, it is clear that hot tearing can be alleviated by minimizing the tensile stress and/or strain during the casting process, increasing the high temperature strength and ductility of the alloy, and/or by narrowing the BTR of the solidifying steel. To predict hot tearing behavior under different conditions, a more reliable predictive model or criterion that can relate these requirements to casting parameters is still needed. Moreover, although various experimental methods have been developed to study the high temperature mechanical properties and evaluating the hot tearing susceptibility for different steels, in order to obtain comparable hot tearing susceptibility, a standardized hot tearing testing approach and evaluation system still needs to be established.

ACKNOWLEDGEMENT

The authors would like to thank Dr. Simon N. Lekakh for his technical advice and contribution within this manuscript. The present work is supported by Peaslee Steel Manufacturing Research Center (PSMRC) at Missouri University of Science and Technology (Missouri S&T). All the faculties and industry mentoring committee of PSMRC are greatly acknowledged.

REFERENCES

- [1] J. Campbell, *Casting*, Oxford, United Kingdom: Butterworth-Heinemann, 1991.
- [2] J. Guo and G. Wen, "Influence of Alloy Elements on Cracking in the Steel Ingot during Its Solidification," *Metals*, vol. 9, no. 8, p. 836, 2019.
- [3] M. Rappaz, J. - M. Drezet, and M. Gremaud , "A New Hot-Tearing Criterion," *METALLURGICAL AND MATERIALS TRANSACTIONS A*, vol. 30A, pp. 449-455, 1999.
- [4] H.F. Bishop, C.G. Ackerlind, and W.S. Pellini, *AFS Trans.* , vol. 60, pp. 818-833, 1952.
- [5] W. Pellini, *Foundry*, vol. 80, pp. 124-133 and 192-199, 1952.
- [6] D.G. ESKIN and L. KATGERMAN, "A Quest for a New Hot Tearing Criterion," *METALLURGICAL AND MATERIALS TRANSACTIONS A*, vol. 38A, pp. 1511-1519, 2007.
- [7] M. O. El_Bealy, "On the Formation of Macrosegregation and Interdendritic Cracks during Dendritic Solidification of Continuous Casting of Steel," *METALLURGICAL AND MATERIALS TRANSACTIONS B*, vol. 45B, pp. 988-1017, 2014.

- [8] Y. M. WON, T.-J. YEO, D. J. SEOL, and K. H. OH, "A New Criterion for Internal Crack Formation in Continuously Cast Steels," *METALLURGICAL AND MATERIALS TRANSACTIONS B*, vol. 31B, pp. 779-794, 2000.
- [9] J. K. Brimacombe, F. Weinberg and E. B. Hawbolt , "Formation of longitudinal, midface cracks in continuously-cast slabs," *Met. Trans. B*, vol. 10, pp. 279-292, 1979.
- [10] K. Miyazawa, K. Schwerdtfeger, "Macrosegregation in continuously cast steel slabs: preliminary theoretical investigation on the effect of steady state bulging," *Steel Research Int.*, vol. 52, no. 11, pp. 415-422, 1981.
- [11] A Grill, K Schwerdtfeger, "Finite-element analysis of bulging produced by creep in continuously cast steel slabs," *Ironmaking Steelmaking*, vol. 6, pp. 131-135, 1979.
- [12] G. Van Drunen, J. K. Brimacombe, and F. Weinberg, "Internal cracks in strand-cast billets," *Ironmaking and Steelmaking*, vol. 2, pp. 125-133, 1975.
- [13] J. K. Brimacombe and K. Sorimachi , "Crack formation in the continuous casting of steel," *Metallurgical Transactions B*, vol. 8, p. 489-505, 1977.
- [14] E. B. Hawbolt, F. Weinberg and J. K. Brimacombe , "Influence of hot working on internal cracks in continuously-cast steel billets," *Metallurgical Transactions B* , vol. 10, pp. 229-236, 1979.
- [15] H. K., *On the hot crack formationh during solidification of iron-base alloys*, Stockholm, Sweden: PhD thesis, Royal Institute of Technology, 2001.
- [16] D.G. Eskin, Suyitno, L. Katgerman, "Mechanical properties in the semi-solid state and hot tearing of aluminium alloys," *Progress in Materials Science*, vol. 49, pp. 629-711, 2004.
- [17] K. Kim, H. N. Han, T. Yeo, Y. Lee, K. H. Oh, and D. N. Lee, "Analysis of surface and internal cracks in continuously cast beam blank," *Ironmaking and Steelmaking*, vol. 24, no. 3, pp. 249-256, 1997.
- [18] W. Wang, L. Ning, R. Bulte, and W. Bleck, "Formation of internal cracks in steel billets during soft reduction," *Journal of University of Science and Technology Beijing*, vol. 15, no. 2, pp. 114-119, 2008.
- [19] T.W. CLYNE, M. WOLF, and W. KURZ, "The Effect of Melt Composition on Solidification Cracking of Steel, with Particular Reference to Continuous Casting," *Met. Trans. B*, vol. 13B, pp. 259-266, June 1982.

- [20] Young Mok WON, K -hyun KIM. Tae-jung YEO and Kyu Hwan OH, "Effect of Cooling Rate on ZST. LIT and ZDT of Carbon Steels Near Melting Point," *ISIJ Int.*, vol. 38, no. 10, pp. 1093-1099, 1998.
- [21] J.-M. Drezet, M. Gremaud, R. Graf, and M. Gäumann, "A new hot tearing criterion for steel," in *4th ECCO*, Birmingham, UK, 2002.
- [22] M. B. Santillana, "Thermo-mechanical properties and cracking during solidification of thin slab cast steel," *Tata Steel Nederland Technology B. V.*, 2013.
- [23] Jiangfeng Song, Fusheng Pan, Bin Jiang, Andrej Atrens, Ming-Xing Zhang, Yun Lu, "A review on hot tearing of magnesium alloys," *Journal of Magnesium and Alloys*, vol. 4, pp. 151-172, 2016.
- [24] D. S. Bhiogaed, S. M. Randiwe and A. M. Kuthe, "Failure analysis and hot tearing susceptibility of stainless steel CF3M," *International Journal of Metalcasting*, vol. 13, no. 1, pp. 166-179, 2019.
- [25] H. Zhong, X. Li, B. Wang, T. Wu, Y. Zhang, B. Liu and Q. Zhai, "Hot Tearing of 9Cr3Co3W Heat-Resistant Steel during Solidification," *Metals*, vol. 9, no. 25, 2019.
- [26] C.H. Dickhaus, L. Ohm, and S. Engler, "Mechanical properties of solidifying shells of aluminum alloys," *Trans. Am. Foundrymen's Soc.*, vol. 101, pp. 677-684, 1993.
- [27] J. Langlais and J.E. Gruzleski, "A Novel Approach to Assessing the Hot Tearing Susceptibility of Aluminium Alloys," *Materials Science Forum*, Vols. 331-337, pp. 167-172, 2000.
- [28] D. J. LahaieM. Bouchard, "Physical modeling of the deformation mechanisms of semisolid bodies and a mechanical criterion for hot tearing," *Metallurgical and Materials Transactions B*, vol. 32, no. 4, pp. 697-705, 2001.
- [29] A. Yamanaka, K. Nakajima, and K. Okamura, "Critical strain for internal crack formation in continuous casting," *Ironmaking and Steelmaking*, vol. 22, no. 6, pp. 508-512, 1995.
- [30] B. Magnin, L. Maenner, L. Katgerman, and S. Engler, "Ductility and Rheology of an Al-4.5% Cu Alloy from Room Temperature to Coherency Temperature," *Materials Science Forum*, Vols. 217-222, pp. 1209-1214, 1996.

- [31] M. RAPPAZ, J.-M. DREZET, and M. GREMAUD, "A New Hot-Tearing Criterion," *METALLURGICAL AND MATERIALS TRANSACTIONS A*, vol. 30A, pp. 449-455, 1999.
- [32] T. Senda, F. Matsuda, G. Takano, K. Watanabe, T. Kobayashi, and T. Matsuzaka, "Fundamental Investigations on Solidification Crack Susceptibility for Weld Metals with Trans-Varestraint Test," *Trans. Jap. Weld. Soc.*, vol. 2, pp. 45-66, 1971.
- [33] SUYITNO, W.H. KOOL, and L. KATGERMAN, "Hot Tearing Criteria Evaluation for Direct-Chill Casting of an Al-4.5 Pct Cu Alloy," *METALLURGICAL AND MATERIALS TRANSACTIONS A*, vol. 36A, pp. 1537-1546, 2005.
- [34] L. Katgerman, "A mathematical model for hot cracking of aluminum alloys during DC casting," *JOM*, vol. 34, no. 2, pp. 46-49, 1982.
- [35] SUYITNO, W.H. KOOL, and L. KATGERMAN, "Integrated Approach for Prediction of Hot Tearing," *METALLURGICAL AND MATERIALS TRANSACTIONS A*, vol. 40A, pp. 2388-2400, 2009.
- [36] M. R. Nasresfahani and B. Niroumand, "A New Criterion for Prediction of Hot Tearing Susceptibility of Cast Alloys," *METALLURGICAL AND MATERIALS TRANSACTIONS A*, vol. 45A, pp. 3699-3702, 2014.
- [37] M. WOLF AND W. KURZ, "The Effect of Carbon Content on Solidification of Steel in the Continuous Casting Mold," *METALLURGICAL TRANSACTIONS B*, vol. 12B, pp. 85-93, 1981.
- [38] C. Bernhard, H. Hiebler and M. M. Wolf, "Simulation of Shell Strength properties by the SSCT Test," *ISIJ Int.*, vol. 36, pp. S163-S466, 1996.
- [39] C. Bernhard, R. Pierer, A. Tubikanec, C.M. Chimani, "Experimental Characterization of Crack Sensitivity under Continuous Casting Conditions," *Materials Science*, no. 06.03, 2004.
- [40] Mikio SUZUKI, Makoto SUZUKI, Chonghee YU and Toshihiko EMI, "In-Situ Measurement of Fracture Strength of Solidifying Steel Shells to Predict Upper Limit of Casting Speed in Continuous caster with Oscillating Mold," *ISIJ Int.*, vol. 37, no. 4, pp. 375-382, 1997.
- [41] A. Yamanaka, K. Nakajima, K. Yasumoto, H. Kawashima, K. Nakai, "New Evaluation of Critical Strain for Internal Crack Formation in Continuous Casting," *Rev. Metall., Cah. Inf. Tech. (France)*, vol. 89, no. 7-8, pp. 627-633, 1992.

- [42] M. Suzuki, H. Hayashi, H. Shibata, T. Emi and In-Jae Lee, "Simulation of transverse crack formation on continuously cast peritectic medium carbon steel slabs," *Steel Research*, vol. 70, no. 10, pp. 412-419, 1999.
- [43] R. Flesch and W. Bleck, "Crack susceptibility of medium and high alloyed tool steels under continuous casting conditions," *Steel research*, vol. 69, no. 7, pp. 292-299, 1998.
- [44] K Marukawa, M Kawasaki, T Kimura, S Ishikawa , "Investigate of the criterion of the internal cracks," *Tetsu to Hagane*, vol. 64, p. S661, 1978.
- [45] YOUNG-MOK WON and BRIAN G. THOMAS, "Simple Model of Microsegregation during Solidification of Steels," *METALLURGICAL AND MATERIALS TRANSACTIONS A*, vol. 32A, pp. 1755-1767, 2001.
- [46] B. BO"TTGER, M. APEL, B. SANTILLANA, and D.G. ESKI, "Relationship Between Solidification Microstructure and Hot Cracking Susceptibility for Continuous Casting of Low-Carbon and High-Strength Low-Alloyed Steels: A Phase-Field Study," *METALLURGICAL AND MATERIALS TRANSACTIONS A*, vol. 44A, pp. 3765-3777, 2013.
- [47] R. Pierer, C. Bernhard, C. Chimani, "A contribution to hot tearing in the continuous casting process," in *Proc. of 2006 ATS Int. Steelmaking Conf.*, Paris, 2006.
- [48] M. R. RIDOLFI, S. FRASCHETTI, A. D. VITO and L. A. FERRO, "Mathematical Modeling of Hot Tearing in the Solidification of Continuously Cast Round Billets," *METALLURGICAL AND MATERIALS TRANSACTIONS B*, vol. 41B , pp. 1293-1309, 2010.
- [49] M. Bellet, G. Qiu, J. Carpreau, "Comparison of two hot tearing criteria in numerical modelling of arc welding of stainless steel AISI 321," *Journal of Materials Processing Technology*, vol. 230, pp. 143-152, 2016.
- [50] Y. M. Wong, H. N. Han, T Yeo and K. H. OH, "Analysis of solidification cracking using the specific crack susceptibility," *ISIJ International*, vol. 40, no. 2, pp. 129-136, 2000.
- [51] Z. HAN, K. CAI and B. LIU, "Prediction and Analysis on Formation of Internal Cracks in Continuously Cast Slabs by Mathematical Models," *ISIJ Int.* , vol. 41, no. 12, pp. 1473-1480, 2001.

- [52] I. I. Novikov, O. E. Grushko, "Hot cracking susceptibility of Al–Cu–Li and Al–Cu–Li–Mn alloys," *Materials Science and Technology*, vol. 11, no. 9, pp. 926-932, 1995.
- [53] Drezet, J. M., Rappaz, M., "Study of hot tearing in aluminum alloys using the ring mold test," in *Modeling of Casting, Welding, and Advanced Solidification Process-XIII*, San Antonio, 1998.
- [54] Yeshuang Wang, Qudong Wang, Guohua Wu, Yanping Zhu, Wenjiang Ding, "Hot-tearing susceptibility of Mg-9Al-xZn alloy," *Materials Letters*, vol. 57, pp. 929-934, 2002.
- [55] G. Gao, S. Kou, "Hot cracking of binary Mg-Al alloy casting," *Materials Science and Engineering A*, vol. 417, pp. 230-238, 2006.
- [56] Shuangshou Li, Bin Tang, Xinyan Jin, Daben Zeng, "An investigation on hot-cracking mechanism of Sr addition into Mg-6Al-0.5Mn alloy," *J Mater Sci.*, vol. 47, pp. 2000-2004, 2012.
- [57] C. Monroe, C. Beckermann, "Simulation of hot tearing and distortion during casting of steel: comparison with experiments," in *60th SFSA Technical and Operating Conf.*, Chicago, IL, 2006.
- [58] C.A. Monroe, C. Beckermann, J. Klinkhammer, "SIMULATION OF DEFORMATION AND HOT TEAR FORMATION USING A VISCO-PLASTIC MODEL WITH DAMAGE," in *Modeling of Casting, Welding, and Advanced Solidification Process - XII*, 2009.
- [59] D. Galles and C. Beckermann, "Measurement and Simulation of Distortion of a Steel Bracket Casting," in *Proceedings of the 66th SFSA Technical and Operating Conference*, Chicago, 2012.
- [60] O., Chastel, Y., Ballet, M, "Hot Tearing in Steels During Solidification: Experimental Characterization and Thermomechanical Modeling," *J. of Eng. Mat. Techn.*, vol. 130, pp. 1-7, 2008.
- [61] S. HADŽIĆ*, E. SCHMIDTNE KELITY, C. SOMMITSCH, "PREDICTION AND VALIDATION OF HOT TEARING IN PERMANENT MOLD STEEL CASTING USING A VISCOPLASTIC DAMAGE MODEL," *COMPUTER METHODS IN MATERIALS SCIENCE*, vol. 13, no. 1, pp. 36-42, 2013.
- [62] Dong Jin SEOL, Young Mok WON, Kyu Hwan OH, Yong Chang SHIN and Chang Hee YIM, "Mechanical Behavior of Carbon Steels in the Temperature Range of Mushy Zone," *ISIJ International*, vol. 40, no. 4, pp. 356-363, 2000.

- [63] Wenli Hu, Yuanxiang Zhang, Guo Yuan, Xiaoming Zhang, and Guodong Wang, "Hot Temperature Mechanical Behavior of High-Permeability 6.5 wt% Si Electrical Steel in a Mushy Zone," *steel research int.*, 2019.
- [64] J. R. ... W.T. LANKFORD, "Some Considerations of Strength and Ductility in the Continuous-Casting Process," *METALLURGICAL TRANSACTIONS*, vol. 3, pp. 1331-1357, 1972 .
- [65] H Sato, T Kitagawa, K Murakami and K Kawawa , " Effect of the local shrinkage to the internal cracks in strand," *Tetsu to Hagane*, vol. 61, p. S471, 1975.
- [66] K Miyamura, K Kanamaru, N Kaneko, A Ochi, "Effects of the internal cracks," *Tetsu to Hagane*, vol. 62, p. S482, 1976.
- [67] K Narita, T Mori, K Ayata, J Miyazaki, M Fujimaki, "Determination of the temperature distribution in continuous casting process," *Tetsu-to-Hagané*, vol. 64, p. S152, 1978.
- [68] H Sato, T Kitagawa, K Murakami, T Kawawa, " Effect of the local shrinkage to the internal cracks in strand," *Tetsu to Hagane*, vol. 61, p. S471, 1975.
- [69] T. Matsumiya, M. Ito, H. Kajioka, S. Yamaguchi and Y. Nakamura, "An Evaluation of Critical Strain for Internal Crack Formation in Continuously Cast Slabs," *Iron Steel Inst. Jpn. Int.*, vol. 26, pp. 540-546, 1986.
- [70] M. BELLET, O. CERRI, M. BOBADILLA, and Y. CHASTEL, "Modeling Hot Tearing during Solidification of Steels: Assessment and Improvement of Macroscopic Criteria through the Analysis of Two Experimental Tests," *METALLURGICAL AND MATERIALS TRANSACTIONS A*, vol. 40A, pp. 2705-2717, 2009.
- [71] C. Olivier, C. Yvan, B. Michel, "Hot Tearing in Steels During Solidification: Experimental Characterization and Thermomechanical Modeling," *Journal of Engineering Materials and Technology*, vol. 130, 2008.
- [72] T Koshikawa, M Bellet, C-A Gandin, H Yamamura, and M Bobadilla, "Experimental study and two-phase numerical modeling of macrosegregation induced by solid deformation during punch pressing of solidifying steel ingots," *Acta Materialia*, vol. 124, pp. 513-527, 2017.
- [73] T Koshikawa, M Bellet, C-A Gandin, H Yamamura, and M Bobadilla, "Study of hot tearing through ingot bending test: thermomechanical and solute transport analysis," in *Czech metallurgical Society*, Ostrava, 2013.

- [74] T Koshikawa, M Bellet, C A Gandin, H Yamamura and M Bobadilla, "Study of hot tearing and macrosegregation through ingot bending test and its numerical simulation," in *IOP Conf. Ser.: Mater. Sci. Eng.*, 2015.
- [75] T Koshikawa, M Bellet, C-A Gandin, H Yamamura, and M Bobadilla, "Study of hot tearing during steel solidification through ingot punching test and its numerical simulation," *Metallurgical and Materials Transactions A*, vol. 47, pp. 4053-4067, 2016.
- [76] P. Ackermann, W. Kurz, W. Heinemann, "In Situ tensile testing of solidifying aluminium and Al-Mg shells," *Mater. Sci. Eng.*, vol. 75, no. 1-2, pp. 79-86, 1985.
- [77] H. Hiebler and C. Bernhard, "Mechanical properties and crack susceptibility of steel during solidification," *Steel Research*, vol. 70, no. 8+9, pp. 349-355, 1999.
- [78] X. Ruan, P. Robert, C. Shi, F. Mei, "Experimental research on hot-tearing crack sensitivity," *Baosteel Technical Research*, vol. 6, no. 3, pp. 18-23, 2012.
- [79] J. Reiter, R. Pierer, "Thermo-mechanical simulation of a laboratory test to determine mechanical properties of steel near the solidus temperature," in *COMSOL*, Burlington, 2005.
- [80] M. ROWAN, B. G. THOMAS, R. PIERER, and C. BERNHARD, "Measuring Mechanical Behavior of Steel During Solidification: Modeling the SSCC Test," *METALLURGICAL AND MATERIALS TRANSACTIONS B*, vol. 42B, pp. 837-851, 2011.
- [81] Y. Lu, L. Bartlett, R. O'Malley, S. Lekakh, M. Buchely, "New Experimental Apparatus to Investigate Hot Tearing Behavior in Steel," in *Proceedings of AISTech 2020*.
- [82] G. Sigworth, "Hot Tearing of Metals," in *AFS Library Copy*, 2002.
- [83] Kyung-hyun KIM. Tae-jung YEO. Kyu Hwan OH and Dong Nyung LEE, "Effect of Carbon and Sulfur in Continuously Cast Strand on Longitudinal Surface Cracks," *ISIJ Int.*, vol. 36, no. 3, pp. 284-289, 1996.
- [84] K. Wunnenberg and R. Flender, "Investigation of internal-crack formation in continuous casting, using a hot model," *Ironmaking and Steelmaking*, vol. 12, no. 1, pp. 22-29, 1985.
- [85] S, N. Singh and K. E. Blazek, "Heat transfer and skin formation in a continuous-casting mold as a function of steel carbon content," *JOM*, vol. 26, no. 10, pp. 17-27, 1974.

- [86] D. R. Poirier, G. H. Geiger, *Transport Phenomena in Materials Processing*, Switzerland: Springer International Publishers, 2006 .
- [87] T. NAKAGAWA, T. UMEDA, J. MURATA, Y. KAMIMUR Aand N. NIWA, "Detormation Behavior during Solidification of Steels," *ISIJ Int.*, vol. 35, no. 6, pp. 723-729, 1995.
- [88] A. Chojecki, I. TeleJko, T. Bogacz, "Influence of chemical composition on the hot tearing formation of cast steel," *Theoretical and Applied Fracture Mechanics* , vol. 27, pp. 99-105, 1997.
- [89] Weiling Wang, Sen Luo, Zhaozhen Cai, Miaoyong Zhu, "THE EFFECT OF PHOSPHORUS AND SULFUR ON THE CRACK SUSCEPTIBILITY OF CONTINUOUS CASTING STEEL," *TMS*, pp. 89-98, 2013.
- [90] Gonzalo Alvarez de Toledo, Oscar Campo and Enrique Lainez, "Influence of Sulfur and Mn/S ratio on the hot ductility of steels during continuous casting," *Steel Research*, vol. 64, no. 4, pp. 292-299, 1993.
- [91] L. K. BIGELOW AND M. C. FLEMINGS , "Sulfide Inclusions in Steel," *METALLURGICAL TRANSACTIONS B* , vol. 6B, pp. 275-283, 1975.
- [92] N. BANDYOPADHYAY and C. L. BRIANT, "The Effect of Phosphorus on Intergranular Caustic Cracking of NiCr Steel," *National Association of Corrosion Engineers*, vol. 38, no. 3, pp. 125-129, 1982.
- [93] E. D. Hondros &M. P. Seah, "Segregation to interfaces," *International Metals Reviews*, vol. 22, no. 1, p. 1977, 262-301.
- [94] F. WEINBERG, "The Ductility of Continuously-Cast Steel Near the Melting Point--Hot Tearing," *METALLURGICAL TRANSACTIONS B*, vol. 10B, pp. 219-227, 1979.
- [95] Y. LI, Q.L. BAI, J.C. LIU, H.X. LI, Q. DU, J.S. ZHANG, and L.Z. ZHUANG, "The Influences of Grain Size and Morphology on the Hot Tearing Susceptibility, Contraction, and Load Behaviors of AA7050 Alloy Inoculated with Al-5Ti-1B Master Alloy," *METALLURGICAL AND MATERIALS TRANSACTIONS A*, vol. 74A, pp. 4024-4037, 2016.
- [96] Hiromu FUJII, Tetsuro OHASHI and Takeshi HIROMOTO, "On the Formation of Internal Cracks in Continuously Cast Slabs," *Transactions ISIJ*, vol. 18, pp. 510-518, 1978.

- [97] SHINOZAKI Kenji, WEN Peng, YAMAMOTO Motomichi, KADOI Kota, KOHNO Yusuke and KOMORI Takuo, "Effect of grain size on solidification cracking susceptibility of type 347 stainless steel during laser welding," *Transactions of JWRI*, vol. 39, no. 2, pp. 136-138, 2010.
- [98] Y Yoshida, H Esaka and K Shinozuka, "Effect of solidified structure on hot tear in Al-Cu alloy," in *IOP Conf. Ser.: Mater. Sci. Eng.*, 2015.
- [99] F. Matsuda, K. Nakata, Y. Shimokusu, K. Tsukamoto, and K. Arai, "Effect of Additional Element on Weld Solidification Crack Susceptibility of Al-Zn-Mg Alloy," *Transactions of JWRI*, vol. 12, no. 1, pp. 81-87, 1983.
- [100] J.E. KELLY, K. R. MICHALEK, T.G. O'CONNOR, B. G. THOMAS, and J. A. DANTZIG, "Initial Development of Thermal and Stress Fields in Continuously Cast Steel Billets," *METALLURGICAL TRANSACTIONS A*, vol. 19A, pp. 2589-2602, 1988.
- [101] Jung-Eui LEE, Heung Nam HAN, Kyu Hwan OH and Jong-Kyu YOON, "A Fully Coupled Analysis of Fluid Flow, Heat Transfer and Stress in Continuous Round Billet Casting," *ISIJ Int.*, vol. 39, no. 5, pp. 435-444, 1999.
- [102] Chong Hee YU, Mikio SUZUKI, Hiroyuki SHIBATA and Toshihiko EM, "Simulation of Crack Formation on Solidifying Steel Shell in Continuous Casting Mold," *ISIJ Int.*, vol. 36, pp. S159-S162, 1996.
- [103] H. G. SUZUKI, S. NISHIMURA, and S. YAMAGUCHI, "Characteristics of Hot Ductility in Steels Subjected to the Melting and Solidification," *Transactions ISIJ*, vol. 22, pp. 48-56, 1982.

II. NEW EXPERIMENTAL APPARATUS TO INVESTIGATE HOT TEARING BEHAVIOR IN STEEL

Yanru Lu, Laura N. Bartlett, Ronald J. O'Malley, Simon N. Lekakh, Mario F. Buchely
Peaslee Steel Manufacturing Research Center, Department of Materials Science and
Engineering

Missouri University of Science and Technology

1400 N Bishop Avenue, Rolla, MO, USA, 65409-0340

Phone: 573-341-4711

Email: lnmkvf@mst.edu

ABSTRACT

Hot Tearing is a complex thermo-mechanical phenomenon occurring in the semi-solid region. Strain in this region can induce cracking and localized alloying element segregation. An apparatus for investigating hot tearing was developed utilizing a servomotor controlled cylinder to apply a predetermined amount of strain to the solidifying shell. A special mold was developed using filling and solidification modeling to ensure that dendrite growth was perpendicular to applied strain. A computer-automated system was utilized to control the strain and strain rate and measure the force and displacement. Solidification experiments utilizing AISI 1020 steel validated the apparatus capabilities and optimized testing parameters.

Keywords: Hot tearing, Strain and strain rate, Directional solidification.

1. INTRODUCTION

Hot tearing is a common irreversible defect that usually appears as cracks, segregation or fractures in the mushy zone during solidification of steel. It occurs when a casting is strained to failure in the semi-solid region during solidification and can lead to alloy and impurity element segregation, porosity formation, and precipitation of inclusions [1-2]. These defects can be accentuated by poor caster alignment and damaged support rolls, as well as non-uniform cooling [3- 4] and soft cooling that can induce shell bulging. During solidification, the existence of residual low melting point liquid results in reduced ductility and increased susceptibility to cracking. This can be magnified by a coarse columnar grain structure, entrapped porosity, and segregation of alloying elements and impurities like Mn, C, Si, S, P [5]. As shown in Figure 1, the ductility of the solidifying steel shell remains almost zero as long as a liquid film exists between the dendrites [6]. Therefore, if there is sufficient strain that is perpendicular to the direction of dendrite growth, a hot tear can be generated.

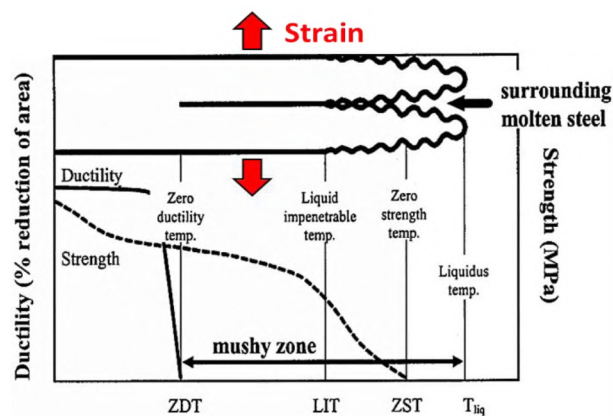


Figure 1. Schematic diagram of mechanical properties in the mushy zone during continuous casting of steels [6].

The ability to fully understand and predict the casting parameters and conditions that cause hot tearing is very important to steel mills and foundries for process design, quality control, and development of new steel grades. Hot tearing has been studied for decades [7-8] by a lot of researchers. However, the effects of segregation of alloying elements such as C, Mn, Al, Si, and S etc. on hot tearing sensitivity are still not well known. This often makes it difficult to predict the hot tearing susceptibility for new steel grades.

Over the years, researchers have developed many different experimental tools to investigate hot tearing behavior. Some of these methods have employed different constraint conditions to induce stress or strain on the solidifying solid shell to promote the formation of hot tearing [9-12] during solidification process. Wang et al. [13] used a ring mold to study the hot tearing susceptibility of Mg alloys. The constrained rod casting (CRC) approach has also been used by several other researchers, which usually consists of rod-shaped castings with different lengths or diameters, as shown schematically in Figure 2 [14-15]. In these tests, the stress is introduced by constraining shrinkage of the solidifying casting to initiate hot tearing in the area that experiences the maximum stress, such as the conjunction area of the round cap and the column in Figure 2 (a).

These CRC experimental methods have been widely used to determine hot tearing sensitivity of both Mg and Al alloys in sand mold as well as in permanent molds, as summarized by J. Song and coworkers [7]. However, both of these methods are qualitative and do not provide a quantitative measure of critical stress or strain for hot tearing.

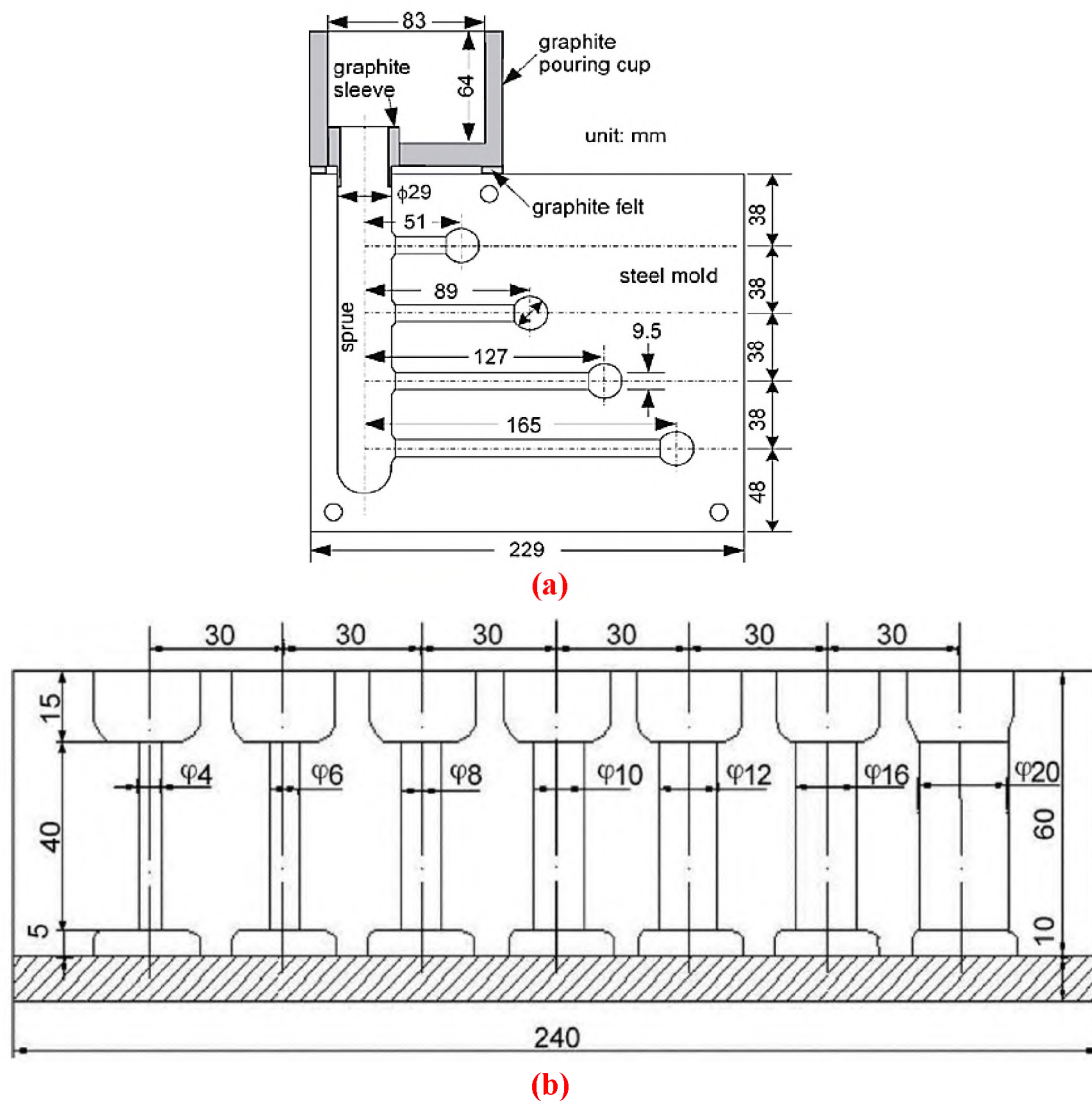


Figure 2. Schematic of different designs of constrained rod castings used to determine hot tearing sensitivity in aluminum and magnesium castings: (a) a design that varies the rod length [14] and (b) a design that varies the rod diameter [15].

Fewer experimental methods have been designed to study the hot tearing susceptibility of steels. One of the most widely used tests is the constrained T-shaped casting. Monroe and Beckermann [16] used a T section setup with a force and displacement measurement devices to quantitatively study the hot tearing behavior of low carbon low alloy steels. The measured force and displacement in this approach were in

good agreement with their simulated force and displacement, respectively. However, the relationship between their measured data with the critical stress or critical strain was not discussed in their work. Bhiogade et al. [17] used the constrained T-shaped casting to study hot tearing susceptibility of a stainless steel and showed that strain and strain rate are more critical for hot tearing than stress. All of the proceeding constrained casting testing approaches share a common drawback; they all rely on solidification shrinkage contraction to develop the strain to form hot tearing. In addition, the amount of contraction and the hot tearing susceptibility will vary as a function of steel composition, which makes it difficult to compare the hot tearing susceptibility for different steel grades at a consistent level of strain.

In recent studies, the submerged split-chill tensile (SSCT) test was developed by Ackermann et al. and applied by Hiebler and other researchers [18-20] to apply controlled deformation to the solidifying steel shell. As shown in Figure 3, a solid copper or steel test body, which can be split into two halves, was submerged into the liquid steel. After a shell of sufficient thickness has formed around the test body, the lower part was moved downwards at a controlled velocity. The force and displacement were recorded during the test. This method allows researchers to study the mechanical behavior of the solidifying steel shell and investigate the relationship between the hot tearing susceptibility and process parameters encountered in the continuous casting process. However, the experiment setup for this test involves immersion of a water cooled copper or steel test body into molten steel contained in an induction furnace. Therefore, this experiment must be extremely well designed for the safety of the operation and to protect the testing devices from high temperature.

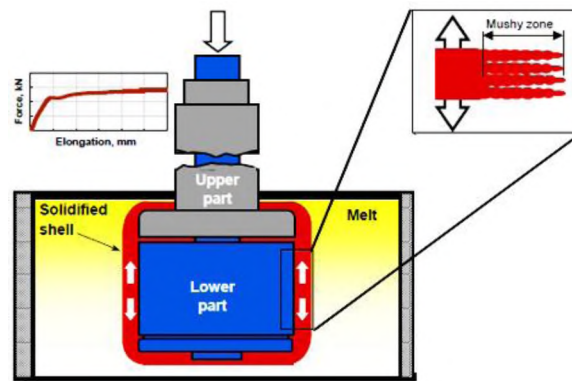


Figure 3. Schematic diagram of the SSCT test method.

To study the hot tearing behavior for different steel grades, a novel approach was developed that overcomes these shortcomings and provides a repeatable and quantitative method of measuring hot tearing susceptibility at controllable strain rates for applications in the continuous casting process.

2. EXPERIMENTAL PROCEDURE

The Controlled Deformation Test (CDT) was developed in the current study to investigate hot tearing in a quantitative way in a solidifying casting. To apply a controlled strain to the mushy zone (see Figure 1) and develop test conditions that are comparable with the continuous casting process, the dendrite growth direction in the solidifying area of casting should be perpendicular to the direction of the applied strain and the solid shell growth in that area should be uniform. Figure 4 shows a schematic of the continuous casting process and highlights the dendritic nature of the expected shell growth. The experimental conditions of the CDT were designed to produce uniform shell growth in a

cylindrical casting in which controlled amounts of deformation could be induced on the shell to replicate strains encountered in continuous casting.

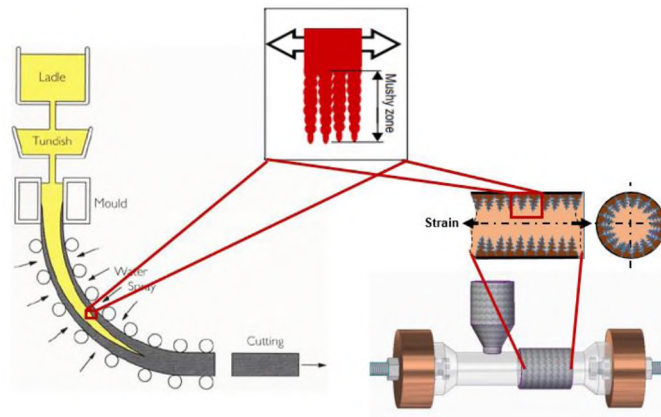


Figure 4. Similarity of the solidification patterns in the continuous casting process and the proposed testing method.

2.1. CASTING AND MOLD DESIGN

A resin bonded, silica sand mold was designed to provide directional solidification and a uniform shell growth in the cylindrical, tensile-bar shaped casting, as shown in Figure 5. A low thermal conductivity insulation sleeve was imbedded into the no-bake sand mold to delay solidification in the test area. The pouring cup also served as a large central riser to ensure proper feeding of the casting during solidification. Two water cooled copper chills were used in the mold to freeze the ends of the bar casting in order to allow transfer of the computer controlled linear displacement to the partial shell in the insulation sleeve area, as shown in Figure 5. The diameter of the reduced section of the casting is 50 mm, and the total length of the casting is 280 mm.

To examine the solidification pattern and evaluate the uniformity of solid shell growth in the insulation sleeve area, filling and solidification software MAGMASOFT

(Version 5.3) was used to simulate the solidification process and determine testing temperature.

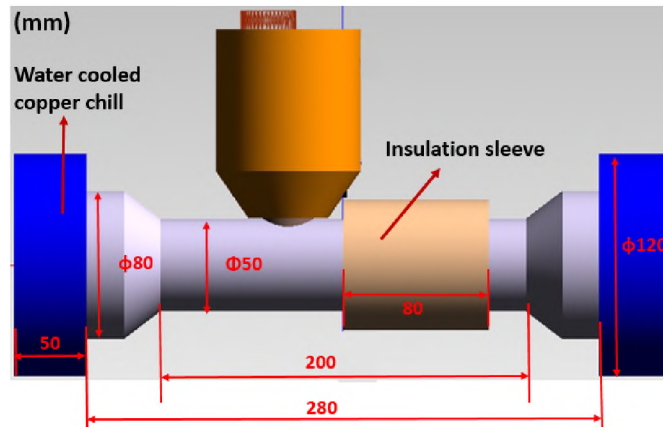


Figure 5. Side view of the test casting design showing the cylindrical test casting, insulation sleeve used to delay solidification in the test area, and water cooled copper chills on each side of the casting used to induce solidification and allow mechanical locking of the test casting.

2.2. TEST APPARATUS

A schematic of the CDT apparatus is shown in Figure 6 (a). The test was designed to control displacement with high precision and measure the resultant displacement and force on the solidifying shell as a function of time. Thus, it is possible to apply a certain amount of strain to the solidifying solid shell at a controlled strain rate. The experimental setup consists of an electric cylinder, which was powered by a servo motor and controlled by an electric drive. Rotational movement of servomotor was translated to reciprocate linear movement using high gear ratio electric cylinder. A 20KN compression & tension load cell and a 25mm linear variable differential transformer (LVDT) were used to control and monitor force and displacement as a function of time. Copper chills were

water cooled to intensify solidification and protect heating the load cell. A threaded steel rod, with two clamping nuts on the end, penetrates the copper chills and protrudes on both sides into the casting cavity, as shown in the detailed view in Figure 6 (b). At the left side, the threaded rod was fixed to the platform, and at the right side, the threaded rod was connected to the load cell (and electric cylinder) by a flange coupling.

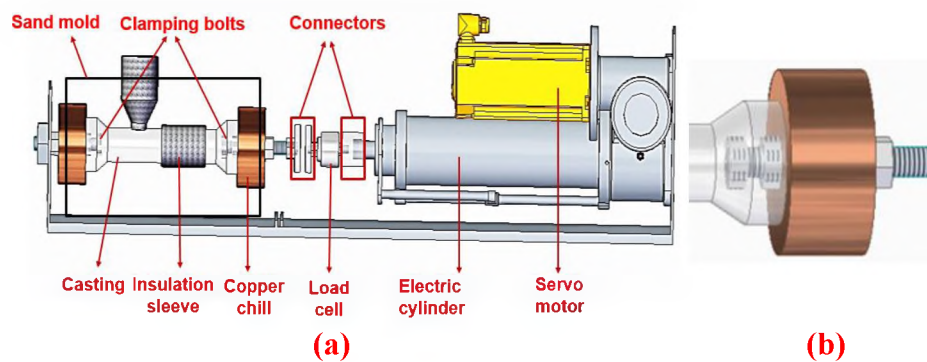


Figure 6. (a) Schematic of the Controlled Deformation Test (CDT) setup showing the main components of this apparatus, and (b) a detailed view of the attachment between the clamping bolts and the copper chill.

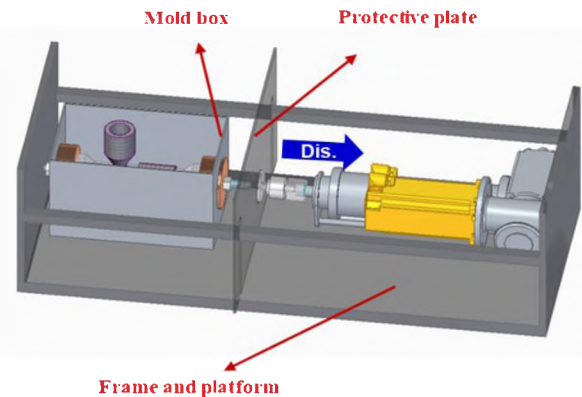


Figure 7. The controlled deformation test setup shows how the mold box and electric cylinder were attached to the steel frame, and the blue arrow in the picture indicates the direction of the movement of the electric cylinder.

All of the components were placed on a custom-made platform, as shown schematically in Figure 7. The electric cylinder, servo motor and drive were fixed to the platform. A protective steel plate was used between the sand mold and the electric cylinder to protect the device. A steel flask was used as the “mold box” to keep the sand mold rigid and to support the copper chills.

2.3. TEST PROCEDURE

Two different experiments were carried out in this study to check the capabilities of the test setup and optimize the test parameters. For both tests, a medium carbon steel with target composition of 0.25 wt% C - 0.3 wt% Si - 0.5 wt% Mn - 0.035 wt% P - 0.03 wt% S were used. For each test, before testing, a no-bake sand mold was prepared separately in the mold box, and then placed in the proper position on the platform. Figure 8(a) shows the experimental setup assembly; Figure 8(b) shows a close view of the LVDT and load cell. LabView software was used to control the movement of the motor. Additionally, LabView data acquisition input modules were connected to the LVDT and the load cell to collect and record the displacement and force data as a function of time.

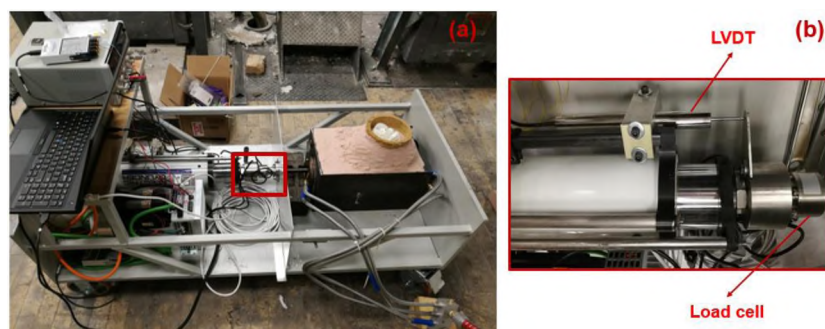


Figure 8. (a) Assembly of the experimental setup, and (b) detail view of the position of the LVDT and load cell.

High purity induction iron, ferrosilicon, electrolytic manganese and cast iron were melted in a coreless 100 lbs capacity induction furnace under argon cover with a flow rate of 45 SCFH. The cast iron served as a source of carbon. When there was a small liquid pool was observed, the pyrite powder was added into the furnace as the source of sulfur. The molten metal was tapped at 1650 °C into a teapot ladle and killed by 0.05 wt.% high purity aluminum shots in the ladle. Then the liquid metal was poured into the sand mold at 1550°C in 5~6 s. At the same time, the force and displacement changes were monitored in the computer. Before the start of the deformation test, to avoid any premature deformation in the casting, the solidification contraction was compensated for by slowly moving the electric cylinder to maintain zero force reading on the load cell. After a specified amount of time, the casting was pulled by the electric cylinder at a constant strain rate.

In the first test (Test 1), multiple deformation steps were applied during the test and the casting was totally fractured after the test. A 4% strain was used at each deformation step in this test and the strain rate was 5×10^{-3} /s. In the second test (Test 2), the test was stopped immediately after a load drop or a load deviation was observed on the load cell readings, which indicates the yield or failure of the material. The strain rate in Test 2 was 10^{-3} /s. These two tests varied the test start time. For Test 1, the test start time was 300 s after pouring. For Test 2, it was 480 s after pouring. The test start time was selected based on the MAGMASOFT solidification analysis of the steel. More details about how to determine the test start time will be discussed in the following section.

3. RESULTS AND DISCUSSION

3.1. THERMODYNAMIC MODELING

To determine the test start time after pouring, the solid fraction vs temperature curve for the current steel grade (0.25 wt% C - 0.3 wt% Si - 0.5 wt% Mn - 0.035 wt% P - 0.03 wt% S) was calculated using the Scheil solidification model in FactSage (Version 7.1) thermodynamic software. Figure 9 shows the calculated solid fraction as a function of temperature. The liquid impenetrable temperature (LIT), which is considered the point below which the dendrites are connected enough to resist the feeding of the interdendritic liquid [4] [21], has been shown to correspond to a solid fraction of 90% [22-23]. Therefore, from the solid fraction – temperature curve, the LIT for the steel composition of interest was determined to be 1420 °C for the current steel composition.

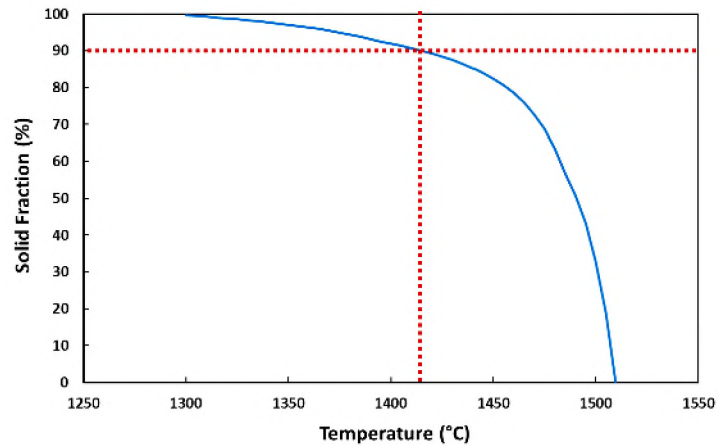


Figure 9. Calculated solid fraction and temperature curve for the studied steel by Scheil equation, which was used to estimate the LIT (dotted lines).

3.2. CASTING SOLIDIFICATION SIMULATION

Figure 10 shows the results of the solidification simulation using MAGMASOFT. Figure 10 (a) shows the predicted fraction of liquid at 6 minutes after solidification. It should be noted that the two sides of the casting were fully solidified because of the water cooled copper chills while the area within the insulation sleeve (short for insulated area) was only partially solidified. A cross section view of solid fraction the insulated area is shown in Figure 10 (b) and this reveals that a uniform solid shell was predicted to form in this area.

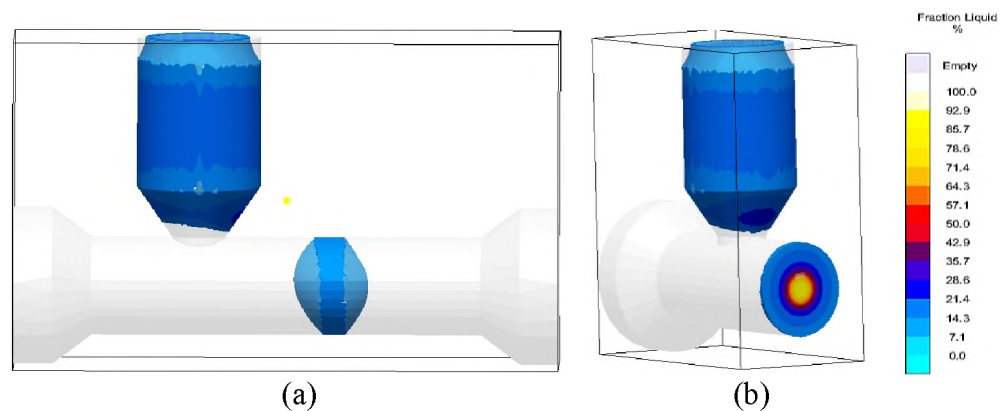


Figure 10. MAGMASOFT solidification modeling shows (a) the solidification sequence of the casting and (b) the cross sectional view of liquid fraction in the insulated area.

The last solidified cross section in the casting was near to the center of the insulated part of the casting, based on the solidification simulation. To establish relationship between the temperature and time, the temperature at two fixed locations within the last solidified cross section was predicted, as shown in Figure 11 (a). One predicted temperature was in the center of the casting and another one was in 10mm radial position from the surface. Figure 11(b) shows the simulated temperature history of

these two points. Test 1 was aimed to check the accuracy of the setup and examine the structure of the fracture surface, so the test start time was decided as 300 s to make sure there still had liquid metal when the start of the test. Test 2 was design to start the test when the solid shell in the insulated area was about 10mm. Thus, when the temperature at the 10mm thickness position is equal to the LIT, the corresponding time is the test start time, which was determined to be 480 s.

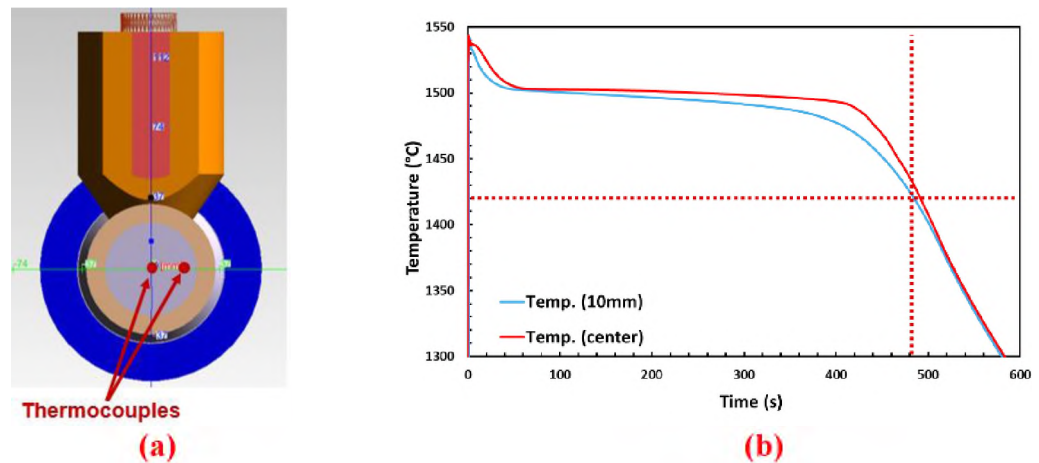


Figure 11. (a) Cross sectional view of the insulated area with the position of the simulated thermocouples and, (b) simulated temperature history in different positions of the casting.

3.3. CDT RESULTS

Table 1 gives the target and measured chemistry of the steels employed in the two tests. The main elements were measured by optical emission spectroscopy (OES).

LECO* combustion method was used for C, S. The measured compositions were in good agreement with the targeted chemistry. It should be noticed that the measured sulfur was slightly higher than the expected amount, which may have been caused by the

segregation of sulfur, since the samples used for measuring the sulfur were cut from the insulated area, which was the last area in the casting to solidify.

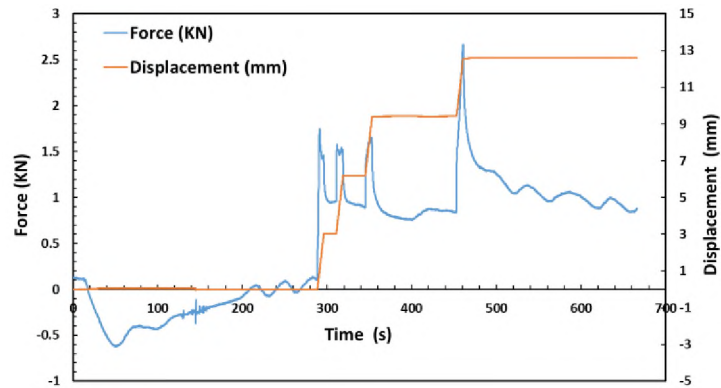
Table 1. Measured steel chemistry in two tests (wt.%).

Element (wt. %)	Fe	*C	Mn	*S (ppm)	P	Si	Al
Target	Bal.	0.17~0.23	0.3~0.6	300	<0.04	0.3~0.4	0.05
Test 1	Bal.	0.23	0.55	319	0.014	0.38	0.054
Test 2	Bal.	0.20	0.59	353	0.021	0.35	0.045

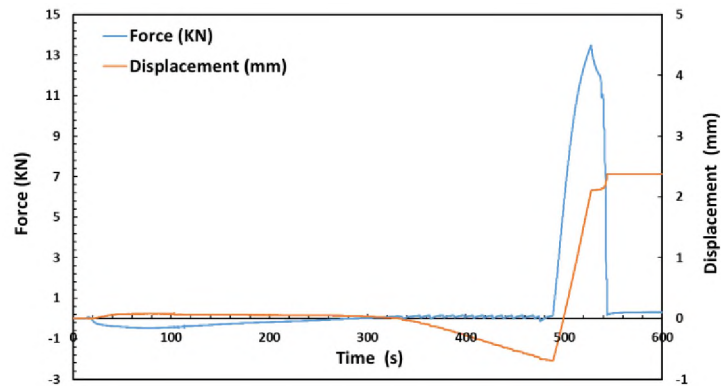
Figures 12 (a) and (b) show the load and displacement measurements obtained during Test 1 and Test 2, respectively. When pouring the metal into the mold, the liquid metal flow pushed the copper chill, which was connected with the load cell and the load cell measured the resultant compression force. As solidification started, the compression force began to decrease because of solidification contraction and solid section shrinkage. For Test 1, the test started 300s after pouring, which is indicated by the change of the displacement. Four deformation steps were applied to the casting in this test at a constant strain rate of 5×10^{-3} /s and each deformation step was at a 4% strain. It should be noted that the amount of strain was calculated using the length of the insulation sleeve as the gauge length. Among these four deformation steps, the last step had the maximum tensile force of about 2.6KN.

For Test 2, before the start of the test, the holding time before applying strain to the casting was longer compared with the waiting time in Test 1 to ensure that a thicker solid shell formed before strain was applied. A larger solidification contraction was observed, which was related to thicker solid shell that formed in the test. To compensate the solidification contraction, a “negative” displacement was applied to keep the

measured force near zero. The deformation test started at 480 s after pouring at the strain rate of 10^{-3} /s. The maximum force in this test was around 13KN. Shell deformation was stopped immediately after the first observed load drop.



(a)



(b)

Figure 12. Load and displacement change during (a) Test 1 and (b) Test 2.

Figure 13 shows the results of the whole test casting, detailing the insulated area after Test 1 and Test 2, respectively. After the Test 1, the casting was totally broken. And the failure position was close to the center of the insulation sleeve, which was expected. For Test 2, some surface cracks were observed on the casting surface.

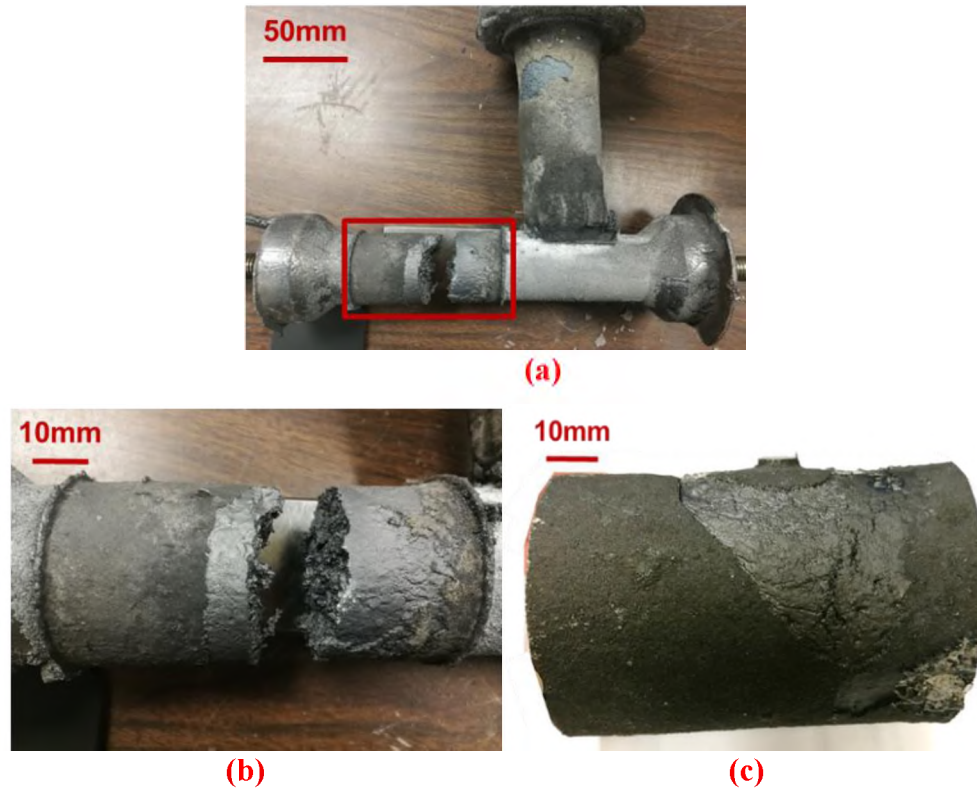


Figure 13. Results of the casting: (a) Complete casting after Test 1, (b) insulated area after Test 1, and (c) insulated area after Test 2.

An overview of the fracture surface after Test 1 is shown in Figure 14 (a). Columnar structure was observed on the upper side of the surface. On the lower side, there was evidence of liquid flow, which means when the test started, liquid was still present in the center of the insulated part and this liquid flowed to the lower side of the fracture site during the test. Figure 14 (b) shows a closer view of a part of the fracture surface, which was highlighted by the red box in the Figure 14 (a). Figure 14 (b) confirms that the dendrite structures grows from the surface towards the center of the casting in the insulated area, which satisfies with the requirement of the experimental design. Under higher magnification Figure 14 (c), single isolated dendrites can also be observed.

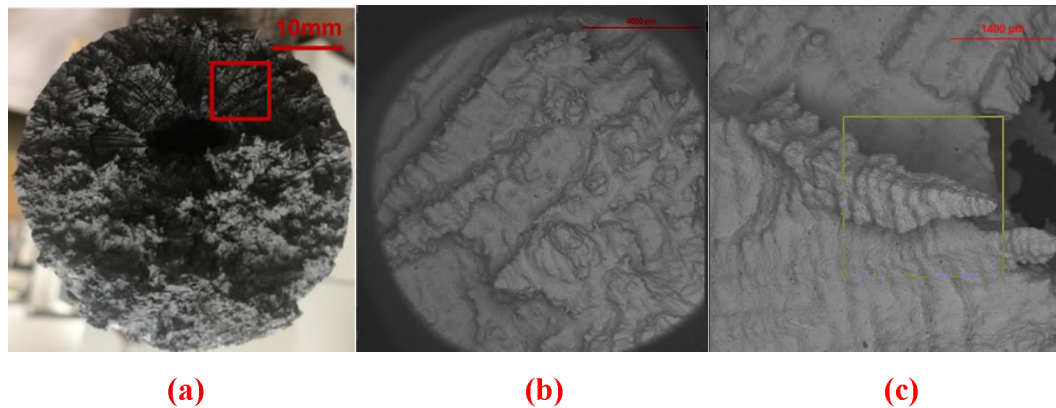


Figure 14. (a) An overview of the fracture surface after Test 1; (b) zoom of part of the fracture surface to show the growth direction of the dendrites; and (c) higher magnification SEM image to show a signal dendrite structure on the fracture surface.

To observe the internal crack, the insulated part of Test 2 was sectioned from top to the bottom along longitudinal direction. Then small specimens were sectioned, mounted and polished for crack observation and chemistry analysis. As shown in Figure 15 (a) and (c), small internal cracks were found to be perpendicular to the direction of the external strain. Figure 15 (b) and (d) show the sulfur distribution in the area of (a) and (c) respectively, which were obtained by ASPEX EDS mapping. It should be noted that in the crack area, the sulfur concentration was higher than other area. It is well known that sulfur has a low partition ratio and it is easy to segregate to the inter-dendritic region, which can flow and accumulate at the crack site as damage occurs [24]. Those low-melting compositions increase the internal crack sensitivity and their enrichment at the crack site serves as a signature of the hot tearing. By comparing the sulfur EDS mapping with the position of the cracks, it can be demonstrated that these internal cracks are the results of hot tearing.

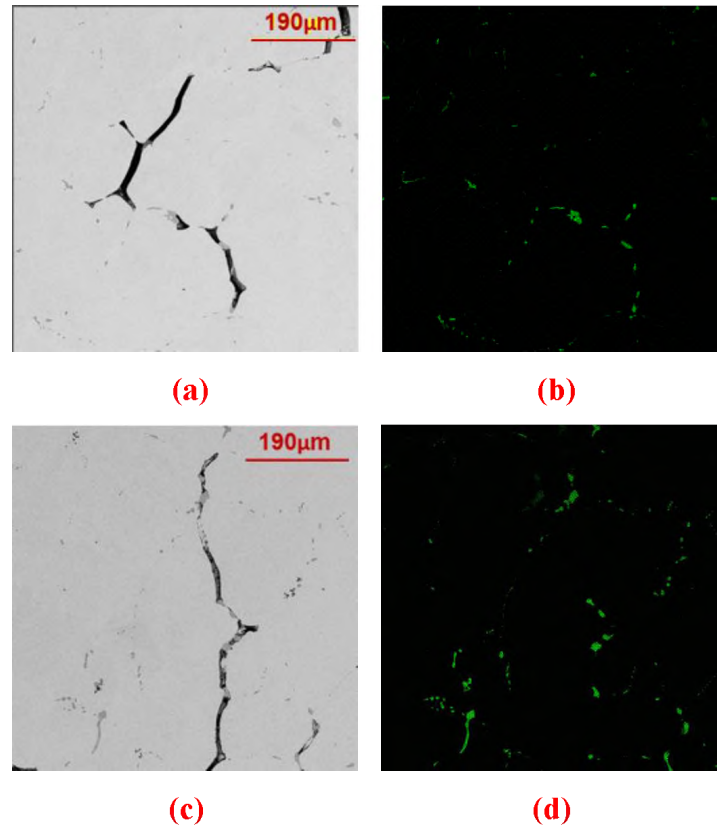


Figure 15. (a) and (c) Internal cracks that were observed in the insulated part after the test 2; (b) and (d) EDS mapping in the area of (a) and (c) to show the sulfur distribution in those area.

4. CONCLUSIONS

In the present study, a laboratory method to investigate hot tearing formation in the continuous casting process was developed and tested. For the mold design, two water cooled copper chills and a centrally located low thermal conductivity insulation sleeve were used to control the solidification of the casting. Solidification simulations show that the insulated area is the last area to solidify in the mold. The solid shell grows from the surface towards the center uniformly in the insulated area, which satisfies the experimental requirements to simulate continuous casting shell growth. Two different

tests were carried out in the present work. These tests confirm the capabilities of this experimental setup to induce hot tearing under controlled thermo-mechanical conditions. Test results indicate that the experimental setup has the ability to monitor the force and displacement change during the solidification of the casting and successfully create conditions for hot tear formation. A test method to quantitatively evaluate and compare the hot tearing susceptibility for different grades of steel has been demonstrated, and testing on a variety of alloy systems of interest are still ongoing.

ACKNOWLEDGEMENTS

The authors would like to thank undergraduate research assistants for their contribution on the sample preparation: Aileen Martinez, Ethan Klafehn, Graham Straley. Acknowledge Brian Bullock for his help with the setup manufacture. This project was supported by Peaslee Steel Manufacturing Research Center (PSMRC) at Missouri University of Science and Technology (Missouri S&T), so special thanks go to all the faculties and industry mentoring committee of PSMRC for their help and guidance. The authors are also grateful to MAGMA LLC for their support to Missouri S&T and their contribution to the simulation work within this project.

REFERENCES

- [1] Junli Guo and Guanghua Wen, "Influence of alloy elements on cracking in the steel ingot during its solidification," *Metals*, vol. 9, no. 8, p. 836, 2019.

- [2] J.-M. D. M. G. M. Rappaz, "A New Hot-Tearing Criterion," METALLURGICAL AND MATERIALS TRANSACTIONS A, vol. 30A, pp. 449-455, 1999.
- [3] L. H. Chown, "The influence of continuous casting parameters on hot tensile behaviour in low carbon, niobium and boron steels," University of the Witwatersrand, Johannesburg, 2008.
- [4] Young Mok Won, Kyung-hyun KIM, Tae-jung Yeo and Kyu Hwan Oh, "Effect of cooling rate on ZST, LIT and ZDT of carbon steel near melting point," ISIJ International, vol. 38, no. 10, pp. 1093-1099, 1998.
- [5] Hirowo G. Suzuki, Satoshi Nishimura and Shigehiro Yamaguchi, "Characteristics of hot ductility in steels subjected to the melting and solidification," ISIJ, vol. 22, p. 48~56, 1982.
- [6] Young Mok Won, Tae-jung Yeo, Dong Jin Seol, and Kyu Hwan Oh, "A New Criterion for Internal Crack Formation in Continuously Cast Steels," Metallurgical and Materials Transactions B, vol. 31B, pp. 779-794, Aug. 2000.
- [7] F. P. B. J. A. A. M. Z. Y. L. J. Song, "A Review on Hot Tearing of Magnesium Alloys," Journal of Magnesium and Alloys, vol. 4, pp. 151-172, 2016.
- [8] J. W. T. Lankford, "Some consideration of strength and ductility in the continuous-casting process," Metallurgical Transactions, vol. 3, pp. 1331-1357, 1972.
- [9] M. R. Nasresfahani and B. Niroumand, "Design of A New Hot Tearing Test Apparatus and Modification of its operation," Met. Mater. Int., vol. 16, no. 1, pp. 35-38, 2010.
- [10] Stephen Instone, David StJohn & John Grandfield, "New apparatus for characterizing tensile strength development and hot cracking in the mushy zone," Int. J. Cast Metals Res., pp. 441-456, 2000.
- [11] L. Bichler, C. Ravindran, "New developments in assessing hot tearing in magnesium alloy castings," Materials and Design, pp. 17-23, 2010.
- [12] H. Z. F. G. S. D. X. T. R. Xu, "A New Investigated Method on Hot Tearing Behavior in Aluminum Alloys," vol. 54, no. 5, pp. 377-382, 2013.
- [13] Yeshuang Wang, Qudong Wang, Guohua Wu, Yanping Zhu, Wenjiang Ding, "Hot-tearing susceptibility of Mg-9Al-xZn alloy," Materials Letters, vol. 57, pp. 929-934, 2002.
- [14] G. Cao, S. Kou, "Hot cracking of binary Mg-Al alloy castings," Materials Science and Engineering A, vol. 417, pp. 230-238, 2006.

- [15] Shuang-Shou Li • Bin Tang • Xin-Yan Jin, Da-Ben Zeng, "An investigation on hot-cracking mechanism of Sr addition into Mg-6Al-0.5Mn alloy," *J Mater Sci*, vol. 47, pp. 2000-2004, 2012.
- [16] C. Monroe, C. Beckermann, "Simulation of hot tearing and distortion during casting of steel: comparison with experiments," in *SFSA 60th Conf. Proc.*, 2006.
- [17] D. S. Bhiogaed, S. M. Randiwe and A. M. Kuthe, "Failure analysis and hot tearing susceptibility of stainless steel CF3M," *International Journal of Metalcasting*, vol. 13, no. 1, pp. 166-179, 2019.
- [18] C. Bernhard, H. Hiebler, and M.M. Wolf, "Simulation of shell strength properties by the SSCT test", *ISIJ Int. (Japan)*, Vol. 36, pp. S163-S166, 1996.
- [19] M. Rowan, B. G. Thomas, R. Pierer and C. Bernhard, "Measuring mechanical behavior of steel during solidification: Modeling the SSCC test," *Metallurgical and Materials Transactions B*, vol. 42B, pp. 837-851, Aug. 2011.
- [20] M. Suauki, C. Yu and T. Emi, "In-Situ Measurement of Tensile Strength of Solidifying Steel Shells to Predict Upper Limit of Casting Speed in Continuous Caster with Oscillating Mold," *ISIJ Int., Iron Steel Inst. Japan*, Vol. 37(4), pp 375-382, 1997.
- [21] Dong Jin SEOL, Young Mok WON, Kyu Hwan OH, Yong Chang SHIN and Chang Hee YIM, "Mechanical Behavior of Carbon Steels in the Temperature Range of Mushy Zone," *ISIL International*, vol. 40, pp. 356-363, 2000.
- [22] M. B. Santillana, "Thermo-mechanical properties and cracking during solidification of thin slab cast steel," *Tata Steel Nederland Technology B.V.*, 2013.
- [23] M. RAPPAZ, J.-M. DREZET, and M. GREMAUD, "A new hot-tearing criterion," *METALLURGICAL AND MATERIALS TRANSACTIONS A*, vol. 30A, pp. 449-455, 1999.
- [24] Gonzalo Alvarez de Toledo, Oscar Campo and Enrique Lainez, "Influence of sulfur and Mn/S ratio on the hot ductility of steels during continuous casting," *Steel Research*, vol. 64, no. 6, pp. 292-299, 1993.

III. DEVELOPING A METHOD TO INVESTIGATE MECHANICAL BEHAVIOR OF STEEL NEAR ITS SOLIDUS TEMPERATURE

Yanru Lu, Laura N. Bartlett, Ronald J. O'Malley, Simon N. Lekakh

Peaslee Steel Manufacturing Research Center, Department of Materials Science and Engineering

Missouri University of Science and Technology

1400 N Bishop Avenue, Rolla, MO, USA, 65409-0340

Phone: 573-341-4711

Email: lnmkvf@mst.edu

ABSTRACT

Crack formation in continuous cast steel is significantly influenced by mechanical properties of the solid shell near its solidus temperature. Thus, a new investigating method to study the high temperature mechanical behavior for solidifying steel shell was introduced in the present work. In this method, an apparatus was designed utilizing an electric cylinder that is controlled by a servo-motor to apply a specified amount of strain to the solidifying steel shell at a controlled strain rate. A special mold configuration was developed to control the dendrite growth in the direction perpendicular to the applied strain and to ensure that the strain is applied in the region of controlled shell growth. Real-time load, displacement and temperature data was monitored by a computer-assisted data acquisition system. The temperature profile of the casting was predicted by MAGMASOFT 5.3.1 and compared with experimental data. Fourier thermal analysis method was applied to calculate solid fraction and coupled with temperature profile to

determine the solid shell thickness/area during the test. The fracture strength at different temperature for a medium carbon steel was determined and compared with that from the other test methods, such as submerged split-chill tensile test and hot tensile test.

Keywords: Experimental apparatus, Solidification crack, Thermal analysis, Temperature profile, Fracture strength

1. INTRODUCTION

In recent years, as a common solidification defect, the hot tearing has been recognized as a major concern that plagues the development of the continuous casting (CC) process. Hot tearing usually appears as a crack in the casting. These cracks have been observed on both surface and inside of the slabs, as shown by the practical data summarized by Brimacombe et al. [1]. The surface cracks were claimed to form at the solidification front at an early stage of solidification and propagates to the surface of the solidifying shell at the lower part of the CC mold or just below the mold [2]. The internal cracks were found to occur in the later stages of solidification when the volume fraction solid is above 85 to 95 percent [3] [4]. The prevention of hot tearing formation during the CC process requires both the well-established understanding of high temperature mechanical properties of the cast material and the analysis of the strand deformation during the casting process.

The thermal mechanical properties of the solidifying steel shell are very critical for the formation of hot tearings, especially for the internal cracks. Industrial and laboratory studies show that most of internal cracks initiate near the equilibrium solidus

temperature and usually appear as interdendritic cracks [5] [6]. During the solidification, the alloy and impurity elements are continuously rejected into the remaining liquid, which makes the melting point of the residual liquid is lower than the equilibrium solidus temperature of the bulk material. The residual low melting point liquid then gathers in the interdendritic region and results in reduced ductility of the material. In CC process, the solidifying steel shell experiences both mechanical and thermal stress loads resulting from the contraction and phase transformation, non-uniform cooling rate from surface to center, friction between the mold and strand, bending and straightening, soft reduction and so on. Under the combined effect of the existence of the low melting liquid and the strain, the interdendritic crack occurs.

The mechanical properties of solidifying steel shell can be characterized by zero strength temperature (ZST) and zero ductility temperature (ZDT), which have been investigated by many other researchers [7] [8] [9]. Many studies show that the ZST and ZDT were related to a solid fraction of 0.6~0.8 and 0.98~1, respectively [3] [9] [10] [11] [12]. The temperature range between ZST and ZDT is the so-called brittle temperature range (BTR). It was reported that there is a critical stress [13] [14] or strain [15] [16] within the BTR, above which the hot tearing happens. The critical stress was estimated as the critical fracture stress [6] or yield stress [17] [18] at that temperature. Thus, the determination of the fracture strength or yield stress of solidifying steel shell is significant for understanding the crack sensitivity of steels.

The conventional hot tensile (CHT) test after re-melting the specimen has been widely used to determine the ZST, ZDT as well as the mechanical properties of the solidifying steel [3] [19] [20] [21]. In this method, the center part of a cylindrical sample,

which usually had a diameter of around 10mm and a length of around 100mm, was heated by an induction coil or joule resistant heater. The center part of the specimen was heated, melted and solidified sequentially under controlled thermal cycle. The tensile tests were performed in the temperature range of liquids temperature and below solidus temperature at certain steps. After the experimental tests, post-mortem analysis was performed to determine the critical temperature points, strength and ductility under different temperatures. However, since the temperature profile in the testing area in this method was nearly uniform during the test and there was temperature gradient along the longitudinal direction, the dendrite growth direction was parallel to the tensile direction. To compare with the solidification conditions in CC process, the submerged split-chill tensile (SSCT) test, which was initially developed by Ackerman et al. [22], was applied by Hiebler et al. [23] and the other researchers [24] [25] [26] to study the mechanical behavior of the solidifying steel shell. The SSCT test consists in a water-cooled cooper or steel test body, which can be split into two halves, was submerged into the liquid steel contained in an induction furnace. After a shell of sufficient thickness has formed around the test body, the lower part was moved downwards at a controlled velocity. The force and displacement were recorded during the test. The cooling conditions and dendrite growth direction in this method were comparable with that in early stage of CC process. Thus, this method was widely used in study the tensile strength and other mechanical properties of the initially formed shell (usually less than 10mm in shell thickness) under CC conditions.

Since the dendrite growth direction cannot be well-controlled in CHT test and SSCT test has been mainly used to study the early stage of solidification in the CC

process, in the present study, a new method has been developed to study the mechanical properties of solidifying steel shell under controlled solidification condition. For this purpose, the in-situ high temperature tensile tests have been conducted using the proposed apparatus. The thermal analysis was performed to analyze the solid shell thickness/area and to choose the representative temperature during the test. The measured fracture strength was determined and compared with the results from CHT test and SSCT test.

2. EXPERIMENTAL PROCEDURE

2.1. CONTROLLED DEFORMATION TEST (CDT)

2.1.1. Experimental Apparatus. The Controlled Deformation Test (CDT) has been initially developed by the Lu et al. and is presented in detail in Reference [27]. The schematic of the CDT apparatus is shown in Figure 1. This test was designed to apply a certain amount of strain to the solidifying or solidified solid shell at a controlled strain rate and measure the resultant displacement and force as a function of time. A resin bonded, no-bake silica sand mold was designed to provide directional solidification and a uniform shell growth in the cylindrical, tensile-bar shaped casting. The dimension of the casting is shown in Figure 2. A low thermal conductivity insulation sleeve was imbedded into the no-bake sand mold to delay solidification in the testing area. Two water cooled copper chills were used in the mold to freeze the ends of the bar casting in order to allow transfer of the computer controlled linear displacement to the partially solidified shell in the insulation sleeve area of casting. An electric cylinder, which was powered by a servo

motor and controlled by an electric drive, was used to apply the controlled strain to the casting. A 20KN compression & tension load cell and a 25mm linear variable differential transformer (LVDT) were used to control and monitor force and displacement during the test. A threaded steel rod, with two clamping nuts on the end, penetrates the copper chills and protrudes on both sides into the casting cavity. At the left side, the threaded rod was fixed to the platform, and at the right side, the threaded rod was connected to the load cell (and electric cylinder) by a flange coupling. The design of the threaded rod and clamping nuts ensures the mechanical lock between the casting and the electric cylinder during the test. LabView software coupled with MotionView software were used to control the movement of the servomotor. The rotational movement of servomotor was translated to reciprocate linear movement of electric cylinder. Additionally, LabView data acquisition input modules were connected to the load cell, LVDT and thermocouples to collect and record the force, displacement and temperature data as a function of time.

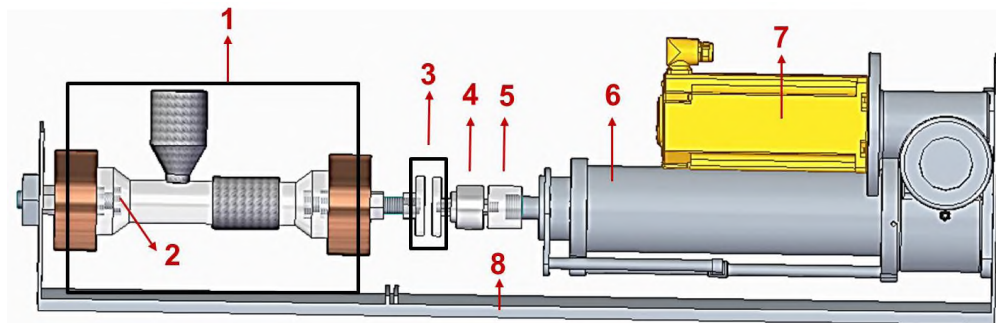


Figure 1. Schematic of the CDT apparatus (front view): (1) sand mold and casting, including insulation sleeve and water-cooled copper chills; (2) steel nuts; (3) flanging connectors; (4) load cell; (5) steel connector; (6) electric cylinder; (7) servo motor; (8) platform.

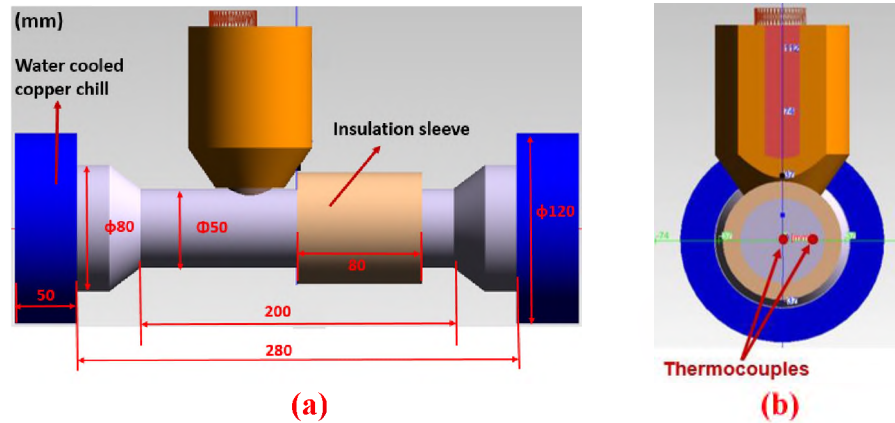


Figure 2. (a) Schematic of the mold and casting design (front view) and (b) the last solidified cross section in insulation area with the positions of the simulated thermocouples.

In the present work, the CDT apparatus was further developed by simultaneously monitoring the temperature history at the different positions in the last solidified cross casting section. The obtained cooling curves were compared to the temperature profile predicted by MAGMASOFT (Version 5.3) simulation and a thickness of solid shell during solidification time were determined. Preliminary simulations were done to find desired thermocouple position in the casting. In actual experiments, two S-type thermocouples were embedded into the sand mold cavity at the locations found from simulation (refer to fig 2 (b)). One thermocouple was in the center of the casting and another one was in around 10mm thickness position from the surface. To protect the thermocouple wires, the bare wires with a diameter of 0.2mm were installed in a double holes ceramic tube, which has an outer diameter of 2.4mm. Then the weld tip of the thermocouple was covered by a thin layer of zircon-colloidal silica slurry used for investment casting ceramic mold, which was mixed in 3 to 1 ratio of 200 mesh zircon powder and liquid colloidal silica. To avoid the influence of the thermocouple on the

crack formation of the casting during deformation, two preliminary repeated tests were performed just to measure the temperature history during solidification without mechanical load. During experiment, temperature sampling rate was 2 readings per second. The actual tests were performed with the same mold configuration and the melt superheat which were used in preliminary trials but without embedded thermocouples.

2.1.2. Experimental Tests. Three different tests were performed to check the capabilities of the test apparatus and estimate the fracture strength of the solid shell under different temperature in this work. The composition of the steels used in these tests is shown in Table 1. High purity induction iron, ferrosilicon, electrolytic manganese and cast iron were melted in a coreless 100 lbs. capacity induction furnace under argon cover with a flow rate of 45 SCFH. The cast iron served as a source of carbon. When a small liquid pool was observed in the furnace, the pyrite powder was added as a source of sulfur. The molten metal was tapped at 1650°C into a teapot ladle and killed in-stream by 0.05 wt.% high purity aluminum shots. The melt was poured into the sand mold installed in the apparatus frame at around 1550°C with 4~5 s mold pouring time. At that moment, the force and displacement changes were monitored and solidification contraction was compensated by slowly moving the electric cylinder to maintain zero force reading on the load cell before the start of the deformation test, to avoid any premature deformation in the casting. After elapsing a certain amount of solidification time, the casting was pulled by the electric cylinder at the strain rate of $10^{-3}/s$ or $5 \times 10^{-3}/s$. Once the measured load started to drop, the applied deformation was stopped. It was done because the drop of the load indicated the failure of the casting. After applied force, the casting was released to freely cool down.

Table 1. Compositions of steels used in this study (weight percent).

Fe	*C	Mn	*S (ppm)	P	Si	Al
Bal.	0.19~0.21	0.50~0.60	300~320	<0.02	0.30~0.40	0.04

2.2. THERMAL ANALYSIS

2.2.1. Cooling Curve Analysis. The Fourier thermal analysis method (short for Fourier method) was adopted to analyze the cooling curves measured during experiments and to estimate the solid fraction. The following analysis was developed based on the methodology suggested by Fras et al. [28]. The critical requirement for this method is determination of “the zero curve (Z curve)” or “the base line”. The Z curve represents the hypothetical first derivative of the cooling curve assuming that the metal doesn’t undergo any phase transformation during the solidification process [29]. In another words, the Z curve overlap the first derivative of the cooling curve in single phase parts (for $T >$ liquidus and $T <$ solidus) of the sample during the cooling process [30]. This method considers the effect of thermal gradient in the casting during solidification and assumes that heat transfer by heat conduction is dominant in the metal-mold systems. Considering a cylindrical mold with a heat source, the Fourier Eq. can be written as:

$$\frac{\partial T}{\partial t} = \alpha \nabla^2 T + \frac{1}{c_V} \frac{\partial Q}{\partial t} \quad (1)$$

where: C_V is the volumetric specific heat, Q is the latent heat of solidification, α is the thermal diffusivity.

Eq. 1 can be rearranged as Eq. 2.

$$\frac{\partial Q}{\partial t} = C_V \left(\frac{\partial T}{\partial t} - z_F \right) \quad \text{with } z_F = \alpha \nabla^2 T \quad (2)$$

where: z_F is the Fourier Z curve.

To determine the Z curve, considering a cylindrical casting, the laplacian $\nabla^2 T$ can be calculated as:

$$\nabla^2 T = \frac{1}{r} \frac{\partial}{\partial r} \left(r \frac{\partial T}{\partial r} \right) \quad (3)$$

Considering the cylindrical casting, which has a symmetric temperature filed with respect to the horizontal axis of the used in experiment cylindrical casting, a minimum data of two temperature points is necessary to determine the ∇^2 . When temperatures T_1 and T_2 in two points, at radii R_1 and R_2 respectively in the test casting are known, then $\nabla^2 T$ in Eq. 3 yields:

$$\nabla^2 T = \frac{4(T_2 - T_1)}{R_2^2 - R_1^2} \quad (4)$$

Determination of the Z curve is also influenced by α . Because before and after solidification, Z curve overlaps the first derivative of the cooling curve, then the thermal diffusivity α can be determined by:

$$\alpha = \frac{\partial T / \partial t}{\nabla^2 T} \quad (5)$$

During the solidification range, since the thermo-physical properties of solid and liquid can be variable, it can be assumed that the change in thermal diffusivity in mushy zone between liquid and fully solid conditions is proportional to the fraction of solid phase. The same assumption can be applied to the specific heat capacity (C_v) as well. To determine the α and C_v value, solid fraction was estimated by a first order approximation:

$$f_s = \frac{t - t_b}{t_e - t_b} \quad (6)$$

where: f_s is the solid fraction, t_b and t_e is the time of beginning and end of solidification determined from the first derivative of the cooling curve.

Hence, the α and C_v value can be determined by:

$$\alpha_{(t)} = \alpha_b(1 - f_s(t)) + \alpha_e f_s(t) \quad (7)$$

$$C_V = C_{Vl}(1 - f_s(t)) + C_{Vs} f_s(t) \quad (8)$$

where, α_b and α_e are the beginning and final values of thermal diffusivity, respectively, determined by Eq. 5 with experimental data, and C_{Vl} and C_{Vs} are the specific heat capacities of liquid and solid.

Then the latent heat and solid fraction can be calculated as [28] [31]:

$$L = \int_{t_b}^{t_e} C_V \left(\frac{\partial T}{\partial t} - z_F \right) (t) dt \quad (9)$$

$$f_s(t) = \frac{1}{L} \int_{t_b}^t C_V \left(\frac{\partial T}{\partial t} - z_F \right) (t) dt \quad (10)$$

In the present work, after each trial experiment, the solidified casting were sectioned at the location of the thermocouples and their position in the casting was measured accurately. The cooling curves obtained in trial experiments were analyzed by the Fourier method. To achieve that, a computer program was developed to process data and calculate the latent heat as well as the relationship between the temperature and solid fraction.

2.2.2. Temperature Profile Simulation. MAGMASOFT (Version 5.3.1) was used to run solidification simulation and to determine the temperature profile at a mesh size of 1mm within the casting. The calculated latent heat and solid fraction by Fourier method were compared with the material properties in MAGMASOFT to validate the database. On the last solidified cross section, 25 thermocouple points were set at a step size of 1mm in radial direction. The measured cooling curves were compared with the simulated cooling curve at same positions. Consequently, the temperature profile

calculated with MAGMASOFT is taken to analyze the solid shell thickness and determine the average temperature of solid shell during tests.

3. RESULTS

3.1. SOLIDIFICATION PATTERN OF THE CASTING IN INSULATING AREA

Figure 3 (a) shows a casting obtained in the trial test. The position of the insulated area was highlighted by the red box. The insulated area of the casting was then sectioned from the top to the bottom along the longitudinal direction. The surface was ground and etched by hot HCl-water solution for 20 minutes to reveal the macro structures, as shown in Figure 3 (b). It can be seen that the columnar structures were formed in the upper side of the insulation area and more equiaxed structures were formed in the lower side. This difference could be caused by the settling of formed solid in the upper part due to the gravity. Similar structures were also observed in another work done by Fujii et al. [32]. The vertical dendritic structures ensure that the applied strain will be in perpendicular to the direction of the dendrite growth.

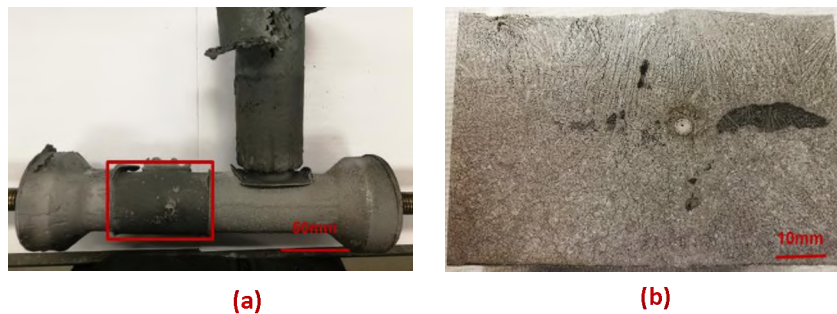


Figure 3. (a) Geometry of the casting with thermocouple tube and (b) the macro structure of the insulated area.

3.2. THERMAL ANALYSIS

Figure 4 shows a cooling curve recorded from the center thermocouple during the solidification, experimental cooling rate, and calculated Fourier Z curve. In this experiment, the actual positions of the thermocouples were measured in the sectioned casting for central as $R=0$ and for wall as $R=15.5\text{mm}$. The start and end solidification time were estimated from the first derivative as $t = 8.5\text{s}$ and $t = 359.5\text{s}$, respectively, using method suggested in the reference [33]. The difference between the first derivative of the cooling curve and the Z curve at any given time represents the generated heat of the solidification reactions at that point. Therefore, the latent heat of solidification can be calculated by Eq. 9 by integrating the area between first derivative and Z curve, which was equals 251249 J/Kg . The latent heat of same steel grade in MAGMASOFT is 256000 J/Kg , which is in reasonable agreement with the calculated latent heat by the Fourier method.

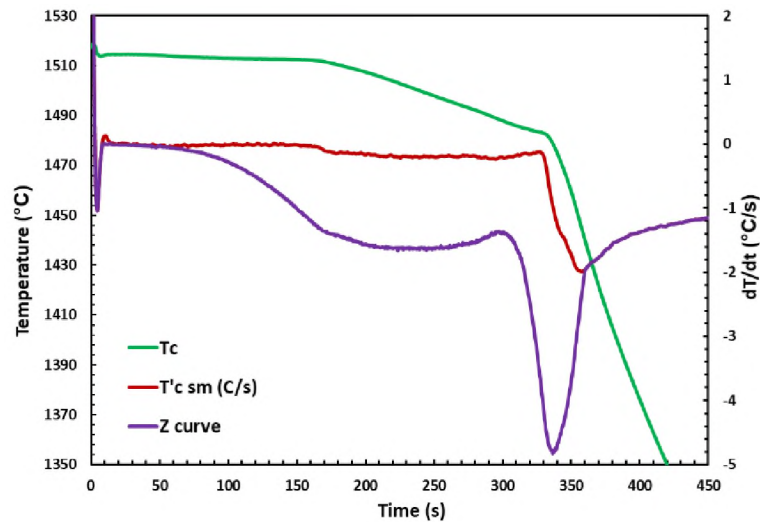


Figure 4. Cooling curve recorded during the test (T_c), its first derivative (T'_c) and the calculated Fourier Z curve.

The calculated solid fraction using Eq. 10 vs time is shown in Figure 5. This calculated result was compared with the solid fraction in MAGMASOFT database used in solidification simulation. It is observed that, in general, the solid fraction by Fourier method shows a reasonable match with that in MAGMASOFT database. Only a slight difference happened in the late stage of solidification. That might be caused by the change of the local composition due to the segregation. Therefore, it is believed that the solid fraction followed from Fourier method analysis of the experimental cooling curve is reasonable valid and was used to determine the solid shell in the casting during experimental trials.

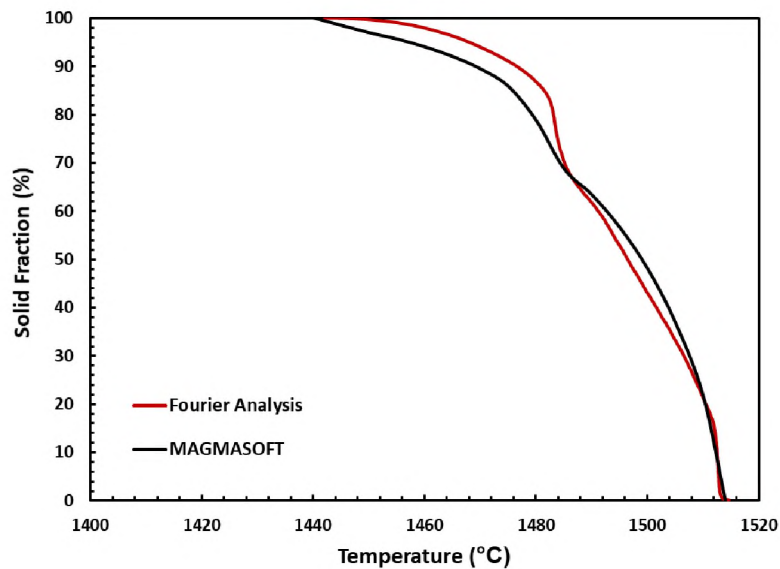


Figure 5. Comparison of the solid fraction calculated with Fourier method and that in MAGMASOFT.

The comparison of the measured temperature in experiments and simulated temperature by MAGMASOFT is shown in Figure 6. The simulated temperatures were in

reasonable agreement with the measured temperatures. Thus, the material properties in MAGMASOFT were valid for the steel studied in the present work and the MAGMASOFT can be used to predict the temperature profile during the tests.

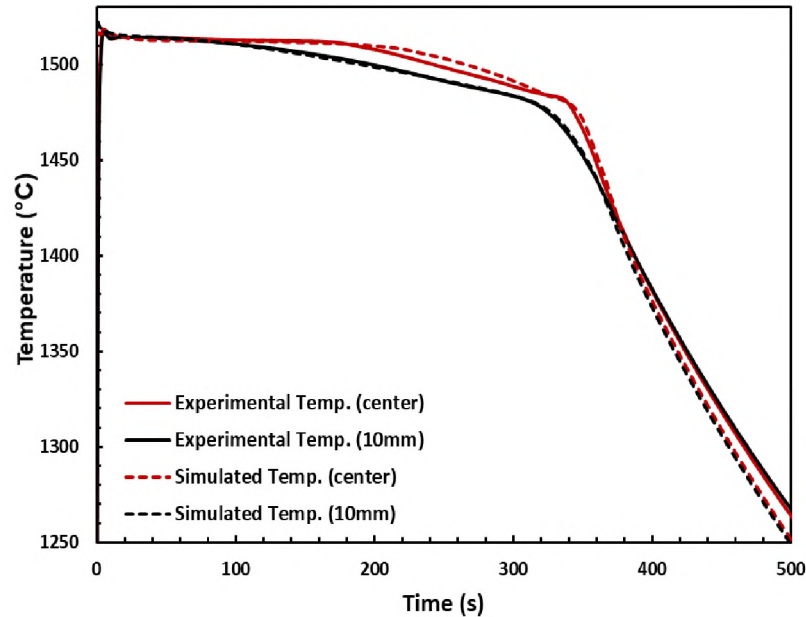


Figure 6. Comparison of the measured temperature in experiment and calculated temperature with MAGMASOFT at two locations: center and 10mm position away from the surface on the last solidified cross section.

3.3. CDT RESULTS

Three formal tests were performed with variation in solidification time and strain rate. Solidification time for Test 1 and Test 2 were 300s and 390s, respectively. These two tests had a same strain rate of $10^{-3}/s$. Test 3 had a longer solidification time of 420s with a higher strain rate of $5 \cdot 10^{-3}/s$. The measured force and displacement are shown in Figure 6.

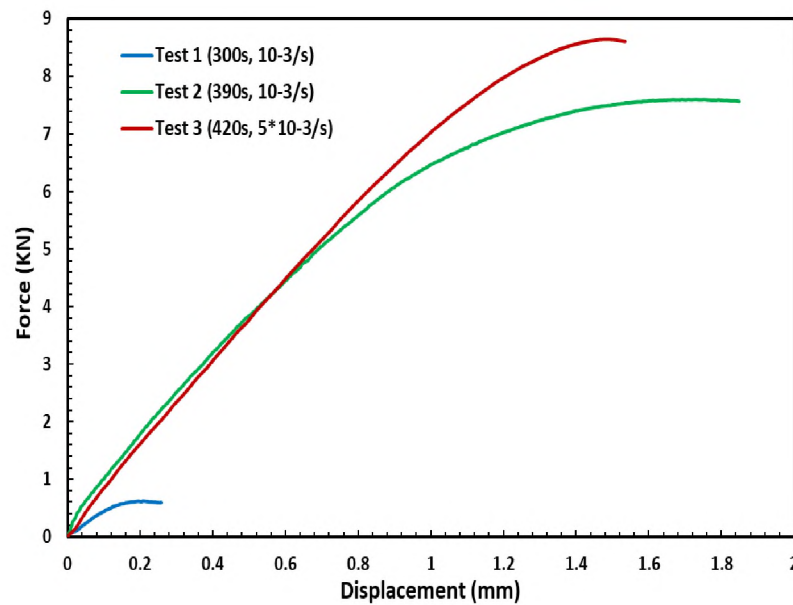


Figure 7. Force and displacement change during experimental tests.

Figure 7 shows the part of casting solidified inside of the insulation sleeve in Test 1 ~ Test 3, respectively. Fracture was observed in the castings after all three tests. From Figure 7 (a) we should noticed that there was a gas bubble on the top of the casting and the fracture was cross the air bubble. The gas bubble may have influence on the crack formation during the deformation test. In order to release the trapped air and improve the surface quality of the casting, a small gas vent was added on the top of insulation part in Test 2 and Test 3. Therefore, the air bubble and surface quality problem were eliminated in Test 2 and Test 3. It was also noticed that the fracture in these two tests happened in the same location in the casting but differed with that in Test 1 due to the existence of the vent.

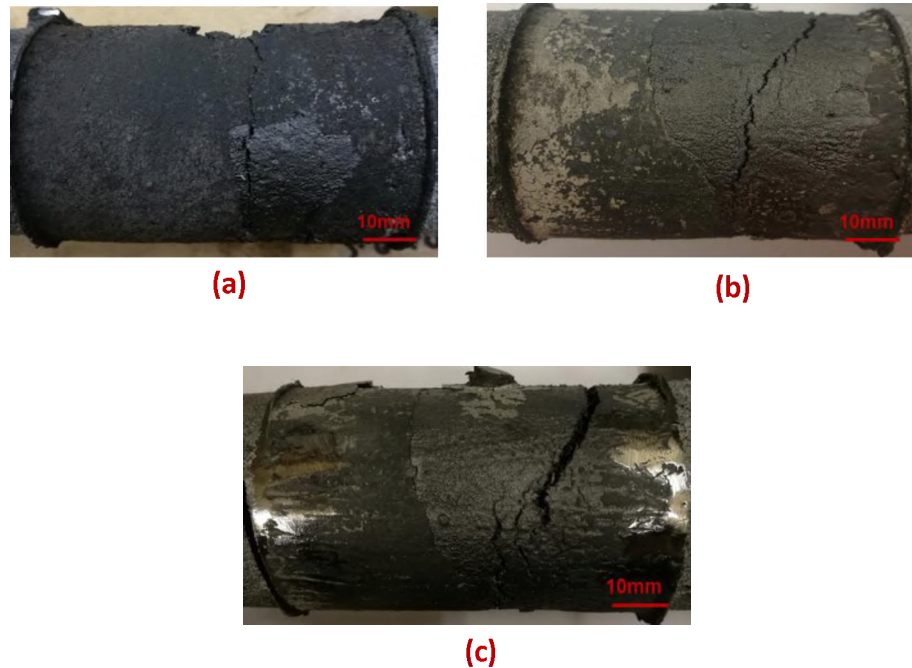


Figure 8. Insulation part of the casting after (a) Test 1, (b) Test 2 and (c) Test 3.

4. DISCUSSION

4.1. TEMPERATURE PROFILE AND SOLID SHELL

The temperature profile of the casting was imported from MAGMASOFT after the solidification simulation, which was taken to analyze the solid shell thickness/area and determine the temperature of solid shell during tests. In the present work, the solid shell was defined as the region where the temperature was below ZST. For carbon steel, the ZST was reported corresponding to a solid fraction of 0.75 [10] [19] [9], which is also used in this work. Based on the thermal analysis in the previous section, the ZST was determined as 1480°C. Compare the start time (300s, 390s and 420s, respectively) to apply strain in three tests and the cooling curve in Figure 6, it was found that in Test 1, the temperature measured in 10mm position was close to the ZST and the center

temperature was above the ZST. While in Test 2 ~ Test 3, the center temperature was below the ZST and the temperature difference in two position was lower than 7°C.

Therefore, in Test 1, around 10mm thick solid shell formed. In Test 2 and Test 3, the whole cross section was in solid state.

4.2. FRACTURE STRENGTH

It is difficult to determine the fracture strength for specific temperature when temperature gradient has taken place in the casting during test. Thus, a “representative temperature” to represent the fracture strength of the shell should be chosen. Yu et al. [34] carried out a hot tensile test with temperature gradient (TG tensile test) in the testing area to study the high temperature mechanical properties of the solidifying steel shell. In this method, one side of the specimen was heated to ZST and the other side was cooled and kept to a temperature that was similar to the interface temperature between the mold and casting in continuous casting process. The tensile force was applied perpendicular to the temperature gradient. The fracture strength measured by this method was compared with that measured using the conventional hot tensile test in uniform temperature profile. It was found that when the average temperature in testing area, $(ZST + \text{temperature in cold side})/2$, in TG tensile test is equal to the temperature in conventional hot tensile test, the measured fracture strengths by these two methods were close. Therefore, the average temperature in solid shell was chosen as the “representative temperature”. Similarly, the average temperature of solid shell was also used as the “representative temperature” when analyzing the fracture strength in SSCT test [35] [36]. In the present study, the test duration for Test 1 ~ Test 3 were 2s, 20s and 3.7s, respectively. Considering the

temperature change during each test, the mean of the “representative temperature” within testing time was elected to calculate the fracture strength. In addition, based on the temperature profile changing during the test, the increment of solid shell thickness in Test 1 can be ignored due to the short testing time. A summary of the experimental conditions and calculated fracture strengths of three tests is shown in Table 2.

Table 2. Test conditions and calculated fracture strength for different tests.

No.	Strain Rate	Solidification Time before the Test (s)	Testing Duration (s)	Max. T_R (°C)	Min. T_R (°C)	Mean T_R (°C)	Fracture Strength (MPa)
Test 1	$10^{-3}/s$	300	2	1475	1474	1474.5	0.47
Test 2	$10^{-3}/s$	390	20	1395	1364	1379.5	3.87
Test 3	$5 \cdot 10^{-3}/s$	420	3.7	1349	1344	1346.5	4.50

(*Max. T_R and Min. T_R : maximum and minimum “representative temperature” within testing time)

4.3. COMPARISON OF FRACTURE STRENGTH DETERMINED BY DIFFERENT EXPERIMENTAL METHODS

The fracture strength tested by the controlled deformation test (CDT) in the present study is plotted against the mean “representative temperature” and compared with that measured with other testing methods (Figure 9). The submerged split-chill tensile (SSCT) test performed by Suzuki et al. [24] had a strain rate of 1/s. The strain rate was $1 \times 10^{-2}/s$ for the conventional hot tensile (CHT) test conducted by Shin et al. [8]. The fracture strength by the CDT increases with decreasing representative temperature, and is in reasonable agreement with that by SSCT test, irrespective of the strain rate. On the other hand, the fracture strength increases steeply with decreasing temperature in CHT

test. The main contributing factor to this discrepancy was the dendrite growth direction in testing area. In both CDT and SSCT test, the dendrite was perpendicular to the applied strain, while in CHT test, radial dendrite growth is hard to control due to the uniform temperature distribution in testing area. Since the cooling rate and solidification pattern within the insulation sleeve in CDT can be controlled by the material type and thickness of the sleeve, the proposed CDT can be used to study the mechanical behavior of the solidifying steel shell in the later stages of solidification in continuous casting (CC) process. Thus, the CDT coupled with the SSCT test will be a valuable tool to study the thermo-mechanical behavior in the different stages of solidification in CC process.

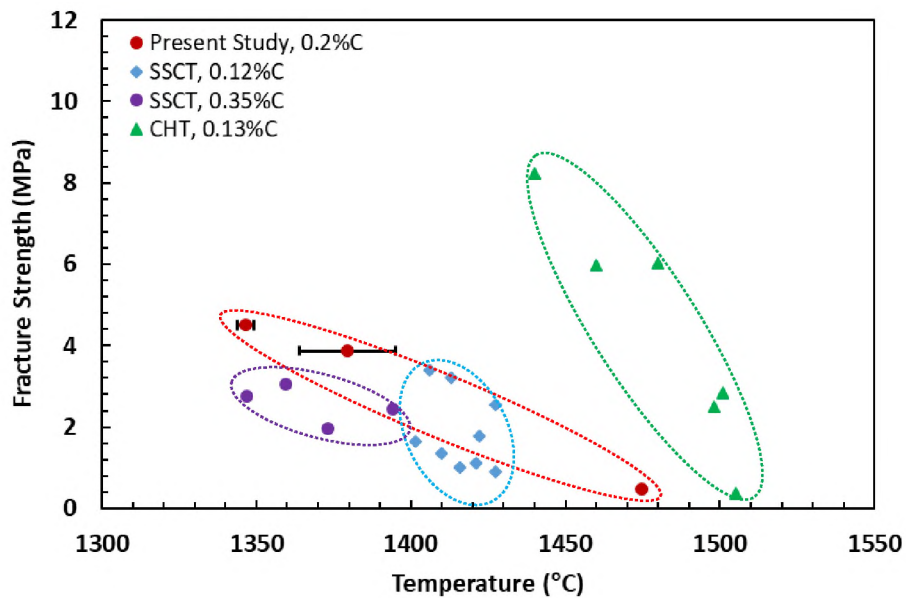


Figure 9. Comparison of fracture strength tested by CDT, SSCT test and CHT test at different representative temperature. Error bar in CDT shows the representative temperature change during each test.

5. CONCLUSIONS

Attempts have been made to develop a new method to determine the high temperature mechanical properties of steel during solidification with the following results:

- 1) Testing apparatus has been developed for applying controlled strain to the solidifying steel shell with controlled dendrite growth. Real-time load, displacement and temperature can be monitored during the test.
- 2) The cooling curves measured in this work was in reasonable agreement with the simulated cooling curves by MAGMASOFT. The calculated latent heat and solid fraction from the measured cooling curve have also matched well with that obtained from MAGMASOFT.
- 3) The fracture strength measured with CDT was in the same order of magnitude with that tested with SSCT tests, although it was lower and increase less with decreasing temperature than the fracture strength determined by the CHT test. It was possibly due to the different dendrite growth directions during the test: in CDT and SSCT test, the dendrite was perpendicular to the applied strain, while in CHT test, the dendrite was randomly distributed or parallel to the tensile direction.

ACKNOWLEDGEMENT

This work was supported by Peaslee Steel Manufacturing Research Center (PSMRC) at Missouri University of Science and Technology (Missouri S&T), so the

authors would like to show their gratitude to all the industry mentoring committee of PSMRC for their financial funding and technical guidance. The authors are also grateful to MAGMA LLC for their support to Missouri S&T and their contribution to the simulation work within this project.

REFERENCES

- [1] J. K. Brimacombe and K. Sorimachi, "Crack Formation in the Continuous Casting of Steel," *METALLURGICAL TRANSACTION B*, vol. 8B, pp. 489-505, 1977.
- [2] C. H. Yu, M. Susuki, H. Shibata and T. Emi, "Simulation of Crack Formation on Solidifying Steel Shell in Continuous Casting Mold," *ISIJ International*, vol. 36, pp. S159-S162, 1996.
- [3] M. B. Santillana, "Thermo-mechanical properties and cracking during solidification of thin slab cast steel," Tata Steel Nederland Technology B.V., geboren te San Nicolás,, 2013.
- [4] D.G. ESKIN and L. KATGERMAN, "A Quest for a New Hot Tearing Criterion," *METALLURGICAL AND MATERIALS TRANSACTIONS A*, vol. 38A, pp. 1511-1519, 2007.
- [5] M. O. EI-Bealy, "On the Formation of Macro-segregation and Interdendritic Cracks during Dendritic Solidification of Continuous Casting of Steel," *METALLURGICAL AND MATERIALS TRANSACTIONS B*, vol. 45B, pp. 988-1017, 2014.
- [6] Y. M. Won, T-J. Yeo, D. J. Seol, and K. H. Oh, "A New Criterion for Internal Crack Formation in Continuously Cast Steels," *METALLURGICAL AND MATERIALS TRANSACTIONS B*, vol. 31B, pp. 779-794, 2000.
- [7] E Schmidtman, F Rakoski, "Influence of the carbon content of 0.015 to 1% and the structure on the high-temperature strength and toughness behavior of structural steels after solidification from the melt," *Arch. Eisenhüttenwes*, vol. 54, no. 9, pp. 357-62, 1983.

- [8] G. Shin, T. Kajitani, T. Suzuki and T. Umeda, "Mechanical properties of carbon steels during solidification," *Tetsu-to-Hagané*, vol. 78, p. 587, 1992.
- [9] T. NAKAGAWA, T. UMEDA, J. MURATA, Y. KAMIMURA and N. NIWA, "Detormation Behavior during Solidification of Steels," *ISIJ International*, vol. 35, no. 6, pp. 723-729, 1995.
- [10] Y. M. WON, K. KIM, T. YEO and K. H. OH, "Effect of Cooling Rate on ZST. LIT and ZDT of Carbon Steels Near Melting Point," *ISIJ International*, vol. 38, no. 10, pp. 1093-1099, 1998.
- [11] H. Hiebler and C. Bernhard, "Mechanical properties and crack susceptibility of steel during solidification," *Steel Research*, vol. 70, no. 8+9, pp. 349-355, 1999.
- [12] Z. Jons'ta, A. Hernas, K. Mazanec, "Contribution to mechanical metallurgy behaviour of steel during continuous casting," *Journal of Materials Processing Technology*, vol. 78, pp. 90-94, 1998.
- [13] C. H. Dickhaus, L. Ohm and S. Engler, "Mechanical properties of solidifying shells of aluminum alloys," *Trans. Am. Foundrymen's Soc.*, vol. 101, pp. 677-684, 1993.
- [14] D.J. LAHAIE and M. BOUCHARD, "Physical Modeling of the Deformation Mechanisms of Semisolid Bodies and a Mechanical Criterion for Hot Tearing," *METALLURGICAL AND MATERIALS TRANSACTIONS B VOLUME 32B*, vol. 32B, pp. 697-705, 2001.
- [15] A. Yamanaka, K. Nakajima, and K. Okamura, "Critical strain for internal crack formation in continuous casting," *Ironmaking and Steelmaking*, vol. 22, no. 6, pp. 508-512, 1995.
- [16] A. Yamanaka, K. Nakkajima, K. Yasumoto, H. Kawashima, K. Nakai, "New Evaluation of Critical Strain for Internal Crack Formation in Continuous Casting," *Revue de métallurgie*, vol. 89, no. 7-8, pp. 627-633, 1992.
- [17] J.E. KELLY, K. R MICHALEK, T.G. O'CONNOR, B. G. THOMAS, and J. A. DANTZIG, "Initial Development of Thermal and Stress Fields in Continuously Cast Steel Billets," *METALLURGICAL TRANSACTIONS A*, vol. 19A, pp. 2589-2602, 1988.
- [18] K. Kim, H. N. Han, T. Yeo, Y. Lee, K. H. Oh, and D. N. Lee, "Analysis of surface and internal cracks in continuously cast beam blank," *Ironmaking and Steelmaking*, vol. 24, no. 3, pp. 249-256, 1997.

- [19] D. J. SEOL, Y. M. WON, K. H. OH, Y. C. SHIN and C. H. YIM, "Mechanical Behavior of Carbon Steels in the Temperature Range of Mushy Zone," *ISIJ International*, vol. 40, no. 4, pp. 356-363, 2000.
- [20] W. Hu, Y. Zhang, G. Yuan, X. Zhang, and G. Wang, "Hot Temperature Mechanical Behavior of High-Permeability 6.5 wt% Si Electrical Steel in a Mushy Zone," *Steel research int.*, p. 1900105, 2019.
- [21] J. R. .. W.T. LANKFORD, "Some Considerations of Strength and Ductility in the Continuous-Casting Process," *METALLURGICAL TRANSACTIONS*, vol. 3, pp. 1331-1357, 1972.
- [22] P. ACKERMANN and W. KURZ, "In Situ Tensile Testing of Solidifying Aluminium and Al-Mg Shells," *Materials Science and Engineering*, vol. 75, pp. 79-86, 1985.
- [23] C. BERNHARD, H. HIEBLER and M. M. WOLF, "Simulation of Shell Strength Properties by the SSCT Test," *ISIJ International*, vol. 36, pp. S163-S168, 1996.
- [24] M. SUZUKI, M. SUZUKI, C. YU and T. EMI, "In-Situ Measurement of Fracture Strength of Solidifying to Predict Upper Limit of Casting Speed in Continuous Caster with Oscillating Mold," *ISIJ International*, vol. 37, no. 4, pp. 375-382, 1997.
- [25] X. Ruan, P. Robert, C. Shi, F. Mei, "Experimental research on hot-tearing crack sensitivity," *Baosteel Technical Research*, vol. 9, no. 3, pp. 18-23, 2012.
- [26] M. Rowan, B. G. Thomas, R. Pierer and C. Bernhard, "Measuring Mechanical Behavior of Steel During Solidification: Modeling the SSCC Test," *METALLURGICAL AND MATERIALS TRANSACTIONS B*, vol. 42B, pp. 837-851, 2011.
- [27] Y. Lu, L. N. Bartlett, R. J. O'Malley, S. N. Lekakh, M. F. Buchely, "New Experimental Apparatus to Investigate Hot Tearing Behavior in Steel," in *Iron & Steel Technology*, Cleveland, 2020.
- [28] E. Fras, W. Kapturkiewicz, A. Burbielko, H. F. Lopez, "A New Concept in Thermal Analysis of Castings," *AFS Transactions*, vol. 101, pp. 505-511, 1993.
- [29] W. T. Kierkus, J. H. Sokolowski, "Recent Advances in CCA: A New Method of Determining Baseline Equation," *AFS Transactions*, vol. 107, pp. 161-167, 1999.

- [30] D. Emadi, L. V. Whiting, M. Djurdjevic, W. T. Kierkus, J. Sokolowski, "COMPARISON OF NEWTONIAN AND FOURIER THERMAL ANALYSIS TECHNIQUES FOR CALCULATION OF LATENT HEAT AND SOLID FRACTION OF ALUMINUM ALLOYS," *MJoM*, pp. 91-106.
- [31] D. M. Stefanescu, "THERMAL ANALYSIS—THEORY AND APPLICATIONS IN METALCASTING," *International Journal of Metalcasting*, vol. 9, no. 1, pp. 7-22, 2015.
- [32] H. Fujii, T. Ohashi, T. Hiromoto, "On the Formation of Internal Cracks in Continuously Cast Slabs," *Transactions ISIJ*, vol. 18, pp. 510-518, 1978.
- [33] Jernkontoret, A Guide to the Solidification of Steels, Stockholm, 1977.
- [34] C. H. Yu, M. Suzuki, H. Shibata and T. Emi, "Simulation of Crack Formation on Solidifying Steel Shell in Continuous Casting Mold," *ISIJ International*, vol. 36, pp. S159-S162, 1996.
- [35] C. Bernhard, R. Pierer, A. Tubikanec, C.M. Chimani, "Experimental Characterization of Crack Sensitivity under Continuous Casting Conditions," in *Proc. of the CCR04 — Continuous Casting and Hot Rolling Conference*, Linz, Austria, 2004.
- [36] M. Suzuki, M. Suzuki and M. Nakada, "Perspectives of Research on High-speed Conventional Slab Continuous Casting of Carbon Steels," *ISIJ International*, vol. 41, no. 7, pp. 670-682, 2001.
- [37] D.G. Eskin, Suyitno, L. Katgerman, "Mechanical properties in the semi-solid state and hot tearing of aluminium alloys," *Progress in Materials Science*, vol. 49, pp. 629-711, 2004.
- [38] J. Song, F. Pan, B. Jiang, A. Atrens, M. Zhang, Y. Lu, "A review on hot tearing of magnesium alloys," *Journal of Magnesium and Alloys*, vol. 4, pp. 151-172, 2016.
- [39] M. Rappaz, J.-M. Drezet, and M. Gremaud, "A New Hot-Tearing Criterion," *METALLURGICAL AND MATERIALS TRANSACTIONS A*, vol. 30A, pp. 449-455, 1999.
- [40] T. Koshikawa, M. Bellet, C-A Gandin, H. Yamamura, M. Bobadilla, "Experimental study and two-phase numerical modeling of macrosegregation induced by solid deformation during punch pressing of solidifying steel ingots," *Acta Materialia*, vol. 124, pp. 513-527, 2019.

- [41] T. KOSHIKAWA, M. BELLET, C.-A. GANDIN, H. YAMAMURA, and M. BOBADILLA, "Study of Hot Tearing During Steel Solidification Through Ingot Punching Test and Its Numerical Simulation," *METALLURGICAL AND MATERIALS TRANSACTIONS A*, vol. 47A, pp. 4053-4067, 2016.
- [42] Y. M. WON, H. N. HAN, T. YEO and K. H. OH, "Analysis of Solidification Cracking Using the Specific Crack Susceptibility," *ISIJ International*, vol. 40, no. 2, pp. 129-136, 2000.
- [43] G. Xia, J. Zirngast, H. Hiebler and M. M. Wolf, "High temperature mechanical properties of in-situ solidified steel measured by the new SSCT-Test," in *Proc. Conf. Continuous Casting of Steel in Developing Countries*, Beijing, 1993.
- [44] T. Matsumiya, M. Ito, H. Kajioka, S. Yamaguchi and Y. Nakamura, "An Evaluation of Critical Strain for Internal Crack Formation in Continuously Cast Alsbs," in *105th ISIJ Meeting Proceedings*, Tokyo, 1985.

SECTION

2. CONCLUSIONS AND RECOMMENDATIONS

2.1. CONCLUSIONS

The purpose of this study has been to provide an understanding of the conditions and mechanisms that cause the hot tearing as well as to develop a quantitative method for measuring the hot tearing formation in continuous casting process. Therefore, the current investigation of hot tearing has been summarized and a new experimental method, the controlled deformation test, was developed and tested.

Most of the hot tears have been found to initiate at the late stage of solidification and appear as interdendritic cracks [14] [23], which usually involves in the existence of the interdendritic liquid film as well as strain and/or stress. To predict the hot tearing formation, both non-mechanical criteria and mechanical criteria have been developed considering the different influence factors under different casting conditions (Paper I). Previous studies show that these alloying elements, like carbon [15] [24] [25], sulfur [26] [25] [27], phosphorus [26] [28] [29] and so on, influence the hot tearing susceptibility of steels mainly by changing the brittle temperature range and the total strain during solidification. It has also been found that the dendrite solidification structure is more vulnerable to crack compared with the equiaxed structure because the interdendritic region can work as a path for the propagation of the crack under tensile strain [30]. However, the synergistic effects of different alloy additions, segregation effects, heating and cooling, solidification structure to hot tear formation during casting are currently not

well known. In addition, although various experimental methods have been developed to evaluate the hot tearing sensitivity of different steels, in order to obtain comparable hot tearing susceptibility, a standardized hot tearing testing approach and evaluation system still needs to be established.

The controlled deformation test was then developed to provide a new tool to study the thermo-mechanical properties of solidifying steel and to assess the hot tearing sensitivity for different steel grades. Experimental results show that the applied strain and strain rate could be well controlled by this apparatus. Real-time load, displacement and temperature were monitored and stable data was obtained during the test. The dendrites grow from surface towards the center of the casting in the part within the insulation sleeve, which make sure the direction of the dendrite growth was perpendicular to the applied strain in the testing area. The measured cooling curves in experiments were in reasonable agreement with that calculated by the filling and solidification software package. Thus, this software was believed to be reasonable valid to predict the temperature profile of casting during test.

The fracture strength at different temperatures of a medium carbon steel was determined with the controlled deformation test (CDT). Results show that the fracture strength measured by the controlled deformation test was in the same order of magnitude with that tested with the submerged-split chill tensile (SSCT) test, while it was lower and increase less with decreasing temperature than the fracture strength determined by the conventional hot tensile (CHT) test (Paper III). It was believed that the dendrite growth direction causes this difference: in CDT and SSCT test, the dendrite was perpendicular to

the applied strain, while in CHT test, the dendrite was randomly distributed or parallel to the tensile direction.

2.2. RECOMMENDATIONS

In current study, the controlled deformation test (CDT) was developed to study the thermo-mechanical properties of the solidifying steel shell and to evaluate the hot tearing sensitivity for different steel grades under continuous casting (CC) condition. Compared with the widely used submerged-split chill tensile (SSCT) test [31] [32] [33], which was mainly used to study the tensile strength and other mechanical properties of the initially formed shell (usually less than 10mm in shell thickness) under CC condition, the current CDT has lower cooling rate in the testing area. Therefore, it is more suitable for the study of the mechanical behavior of the steel shell at later stage of solidification in CC process. Since the cooling rate and temperature gradient in the testing area are mainly controlled by the mold material and sleeve, this method can be potentially designed to mimic the different solidification conditions during different casting processes. Figure 2.1 provides an example to show the influence of the thickness of the insulation sleeve on the solidification structure within testing area. It was shown that more dendritic structures were formed with a thinner insulation sleeve. In addition, the solid shell thickness during the test was significantly determined by the elapsed solidification time before the applied strain. Thus, experiments can be designed and performed to study the mechanical properties of the casting at different solidification stages.

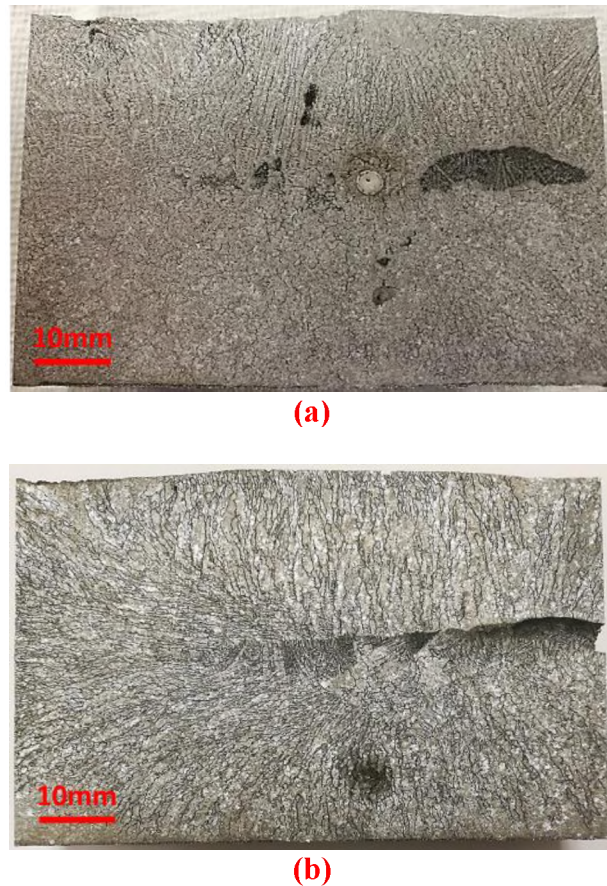


Figure 2.1. Solidification structure of the insulated area with (a) 10mm thick insulation sleeve, (b) 4mm thick insulation sleeve. Samples were etched with HCl-water solution at the temperature range of 65~70°C for 25 minutes.

Fracture strength of solidifying steel shell at different temperature was measured and discussed in Paper III. However, to determine the critical strain/stress for the hot tearing formation, it is important to capture the point where the hot tearing was just initiated. Current load curves show that the casting underwent the elastic deformation first during the test, then it was plastic deformation. The transformation from elastic deformation to plastic deformation might be an indicator for the hot tearing initiation. Therefore, in order to decide the critical strain/stress, different experiments should be conducted to stop the deformation before and after the load deviation occurs.

The stress can be directly calculated based on the solid shell area and measured force during the test. While the local strain happened within the “gauge length” is hard to determine since the total strain is applied to the whole casting as well as the parts in the setup. In addition, the solidification process proceeds during the test and the solid shell changes all the time, which makes it much more difficult to determine the real strain during the test. A possible solution to help analyzing the real strain is to develop a numerical model that can simulate the thermo-mechanical process during the test, which requires the accurate temperature profile prediction, material properties, and proper models that can be used to describe the thermal mechanical behaviors for both semi-solid and solid material.

BIBLIOGRAPHY

- [1] C. Monroe, C. Beckermann, "Development of a hot tear indicator for steel castings," *Materials Science and Engineering A*, pp. 30-36, 2005.
- [2] J. B. Mitchell, S. L. Cockcroft, D. Viano, C. Davidson & D. StJohn , "Determination of Strain during Hot Tearing by Image Correlation," *Metallurgical and Materials Transactions A*, vol. 38, pp. 2503-2512, 2007.
- [3] M. A. Easton, H. Wang, J. Grandfield, C. J. Davidson, D. H. StJohn, L. D. Sweet & M. J. Couper, "Observation and Prediction of the Hot Tear Susceptibility of Ternary Al-Si-Mg Alloys," *Metallurgical and Materials Transactions A*, vol. 43, pp. 3227-3238, 2012.
- [4] R. XU, H. ZHENG, J. LUO, S. DING, S. ZHANG, X. TIAN, "Role of tensile forces in hot tearing formation of cast Al-Si alloy," *Trans. Nonferrous Met. Soc. China*, vol. 24, pp. 2203-2207, 2014.
- [5] J. Campbell, *Complete Casting Handbook*, Oxford: Butterworth-Heinemann, 2011.
- [6] M. R. RIDOLFI, "Hot Tearing Modeling: A Microstructural Approach Applied to Steel Solidification," *METALLURGICAL AND MATERIALS TRANSACTIONS B*, vol. 45B, pp. 1425-1438, 2014.
- [7] M. BELLET, O. CERRI, M. BOBADILLA, and Y. CHASTEL, "Modeling Hot Tearing during Solidification of Steels: Assessment and Improvement of Macroscopic Criteria through the Analysis of Two Experimental Tests," *METALLURGICAL AND MATERIALS TRANSACTIONS A*, vol. 40A, pp. 2705-2717, 2009.
- [8] J. Dantzig and M. Rappaz, *Solidification*, Lausanne: EPFL, 2016.
- [9] M. B. Santillana, *Thermo-mechanical properties and cracking during solidification of thin slab cast steel*, Argentina, 2013.
- [10] D.G. ESKIN and L. KATGERMAN, "A Quest for a New Hot Tearing Criterion," *METALLURGICAL AND MATERIALS TRANSACTIONS A*, vol. 38A, pp. 1511-1519, 2007.
- [11] Hansson K., *On the hot crack formationh during solidification of iron-base alloys*, Stockholm: Royal Institute of Technology, 2001.

- [12] D. G. Eskin, Suyitno, L. Katgerman, "Mechanical properties in the semi-solid state and hot tearing of aluminium alloys," *Progress in Materials Science*, vol. 49, pp. 629-711, 2004.
- [13] Y. M. WON, K. KIM, T. YEO and K. H. OH, "Effect of Cooling Rate on ZST, LIT and ZDT of Carbon Steels Near Melting Point," *ISIJ International*, vol. 38, no. 10, pp. 1093-1099, 1998.
- [14] Y. M. WON, T. YEO, D. J. SEOL, and K. H. OH, "A New Criterion for Internal Crack Formation in Continuously Cast Steels," *Metallurgical and Materials Transactions B*, vol. 31B, pp. 779-794, 2000.
- [15] A. Chojecki, I. Telejko, and T. Bogacz, "Influence of chemical composition on the hot tearing formation of cast steel," *Theoretical and Applied Fracture Mechanics*, vol. 27, pp. 99-105, 1997.
- [16] M. RAPPAZ, J.-M. DREZET, and M. GREMAUD, "A New Hot-Tearing Criterion," *METALLURGICAL AND MATERIALS TRANSACTIONS A*, vol. 30A, pp. 449-455, 1999.
- [17] Suyitno, W.H. Kool, and L. Katgerman, "Micro-Mechanical Model of Hot Tearing at Triple Junctions in DC Casting," *Mater. Sci. Forum Vols.*, Vols. 179-184, pp. 396-402, 2002.
- [18] J.A. Williams and A.R.E. Singer, "Deformation, strength, and fracture above the solidus temperature," *J. Inst. Met.*, vol. 96, pp. 5-12, 1968.
- [19] B. G. Thomas, "Modeling of Hot Tearing and Other Defects in Casting Processes," in *ASM Handbook Vol 22: Fundamentals of Modeling for Metals Processing*, ASM International, 2009, pp. 362-374.
- [20] C. H. Dickhaus, L. Ohm, and S. Engler, "Mechanical properties of solidifying shells of aluminum alloys," *Trans. Am. Foundrymen's Soc.*, vol. 101, pp. 677-684, 1993.
- [21] I.I. Novikov and F.S. Novik, "Mechanism of plastic deformation of alloys in the range of melting temperatures," *Dokl. Akad. Nauk SSSR. Ser. Fiz.*, vol. 7, pp. 1153-1155, 1963.
- [22] H. Fredriksson, M. Haddad-Sabzevar, K. Hansson and J. Kron, "Theory of hot crack formation," *Materials Science and Technology*, vol. 21, no. 5, pp. 521-529, 2005.

- [23] M. O. El-bealy, "On the Formation of Macrosegregation and Interdendritic Cracks During Dendritic Solidification of Continuous Casting of Steel," *Metall Mater Trans B*, vol. 45B, pp. 988-1017, 2014.
- [24] Y. M. Won, H. N. Han, T. Yeo and K. H. Oh, "Analysis of Solidification Cracking Using the Specific Crack Susceptibility," *ISIJ International*, vol. 40, no. 2, pp. 129-136, 2000.
- [25] K. Kim, T. Yeo, K. H. Oh and D. N. Lee, "Effect of Carbon and Sulfur in Continuously Cast Strand on Longitudinal Surface Cracks," *ISIJ International*, vol. 36, no. 3, pp. 284-289, 1996.
- [26] W. Wang, S. Luo, Z. Cai, M. Zhu, "The Effect of Phosphorus and Sulfur on the E Crack Susceptibility of Continuous Casting Steel," *Materials Processing Fundamentals*, pp. 89-98, 2013.
- [27] G. A. de Toledo, O. Campo and E. Lainez, "Influence of sulfur and Mn/S ratio on the hot ductility of steels during continuous casting," *Steel Research*, vol. 64, no. 6, pp. 292-299, 1993.
- [28] F. WEINBERG, "The Ductility of Continuously-Cast Steel Near the Melting Point-Hot Tearing," *METALL. TRANS. B*, vol. 10B, pp. 219-227, 1979.
- [29] T. Nakagawa, T. Umeda, J. Murata, Y. Kamimura and N. Niwa, "Detormation Behavior during Solidification of Steels," *ISIJ International*, vol. 35, pp. 723-729, 1995.
- [30] H. Fujii, T. Ohashi and T. Hiromoto, "On the Formation of Internal Cracks in Continuously Cast Slabs," *Transactions ISIJ*, vol. 18, pp. 510-518, 1978.
- [31] M. Suzuki, M. Suzuki, C. Yu and T. Emi, "In-Situ Measurement of Fracture Strength of Solidifying Steel Shell to Predict Upper Limit of Casting Speed in Continuous Caster with Oscillating Mold," *ISIJ International*, vol. 37, no. 4, pp. 375-382, 1997.
- [32] C. Bernhard, R. Pierer, A. Tubikanec, C.M. Chimani, "Experimental Characterization of Crack Sensitivity under Continuous Casting Conditions," *Materials Science*, no. 06.03, 2004.
- [33] M. Rowan, B. G. Thomas, R. Pierer, and C. Bernhard, "Measuring Mechanical Behavior of Steel During Solidification: Modeling the SSCC Test," *METALLURGICAL AND MATERIALS TRANSACTIONS B*, vol. 42B, pp. 837-851, 2011.

VITA

Yanru Lu was born in 1992 in Inner Mongolia, China. After completing her schoolwork at Inner Mongolia No. 1 Senior Middle School No. 1 Machinery Group in Baotou in June 2011, she entered Xi'an Jiaotong University in China, and received her bachelor's degree in Material Science and Engineering and bachelor's degree in Finance in June of 2015. In August 2018, she attended Missouri University of Science and Technology studying hot tearing behavior of continuous casting steel. She received her Master of Science in Materials Science & Engineering from Missouri S&T in December 2020 under the guidance of Dr. Laura Bartlett, Dr. Ronald O'Malley and Dr. Simon Lekakh.